Regional Inkamulla-aged (ca. 1740–1755 Ma) tectonism along strike of the Mt Hay-Redbank Hill region, southern Aileron Province, central Australia

Thesis submitted in accordance with the requirements of the University of Adelaide for an Honours Degree in Geology.

Maddison Lawson-Wyatt

November 2012

THE UNIVERSITY of ADELAIDE

TITLE

Regional Inkamulla-aged (ca. 1740–1755 Ma) tectonism along strike of the Mt Hay-Redbank Hill region, southern Aileron Province, central Australia

RUNNING TITLE

Inkamulla-aged tectonism, Aileron Province

ABSTRACT

LA-ICP-MS U-Pb monazite and zircon geochronology from granulite facies metapelites and granites indicate Inkamulla-aged metamorphism has occurred in the southern Aileron province, immediately east of the Mt Hay and Mt Chapple mastiffs. Gneissic metasediments and a granitic gneiss from an EW-striking structural belt in the southern Aileron Province yield ages reflective of the Inkamulla Igneous Event (1754-1741 Ma) and the Chewings Event (1593-1545 Ma), along with magmatic ages of 1627 and 1641 Ma. The Chewings age is interpreted to represent structural reworking associated with discrete shear zones along the northern margin of the EW belt. Magmatic ages of ca. 1640 Ma typically associated with Warumpi Province magmatism and deformation are found within the study area, which weakens the argument that the Warumpi terrane is exotic from the Aileron Province. The metamorphic conditions of 780-920°C and 5-10 kbars indicate an elevated geothermal gradient.

KEYWORDS

Arunta, Aileron Province, U-Pb geochronology, monazite, reworking, migmatite, Proterozoic Australia, Inkamulla, Chewings

TABLE OF CONTENTS

LIST OF FIGURES AND TABLES

INTRODUCTION

The Arunta Complex is the southernmost portion of the North Australian Craton (NAC) (Figure 1), and is a key region of Proterozoic Australia because it is considered to represent a long-lived active margin (several hundred million years) that preserves a cryptic history of the growth and/or assembly of the Australian continent (Scrimgeour *et al.* 2005b, Betts & Giles 2006). Unravelling the Proterozoic history of the Arunta Complex is challenging due to the large number of ductile deformation events that have affected the region (Scrimgeour 2003). Despite the geographic importance of the Arunta Complex for models of Australian Proterozoic continental growth and assembly there have been relatively few studies that have specifically targeted the age of fabric elements and fabric domains, data which is fundamental for the underpinning of large-scale tectonic models. As an example, the Warumpi and southern Aileron Provinces (Figure 1), which comprise the southernmost part of the Arunta Complex, have been cited as preserving evidence for the creation of continental crust in extensional and collisional settings at different time intervals (Scrimgeour *et al.* 2005b, Betts & Giles 2006, Morrissey *et al.* 2011). However there is a distinct paucity of geochronological constraints on the rocks and structural fabrics located within this region on which models can be based.

This study focuses on rocks outcropping within a large (approximately 1120 km^2) and pronounced E-W striking geophyscially-defined magnetic belt located in the southernmost portion of the Aileron Province (Figure 2). There is no existing geochronological data that constrains the age of deformation and metamorphism of the crust during the Proterozoic from this part of the Aileron Province. The purpose of this

study is to determine the timing of fabric development and to determine the *P-T* conditions of metamorphism. The data collected in this study, as well as concurrently running projects in the Warumpi and Aileron Provinces, will assist in addressing the larger question of the tectonic and geodynamic significance of major event timelines in Proterozoic Australia.

GEOLOGICAL SETTING

Regional Setting

The Arunta Complex defines the southern part of the NAC and comprises an area of 200,000 km^2 (Shaw *et al.* 1984) that can be divided into three separate provinces on the basis of geological history and event chronology, the Aileron, Warumpi and Irindina Provinces (Hand & Buick 2001, Claoué-Long *et al.* 2008a). The Aileron Province is the oldest, preserving depositional and intrusive ages of 1870–1710 Ma (Scrimgeour *et al.* 2005b, Claoué-Long *et al.* 2008b). The Warumpi Province along the southern margin of the Arunta Complex is separated from the much larger Aileron Province by the

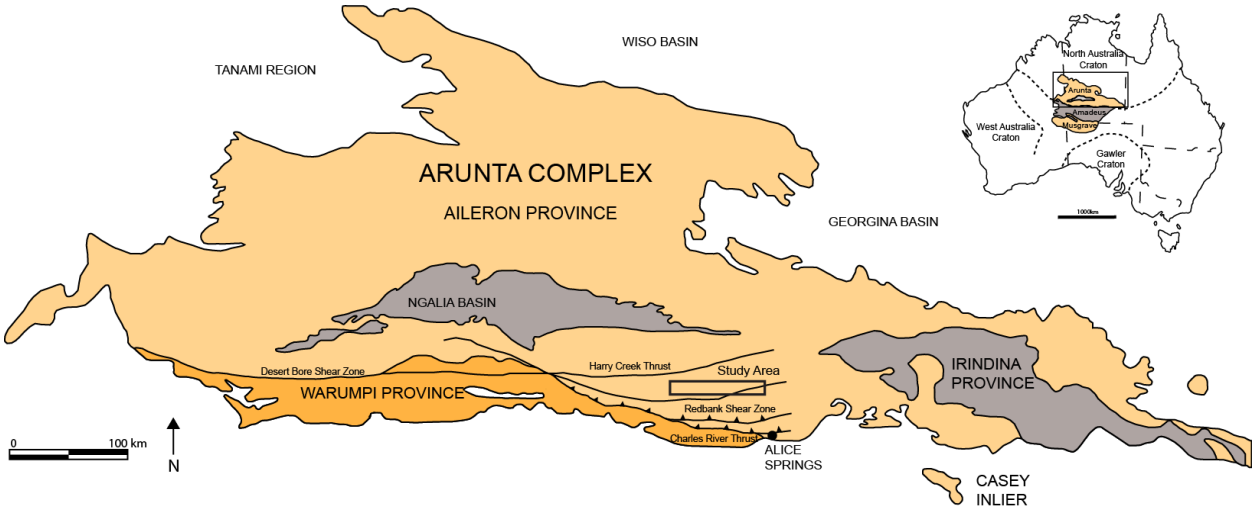

Figure 1- Simplified regional map showing the location of the study area in relation to the Aileron Province and Warumpi Province (modified from Scrimgeour *et al.* 2005). The major faults within the region (Charles River Thrust, Redbank Shear Zone, Harry Creek Thrust and Desert Bore Shear Zone) are marked.

Redbank deformed zone and the Charles River Thrust. The Warumpi Province has protolith ages in the range of 1690–1600 Ma (Scrimgeour *et al.* 2005b) and, based upon limited isotope data, interpreted to be isotopically more juvenile than the Aileron Province. Using these two pieces of evidence the Warumpi Province has been interpreted as exotic to the NAC (Scrimgeour et al 2005). The Irindina Province is located in the eastern Arunta Complex and is associated with Neoproterozoic to Cambrian depositional ages related to the surrounding sedimentary basins and high-grade metamorphism and deformation occurring between 480–320 Ma (Mawby *et al.* 1999, Scrimgeour 2003, Buick *et al.* 2005, Scrimgeour *et al.* 2005a).

The Aileron Province comprises the largest component of the Arunta Complex, but it is predominately covered by recent sediment, leaving only scattered outcrop available to study the Proterozoic history. Regions of large outcrop of Proterozoic rock include the Reynolds-Anmatijira Ranges, the Strangways Range, the Mt Hay–Mt Chapple–Redbank Hill massifs and hill country immediately north and NW of Alice Springs (Figure 2). These regions preserve a complex and protracted record of a series of magmatic and metamorphic events occurring over approximately 1600 million years from ca. 1850 Ma to 300 Ma (Table 1). Proterozoic tectonism in the Arunta Complex is consistently characterised by elevated/high thermal gradients (Scrimgeour *et al.* 2005b). The Stafford Event at ca. 1810–1800 Ma (Scrimgeour 2003) and the Yambah Event at ca. 1770–1780 Ma (Zhao & Bennett 1995, Hoatson *et al.* 2002) both resulted in voluminous magmatism and low-pressure, high-temperature granulite facies metamorphism (Hand & Buick 2001). The Strangways Orogeny, ca. 1740–1690 Ma (Claoué-Long *et al.* 2008b) involved high-grade, granulite facies metamorphism in the Strangways Ranges and southeastern Aileron Province (Scrimgeour 2003, Claoué-Long

et al. 2008b). The Strangways Range and adjacent Harts Range also records evidence for the Inkamulla Igneous Event, between ca. 1760-1740 Ma (Scrimgeour 2003), involving granitic suites in the Entia Dome region of the eastern Aileron Province (Cooper *et al.* 1988, Foden *et al.* 1988, Zhao & Cooper 1992). No metamorphism has been documented from this time period (Scrimgeour 2003).

The eastern Warumpi Province is characterised by abundant outcrop in hilly country defining an E-W trending belt between the Redbank and Desert Bore Shear Zones and sedimentary rocks of the Amadeus Basin (Figure 2) which outcrop continuously over a strike length of approximately 500 km. The Warumpi central western Province is documented as recording an event at ca. 1645–1635 Ma referred to as the Liebig Orogeny. This event involved granulite facies metamorphism (>800°C and 9–10 kbar) and voluminous magmatism (Scrimgeour *et al.* 2005b). The ca. 1640 Ma magmatism is suggested to be characteristic of the Warumpi Province and is suggested to be the result of subduction-related suturing of the exotic Warumpi Terrane with the Aileron Province (Scrimgeour *et al.* 2005b). However, mafic-ultramafic intrusions such as the Andrew Young Complex were emplaced into the Aileron Province at this time. Claoué-Long & Hoatson (2005) and Wong (2011) found evidence of ca. 1650-1630 Ma magmatism in the southern Aileron Province suggesting magmatism of this age is not restricted to the Warumpi Province.

Post-Liebig Orogeny, the Chewings Orogeny (1590-1570 Ma) reworked the Aileron and Warumpi Provinces. More regionally, the Chewings Orogeny corresponds to a continental-scale event that is recorded throughout Proterozoic Australia (Neumann & Fraser 2007).

Table 1- Summary of the deformational events that have affected the Arunta over a 1600 Ma time period.

Event Name	**Event Range**	**Event Characteristics**
Stafford Event	1810-1800 Ma	Widespread deformation recorded across the Arunta Region. The northern Arunta preserved high-temperature, low-pressure metamorphism with rapid lateral changes in the metamorphic grade. The eastern Arunta preserved no associated metamorphism but instead preserved widespread volcanism, mafic and felsic magmatism (Betts & Giles 2006).
Yambah Event (Early Strangways Event)	1780-1770 Ma	Magmatic event affecting the Arunta Complex, preserving felsic and minor mafic magmatism, along with metamorphism and deformation. The eastern Arunta preserves widespread mafic and felsic magmatism (Zhao & Bennett 1995). Also preserved from this time period is mafic magmatism in the Mount Chapple region and granitic magmatism in the northern Arunta (Young *et al.* 1995, Hoatson *et al.* 2002). Metamorphism from this time period is also preserved in the Strangways range and Mt Hay region (Hoatson *et al.* 2002).
Inkamulla Igneous Event	1760-1740 Ma	A voluminous magmatic event associated with granitic and less abundant mafic magmatism. This event was restricted to the southern and eastern Arunta, western Strangways Range and Entia Dome (Scrimgeour 2003). There has been no evidence to suggest any metamorphism was associated with this period of magmatism (Scrimgeour 2003).
Strangways Orogeny	1730-1715 Ma	The most dominant tectonic event in the eastern Arunta. It is preserved as granulite facies metamorphism in the Strangways range, and as amphibolites facies metamorphism south of the Harry Creek Shear Zone (Claoué-Long *et al.* 2008b). Granite intrusion also occurred during this time in the eastern Arunta. The granite intrusions can also be seen in the northern Arunta Complex (Claoué-Long & Hoatson 2005).
Liebig Orogeny	1640-1630 Ma	Proposed as a major orogenic event which resulted in the Warumpi Province accreting to the North Australian Craton (Aileron Province). In the Warumpi Province it is preserved as granulite facies metamorphism with suggested local temperatures of 9 kbar and 900°C. It is also associated with granitic intrusions (Scrimgeour *et al.* 2005b). North of the Redbank Shear Zone mafic complexes and granites intruded which are associated with high-temperature, low-pressure metamorphism (Scrimgeour *et al.* 2005b).
Chewings Orogeny	1590-1560 Ma	This event had a variable impact on the Arunta Complex. It is expressed as pervasive amphibolites facies metamorphism in the Warumpi region. High-temperature, low-pressure metamorphism in the south-eastern Reynolds Range can also be attributed to this event (Hand & Buick 2001). The remainder of the Arunta was affected by low grade deformation and metamorphism associated with this event. Magmatism associated with this event includes the Southwark suite in the western Aileron Province and the Ormiston Pound granite in the Warumpi Province (Collins et al. 1995, Young et al. 1995).
Teapot Event	1150-1130 Ma	A magmatic and thermal event associated with intrusions in the southern region of the Arunta. It included the intrusion of the Teapot granite in the Warumpi and the Mordor Complex in the eastern Arunta (Black & Shaw 1995, Hoatson *et al.* 2002). This Grenvillian aged deformation recorded conditions of 800°C and 8.5 kbar in the central Wigley Block (Wong 2011). The eastern Warumpi region preserves Grenvillian age deformation with temperatures and pressures of 530-570°C and 3.5-4.5 kbar (Morrissey *et al.* 2011).
Alice Springs Orogeny	450-300 Ma	A long lived event with varying amounts of deformation spread across the Arunta Complex. Basin inversion in the Irindina province resulted in amphibolite facies shear zones being activated along the Strangways Complex rock unit (Ballèvre *et al.* 2000). There was increased deformation recorded along the Redbank and Delny Shear Zones associated with the exhumation of buried rock packages (Ballèvre *et al.* 2000) . Geophysical data shows that the Redbank shear zone causes a vertical offset of the Moho by 25 kilometres (Korsch *et al.* 1998). Large scale fluid flow is heavily associated with this orogenic event (Ballèvre *et al.* 2000).

In the Arunta Complex, the Chewings Orogeny resulted in regional high thermal gradient metamorphism in the Reynolds-Anmatijira Ranges (Hand & Buick 2001). Amphibolite metamorphism of this age is also recorded in the central western Warumpi Province (Table 1) (Scrimgeour *et al.* 2005b). At ca. 1130–1150 Ma the Warumpi and southernmost Aileron Province were reworked by regional E-W-trending isoclinal folds (Morrissey *et al.* 2011, Wong 2011) and crustal anatexis (Black & Shaw 1995, Sun *et al.* 1995, Claoué-Long & Hoatson 2005). This Grenvillian-aged reworking is synchronous with the long-lived Musgrave Orogeny (Smithies *et al.* 2011) and appears to be extensive and pervasive, recording a high thermal gradient associated with high pressure (6-10 kbars) and high temperature (775-830°C) metamorphism (Morrissey *et al.* 2011, Wong 2011).

Between ca. 400–300 Ma (Sandiford & Hand 1998, Haines *et al.* 2001) the Alice Springs Orogeny resulted in the exhumation of the Arunta Complex from beneath the Centralian Superbasin (Table 1).

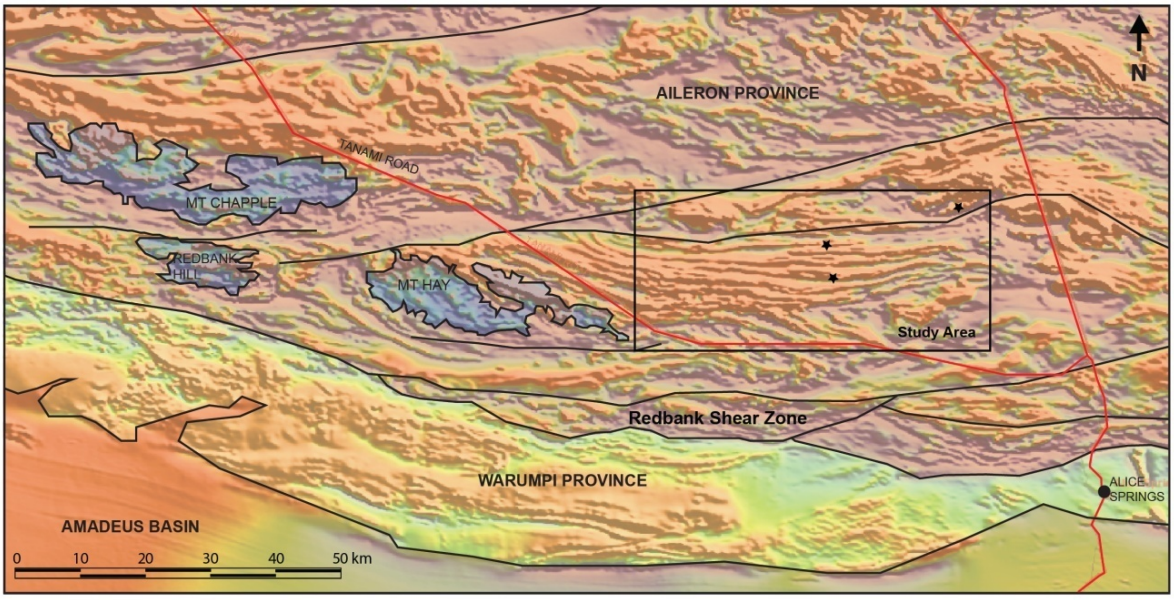

Figure 2- Location map overlain with TMI geophysical image. Mt Hay, Mt Chapple and Redbank Hill are highlighted. The boxed area indicates the EW trending geophysical belt which is the target of this study. The stars indicate sampling locations.

Study Area

The field area lies to the northeast of Alice Springs in the southern region of the Aileron Province (Figure 1, 2). The central southern part of the Aileron Province is only well exposed in the Mt Chapple, Mt Hay and Redbank Hill massifs and in the portion of hill country immediately north of the Charles River Thrust. These massifs comprise granulite facies meta-igneous rocks and subordinate metasedimentary (garnet-sillimanite-bearing) rocks. Elsewhere, outcrop of the southernmost Aileron Province is sparse. However, total magnetic intensity (TMI) geophysical imagery of the southernmost Aileron Province indicates large regions of 'straight belts' wrapping mega-scale boudins (Figure 2). Mt Chapple and Mt Hay are outcropping examples of mega-boudins. The 'straight' belts rarely outcrop. The Mt Chapple–Mt Hay region records at least three Proterozoic high-grade deformational events (Gage *et al.* 2011). Granites in the Mt Chapple area have emplacement ages of 1774–1771 Ma, corresponding to the Yambah Event (Claoué-Long & Hoatson 2005). Other locations in the Mt Chapple region preserve metamorphism dated at ca. 1725 Ma and ca. 1591 Ma which corresponds to the Strangways and the Chewings Events respectively (Claoué-Long & Hoatson 2005). Mt Chapple contains rare metasedimentary granulite facies rocks which record age-unconstrained peak metamorphic temperatures and pressures of 770 °C, 8.1 kbar and 680 °C, 7.3 kbar (Glikson 1984).

Mafic granulites and associated anorthosites that predominately comprise Mt Hay have an emplacement age of ca. 1803 Ma and an overprinting metamorphic age of ca. 1700 Ma (Claoué-Long & Hoatson 2005). Mount Hay records peak granulite facies metamorphism at temperatures and pressures of 770–875 °C and 6–9 kbar during the 1700 Ma metamorphic event (Harley *et al.* 1994, Bonamici *et al.* 2011).

Little is known about the age of protolith and fabrics in the 'straight belts' that wrap the mega-boudins. Sparse outcrops of a 'straight belt' are the focus of this study and comprise mostly migmatitic metasedimentary gneisses (garnet-sillimanite metapelite and garnet-biotite psammite) with lesser granitic gneiss (Table 1). The outcropping rocks in this study are classified as part of the Strangways Metamorphic Complex, specifically the Adla Granulite (Warren & Shaw 1995).

METAMORPHIC PETROLOGY

Table 2- Summary of sample location, rock type and analysis conducted in this study.

Sample	Location Easting (m)	(zone 53K) Southing (m)	Lithology	Type of analysis	Relative Location*
RBN-11	353106	7412191	Garnet-sillimanite metapelitic gneiss	U-Pb monazite + P-T pseudosection	North
RBN-12	352135	7412382	Garnet-sillimanite metapelitic gneiss	U-Pb monazite + garnet mapping	North
RBN-26	352186	7407423	Garnet-biotite granitic gneiss	U-Pb monazite	Central
RBN-28	351666	7408488	Garnet-sillimanite metapelitic gneiss	U-Pb monazite + garnet mapping	Central
RBN-31	351661	7408408	Garnet-biotite psammitic gneiss	U-Pb monazite	Central
RBN-34	367471	7417565	Granitic gneiss	U-Pb zircon	North east
RBN-45	352159	7412509	Garnet-bearing pegmatite	U-Pb monazite and zircon	North
RBN-46	352139	7412379	Garnet-biotite pegmatite	U-Pb monazite	North
RBN-47	352111	7412277	Garnet-bearing leucosome	U-Pb monazite	North

* With respect to northern and southern margins of EW straight belt visible on TMI aeromagnetic image.

Outcrop style

Samples for this study come from regions of outcrop that comprise the northern and central region of the 'straight belt' as well as immediately NE of the belt (Figure 2). Sample numbers, locations (UTM, WGS84) and brief descriptions are provided in Table 2. The northernmost outcrops sampled are dominated by migmatites, commonly with stromatic leucosomes. These outcrops preserve a strong planar fabric trending 090 and dipping steeply (>80°) to vertically, with a lineation plunging steeply to the east. Despite the intensity of the magnetic structural strike, the rocks are not mylonitic. Garnet-bearing mafic boudins are present within the outcrop, which are commonly

folded around gently east plunging axes. Stromatic leucosomes and pegmatites are common, with some pegmatites having a low angle discordance (300/90) to the main gneissic/migmatitic fabric. However, the pegmatites are foliated parallel to the gneissic fabric. The southernmost outcrops (labelled 'Central' in Table 2) have a well-defined, steeply dipping gneissic foliation trending approximately 075 to 090. The migmatitic fabric is locally folded around gentle open upright folds that plunge shallowly to the east. Northeast of the E-W 'straight belt' granitic gneisses contain folded mafic boundins with fold axes of 60→064. Kinematic indicators in the form of S-C fabrics were observed in only one outcrop which was protomylonitic and displayed south down movement on a steep south dipping fabric, associated with a steeply plunging lineation.

Petrography

ADLA GRANULITE METAPELITES (SAMPLES RBN-11, 12, 26, 28, 31)

Adla Granulite metapelitic samples contain garnet, sillimanite, quartz, plagioclase, K-feldspar and variable amounts of biotite (Figure 3). Accessory minerals include zircon, monazite and apatite. Anhedral garnet poikiloblasts (up to 1 cm in diameter) contain fibrous, unoriented sillimanite grains up to 2 mm in length, and prismatic biotite and quartz grains up to 1 mm in size. Garnet grains are highly fractured and biotite occurs within the fractures. Garnet grains are wrapped by a fabric defined by coarse-grained, prismatic sillimanite (up to 6 mm in length) and platy to tabular biotite (1–2 mm). Plagioclase (<1 mm) occurs in quartz and k-feldspar rich layers that alternate in the matrix with the garnet-sillimanite-rich layers. Quartz grains are 1–4 mm in size and are slightly elongate parallel to the fabric. Monazite and zircon occur as inclusions within

garnet, biotite and quartz, in the matrix and along grain boundaries. RBN 31 is an exception, with grain sizes of <1mm.

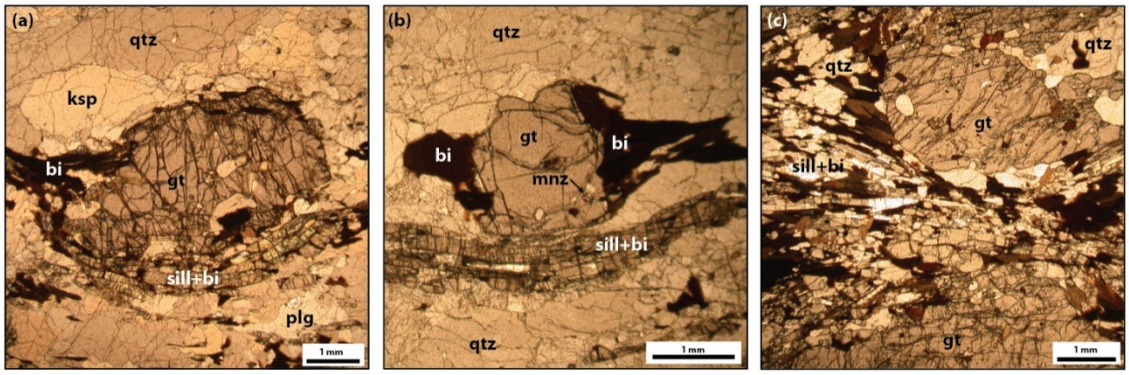

Figure 3- Photomicrographs of key petrological relationships: (a) RBN-11: garnet with inclusions of quartz, biotite and sillimante, being wrapped by a linear biotite/sillimanite foliation. (b) RBN-12: garnet with inclusions of monazite and biotite sitting above a biotite/sillimanite rich band. Biotite can also be seen elongated in the orientation of the fabric. (c) RBN-28: two garnet grains containing inclusions of quartz and biotite are separated by a biotite/sillimanite rich band which preserves a foliation.

UNNAMED GRANITE (SAMPLE RBN-34)

This sample contains quartz, K-feldspar, plagioclase and biotite. The rock contains a planar foliation which is weakly defined by platy biotite (<1mm) and elongated quartz grains (2-5mm). K-feldspar and plagioclase are intergrown with the quartz and biotite. The rock is homogenous in texture, with no mineralogical layering.

ADLA GRANULITE PEGMATITES (RBN-45, 46)

RBN-45 contains garnet, quartz, feldspar and small amounts of biotite. Garnet appears to occur with two distinct sizes; a smaller, more euhedral population (<5mm in diameter) and a larger-grained (up to 2 cm in diameter) population that has a more anhedral grain shape. Garnet contains inclusions of unorientated quartz and biotite. Elongate quartz and feldspar grains define the foliation in the sample (2–3 mm). Biotite-rich layers (2mm wide) can be found throughout the pegmatite, which are parallel to the foliation and wrap around the garnet grains.

RBN-46 is a pegmatite that has a low angle discordance. It contains quartz, K-feldspar, plagioclase and tourmaline. Platy biotite (3–4mm) can also be found on the outside of the pegmatite close to the wall rock. Tourmaline is euhedral with grains 1cm in size. Quartz and feldspar grains are coarse (1–2cm) and are not oriented in the centre of the pegmatite. Towards the outside of the pegmatite, the quartz, feldspar and biotite are weakly aligned with the gneissic fabric of the host metasedimentary rock.

ADLA GRANULITE LEUCOSOME (RBN-47)

This sample is a stromatic leucosome approximately 10 centimetres wide. It contains quartz, garnet, biotite and feldspar. Layers of quartz with inclusions of minor biotite define the fabric in the sample. Quartz is slightly elongate in the direction of the foliation and is up to 3mm in length. Garnet grains are euhedral, up to 1cm in size and contain inclusions of quartz and biotite. Minor amounts of platy biotite are present, with grains being between 1–2 mm in length.

METHODS

Bulk rock and mineral chemistry

Metamorphic phase diagrams were created using bulk rock chemical compositions obtained from Amdel Laboratories, Adelaide (Appendix C). Major element abundances were measured by fusing the crushed/powdered sample with lithium metaborate before dissolution and analysis using ICP–MS (Payne *et al.* 2010, Morrissey *et al.* 2011). REE abundances were measured by digesting the analytical pulp in HF solution before analysis using the ICP–MS.

Chemical analyses of minerals and elemental x-ray maps were obtained using a Cameca SX51 Electron Microprobe at the University of Adelaide. Elemental x-ray maps of garnet grains were undertaken for the following elements: Fe, Mg, Mn and Ca using WDS and EDS spectrometers. The operating conditions of the beam for x-ray maps were 100 nA and 20 kV and for elemental analysis were 20 nA and 15 kV.

Mineral Equilibria Modelling

P–T pseudosection calculations were run in Theriak-Domino (de Capitani & Petrakakis 2010) using the whole rock chemical composition (in mole% element). Theriak-Domino is a program that outputs a graphical pseudosection of mineral assemblage stability as a function of pressure and temperature. The calculation procedure is based on the minimisation of Gibbs Energy for a rock composition in a set chemical system at specified pressure and temperature nodes. The internally consistent dataset of Holland and Powell (1998; dataset tcds55 November 2003 update) was used for calculations in the geologically realistic chemical system NCKFMASHTO (Na_2O–CaO–K_2O–FeO–MgO–Al_2O_3–SiO_2–H_2O–TiO_2–Fe_2O_3). The modelling for this system uses the *a–x* relationships of (White *et al.* 2007) for silicate melt, garnet and biotite; (Coggan & Holland 2002) for muscovite; (White *et al.* 2002) for orthopyroxene, spinel and magnetite; (White *et al.* 2000) for ilmenite and hematite; (Holland & Powell 1998) for cordierite; (Holland & Powell 2003) for ternary plagioclase and ternary K-feldspar.

Geochronology

U-PB MONAZITE LA–ICP–MS GEOCHRONOLOGY

Single grain U-Pb monazite dating was undertaken using the LA–ICP–MS located at Adelaide Microscopy. The method used for dating monazite is outlined comprehensively in Payne *et al.* (2008). Monazite was separated from the bulk rock sample by routine crushing, sieving, panning, Frantz Isodynamic separation and heavy liquid separation. Monazite grains were mounted in epoxy resin to produce a grain mount. Monazite grains were imaged using backscatter electron (BSE) on a Phillips XL-20 scanning electron microscope (SEM). U-Pb isotope analyses were obtained by an Agilent 7500cx ICP–MS with an attached New Wave UP-213 laser ablation system. A 40 s gas blank was analysed prior to each 40 s measurement of monazite ablation. Prior to each ablation, the shutter remained closed while the laser was firing for 10 seconds to stabilise the beam. The beam diameter was 15 μm for the analyses. The isotopes ^{204}Pb, ^{206}Pb, ^{207}Pb and ^{238}Pb were measured with dwell times of 10, 15, 30 and 15 ms respectively. Monitoring of the ^{204}Pb isotope levels allowed for analyses with high common Pb to be recognised, as ^{204}Pb is a proxy for common Pb. Raw LA–ICP–MS data was processed using 'GLITTER', a data reduction program developed at Macquarie University, Sydney (Griffin et al. 2008). An internal monazite standard, MAdel, was used to correct for U-Pb fractionation (TIMS normalisation data: 207Pb/206Pb age= 491.0 ± 2.7 Ma; 206Pb/238U age= 518.37 ± 0.99 Ma; 207Pb/235U age= 513.13 ± 0.19 Ma: (Payne et al. 2008; updated with additional TIMS data)). The accuracy of data correction was monitored by repeated analysis of the in-house monazite standard 94-222/Bruna NW (ca. 450 Ma, Payne et al. 2008). Signals were examined carefully for anomalous portions of signal related to zones of Pb loss or gain

and the best portion of each ablation signal was selected for age and error determination. Common lead (proxied by ^{204}Pb) was not corrected for during data reduction; however, analyses were discarded if ^{204}Pb levels rose to levels high enough to compromise the integrity of the output age. Throughout the study, the weighted averages obtained for MAdel are ^{207}Pb/^{206}Pb= 490.7±5.5 Ma (*n*=121, MSWD=0.51), ^{206}Pb/^{238}U= 515.8±1.5 Ma (*n*=121, MSWD=0.33) and ^{207}Pb/^{235}Pb= 510.9±1.4 Ma (*n*=121, MSWD=0.48), and for 222: ^{207}Pb/^{206}Pb= 471±11 Ma (*n*=30, MSWD=0.99), ^{206}Pb/^{238}U= 448.6±2.8 Ma (*n*=30, MSWD=0.43) and ^{207}Pb/^{235}Pb= 451.5±2.6 Ma (*n*=30, MSWD=0.99).

U-PB ZIRCON LA–ICP–MS GEOCHRONOLOGY

Single grain zircon mounts were prepared in the same manner as the monazite mounts and were also dated using the LA–ICP–MS. For the comprehensive zircon dating method refer to the method outlined in Payne *et al.* (2006). Prior to LA–ICP–MS analysis all zircon grains were imaged using BSE and cathodoluminescence (CL) on a Phillips XL20, to determine the internal structure of the grains. Laser ablation was performed with a beam diameter of 30 μm for all samples and standards. Each analysis ran for 120 s with 30 s of background measurement before firing, 10 s of firing with the shutter closed and 80 s of sample ablation. The isotopes ^{204}Pb, ^{206}Pb, ^{207}Pb, ^{208}Pb, ^{232}Th and ^{238}Pb were measured with dwell times of 10, 15, 30, 10, 10 and 15 ms respectively. The external zircon standard GJ was used to correct for U-Pb fractionation (TIMS normalisation data: ^{207}Pb/^{206}Pb age= 607.7 ± 4.3 Ma; ^{206}Pb/^{238}U age= 600.7 ± 1.1 Ma; ^{207}Pb/^{235}U age= 602.0 ± 1.0 Ma: (Jackson et al. 2004)). The accuracy of data correction was monitored by repeated analysis of the internal zircon standard Plešovice (ID–TIMS normalisation data: ^{207}Pb/^{206}Pb age= 337.13 ± 0.37 Ma (Sláma et al. 2008)). Raw data

was reduced using 'GLITTER' and common lead was not corrected for as outlined above in the monazite methodology. Throughout the study, the weighted averages obtained for GJ are $^{207}Pb/^{206}Pb$= 608.3 ± 3.6 Ma (*n*=236, MSWD=0.39), $^{206}Pb/^{238}U$= 601.1 ± 1.8 Ma (*n*=236, MSWD=3.4) and $^{207}Pb/^{235}Pb$= 602.7 ± 1.6 Ma (*n*=236, MSWD=3.4), and for Plešovice: $^{207}Pb/^{206}Pb$= 344.8 ± 8.5 Ma (*n*=40, MSWD=0.87), $^{206}Pb/^{238}U$= 334.5 ± 1.8 Ma (*n*=40, MSWD=1.8) and $^{207}Pb/^{235}Pb$= 335.7 ± 1.8 Ma (*n*=40, MSWD=2.0).

Reduced monazite and zircon data were exported into Excel where conventional and weighted average concordia plots were generated using Isoplot v4.11 (Ludwig 2012). Ages quoted throughout this study are $^{207}Pb/^{206}Pb$ ages, with all errors stated in data tables and on concordia diagrams at the 1σ level. Concordancy was calculated using the ratio of $^{206}Pb/^{238}U$ age / $^{207}Pb/^{206}Pb$ age.

RESULTS

Geochronology

U-PB MONAZITE LA–ICP–MS GEOCHRONOLOGY

Grain mounted monazite LA–ICP–MS geochronology was conducted on samples RBN-11, 12, 26, 28, 31, 45, 46 and 47 (Tables 2 and 3). Monazite is abundant in all samples, and was identified in garnet, biotite and within the matrix. Monazites ranged in size from 100–400 μm, with monazite from samples RBN-12 and 31 showed slight zoning in BSE images (Figure 4b, 5a). The grains are rounded with a slight elongation, for more specific detail see Appendix D. The data is presented on U-Pb concordia plots and ages are presented as $^{207}Pb/^{206}Pb$ weighted averages, with the exception of RBN-11,

which is presented as an upper intercept age with the lower intercept age anchored to 1150 Ma.

Sample RBN-11

Seventy analyses were obtained from 35 individual unzoned monazite grains (Figure 4a). The analyses were plotted on a U-Pb concordia plot, and anchored to 1150 ± 10 Ma to correct for a disturbance caused by the 1150 Ma overprint/reworking. The upper intercept age was calculated to be 1743 ± 11 Ma (*n*=70, MSWD=1.3)

Sample RBN-12

Seventy analyses were obtained from 64 individual weakly zoned monazite grains (Figure 4b). Of these, two analyses were rejected due to high ^{204}Pb values. Multiple age populations within the data set are distinguishable on the concordia plot (Figure 4b). The ^{207}Pb/^{206}Pb weighted average age for the older population gives a mean of 1750 ± 6 Ma (*n*=57, MSWD=0.57). The younger population gives an age of 1593 ± 20 Ma (*n*=5, MSWD=1.13).

Sample RBN-26

Forty analyses were obtained from 40 individual unzoned monazite grains (Figure 4c). Of these, one analysis was rejected due to poor signal from the ICP–MS. The analyses were plotted on a U-Pb concordia plot (Figure 4c), and the ^{207}Pb/^{206}Pb weighted average age was calculated to be 1745 ± 6 Ma (*n*=39, MSWD=0.54). One outlier was not included in this calculation and has an age of 1642 ± 21 Ma.

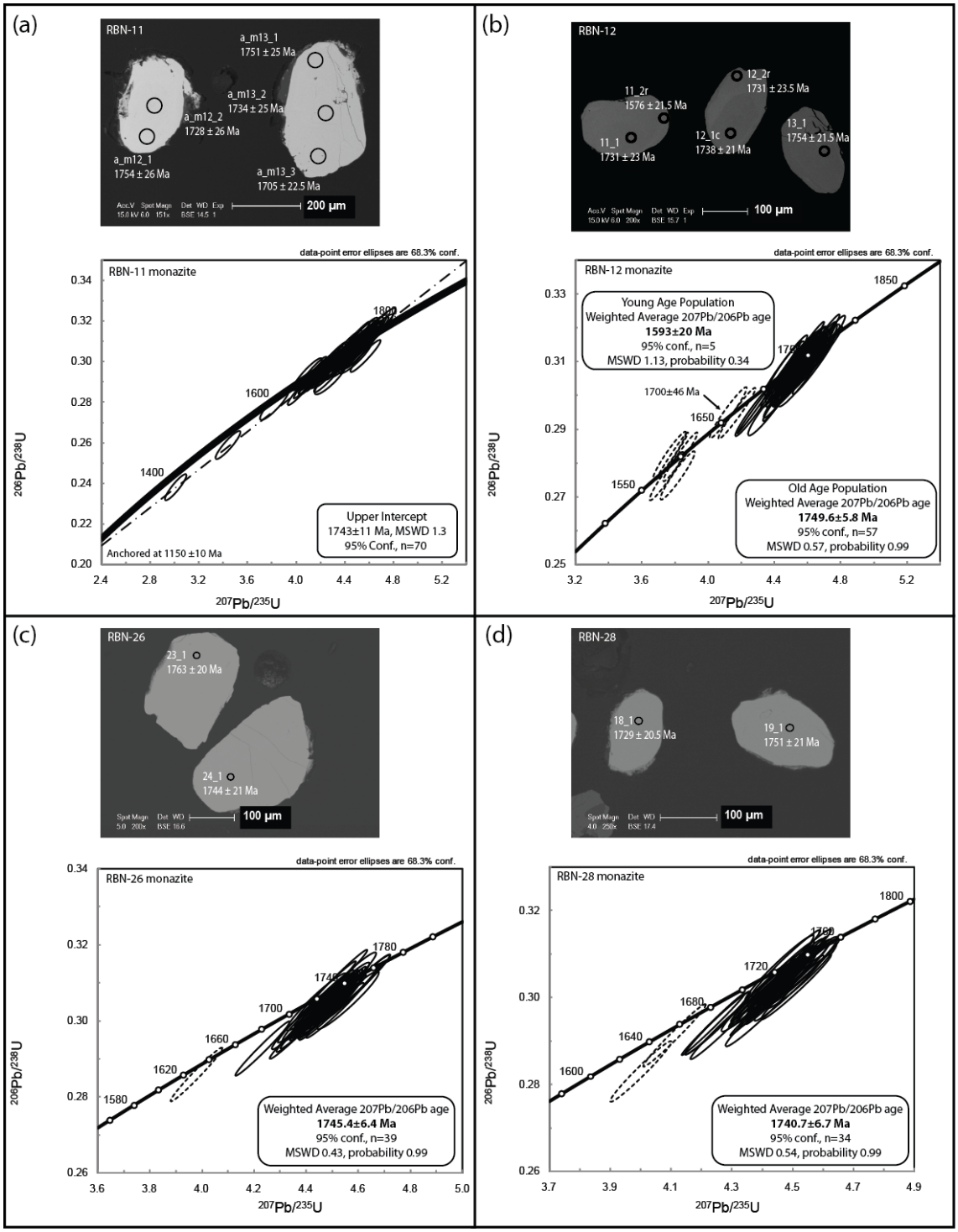

Figure 4- Concordia plots and representative BSE images showing the results of U-Pb monazite geochronology for samples analysed in this study. All the analyses were conducted on grain mounts of monazite separated from crushed rock using a 15 µm beam width as shown on the BSE images by the black circle. (a) sample RBN-11: One distinct population present, with an upper intercept age of 1743 ± 11 Ma (n=70). The lower intercept age was anchored to 1150 Ma to correct for disturbances in the data. No zoning present, grains are rounded and some contain large cracks. (b) sample RBN-12: two distinct age groupings are present with weighted average 207Pb/206Pb ages of 1593 ± 20 Ma (n=5) and 1750 ± 6 Ma (n=57), and a less well defined age grouping at ca. 1700 Ma (n=3). Elemental zonation present in monazite does not correspond to age differences. Younger ages correspond to edges of grains or broken segments. (c) sample RBN-26: one distinct age grouping present with a weighted average 207Pb/206Pb age of 1745 ± 6 Ma (n=39), and one outlier at ca. 1642 Ma. No zoning present, sub rounded to elongate grain shapes. (d) RBN-28: one distinct age grouping present with a weighted average 207Pb/206Pb age of 1741 ± 7 Ma (n=34), and a less well defined age grouping at ca. 1670 Ma (n=2). No zoning present, well-rounded grains, with younger ages found on smaller grains (100 µm).

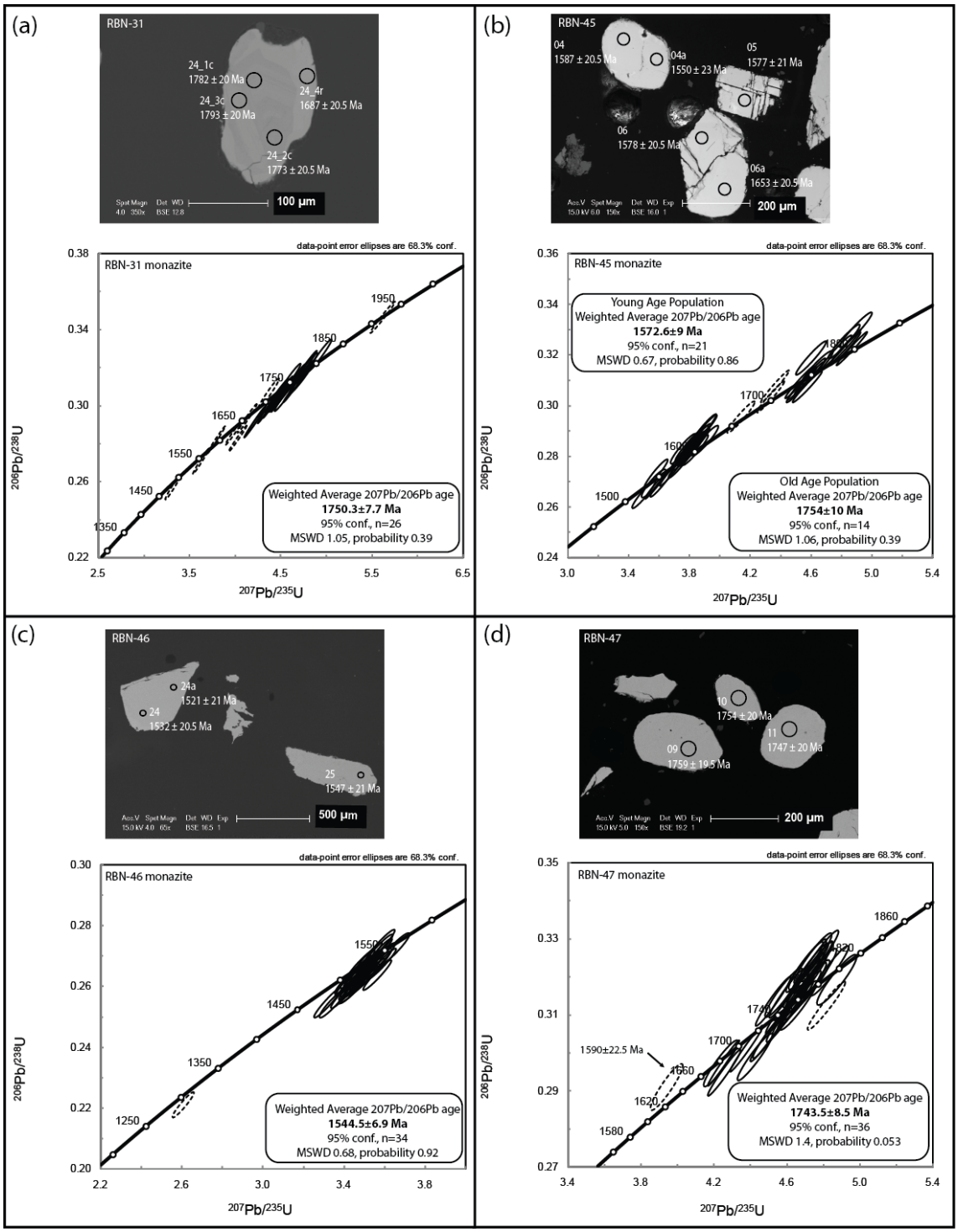

Figure 5- Concordia plots and representative BSE images showing the results of U-Pb monazite geochronology for samples analysed in this study. All the analyses were conducted on grain mounts of monazite separated from crushed rock , using a 15 µm beam width as shown on the BSE images with a black circle. (a) RBN-31: one distinct age grouping present with a weighted average 207Pb/206Pb age of 1750 ± 8 Ma (n=26), and a series of rims with no definitive population age younger than ca. 1750 Ma. Elemental zonation in this sample corresponds to clear core-rim age relationships, as shown. (b) RBN-45: two distinct age groupings are present with weighted average 207Pb/206Pb ages of ca. 1573 ± 9 Ma (n=21) and 1754 ± 10 Ma (n=14), and a less well defined age grouping at ca. 1674 Ma (n=3). No zoning, partial grains, very angular and fractured. The smaller, more rounded and less fractured grains represent the younger age population. (c) RBN-46: one distinct age grouping present with a weighted average 207Pb/206Pb age of 1545 ± 7 Ma (n=34), and one outlier at ca. 1328 Ma. No zoning present, large, angular grains showing fracturing. (d) RBN-47: one distinct age grouping present with a weighted average 207Pb/206Pb age of 1744 ± 9 Ma (n=36), and one outlier at ca. 1590 Ma. No zoning, grains are rounded and show no elongation.

Sample RBN-28

Forty analyses were obtained from 40 individual unzoned monazite grains (Figure 4d). Of these, four analyses were rejected due to the concordancy values lying outside the set ±5% range. The analyses were plotted on a U-Pb concordia plot (Figure 4d), and the $^{207}Pb/^{206}Pb$ weighted average age was calculated to be 1741 ± 7 Ma (*n*=34, MSWD=0.54). Two outliers were not included in this calculation and had ages of 1668 ± 20 Ma and 1672 ± 21 Ma.

SAMPLE RBN-31

Forty analyses were obtained from 33 individual zoned monazite grains (Figure 5a). Of these, six analyses were rejected due to the concordancy values lying outside the set ±5% range and a poor signal from the ICP–MS. Rim and core analyses were plotted on the same U-Pb concordia plot (Figure 5a), which showed one main population with a series of younger analyses corresponding to monazite rims. These rims were not used to calculate the $^{207}Pb/^{206}Pb$ weighted average age of the main population, which was calculated to be 1750 ± 8 Ma (*n*=26, MSWD=1.05). An older outlier, excluded from the weighted average age calculation, has an age of 1920 ± 20 Ma.

Sample RBN-45

Forty analyses were obtained from 23 individual unzoned monazite grains (Figure 5b). Of these, one analysis was rejected due to the concordancy values lying outside the set ±5% range. The analyses were plotted on a U-Pb concordia plot (Figure 5b), which showed multiple populations in the data set. The $^{207}Pb/^{206}Pb$ weighted average age of the older population is 1754 ± 10 Ma (*n*=14, MSWD=1.06). The younger population gave an age of 1573 ± 9 Ma (*n*=21, MSWD=0.67). There were three analyses that were

not included in either population and these gave an age of 1674 ± 23 Ma (MSWD=0.85).

Sample RBN-46

Forty analyses were obtained from 36 individual unzoned monazite grains (Figure 5c). Of these, five analyses were rejected due to the concordancy values lying outside the set ±5% range. The analyses were plotted on a U-Pb concordia plot (Figure 5c), and the $^{207}Pb/^{206}Pb$ weighted average age was calculated to be 1545 ± 7 Ma (*n*=34, MSWD=0.68). One outlier with an age of 1329 ± 21 Ma was excluded from this calculation.

Sample RBN-47

Forty analyses were obtained from 37 individual unzoned monazite grains (Figure 5d). Of these, four analyses were rejected due to the concordancy values lying outside the set ±5% range. The analyses were plotted on a U-Pb concordia plot (Figure 5d), and the $^{207}Pb/^{206}Pb$ weighted average age was calculated to be 1744 ± 9 Ma (*n*=36, MSWD=1.4). Two outliers with ages of 1590 ± 23 Ma and 1830 ± 20 Ma were excluded from the weighted average calculation.

U-PB ZIRCON LA–ICP–MS GEOCHRONOLOGY

Grain mounted zircon LA–ICP–MS was conducted on samples RBN-34 and 45 (Tables 2 and 3). Zircon is abundant in both samples. Zircons ranged in size from 100–400 μm and showed oscillatory zoning in CL images consistent with igneous morphology (Corfu *et al.* 2003). The grains appeared either euhedral with a slight elongation or rounding, for more specific detail see Appendix C.

Sample RBN-34

Fifty-eight analyses were obtained from 48 individual concentric oscillatory-zoned zircon grains (Figure 6a). Of these, twenty-two analyses were rejected due to high ^{204}Pb causing concordancy outside the set ±10% range. The analyses were plotted on a U-Pb concordia plot (Figure 6a), and the $^{207}Pb/^{206}Pb$ weighted average age was calculated to be 1641 ± 10 Ma (*n*=26, MSWD=0.61).

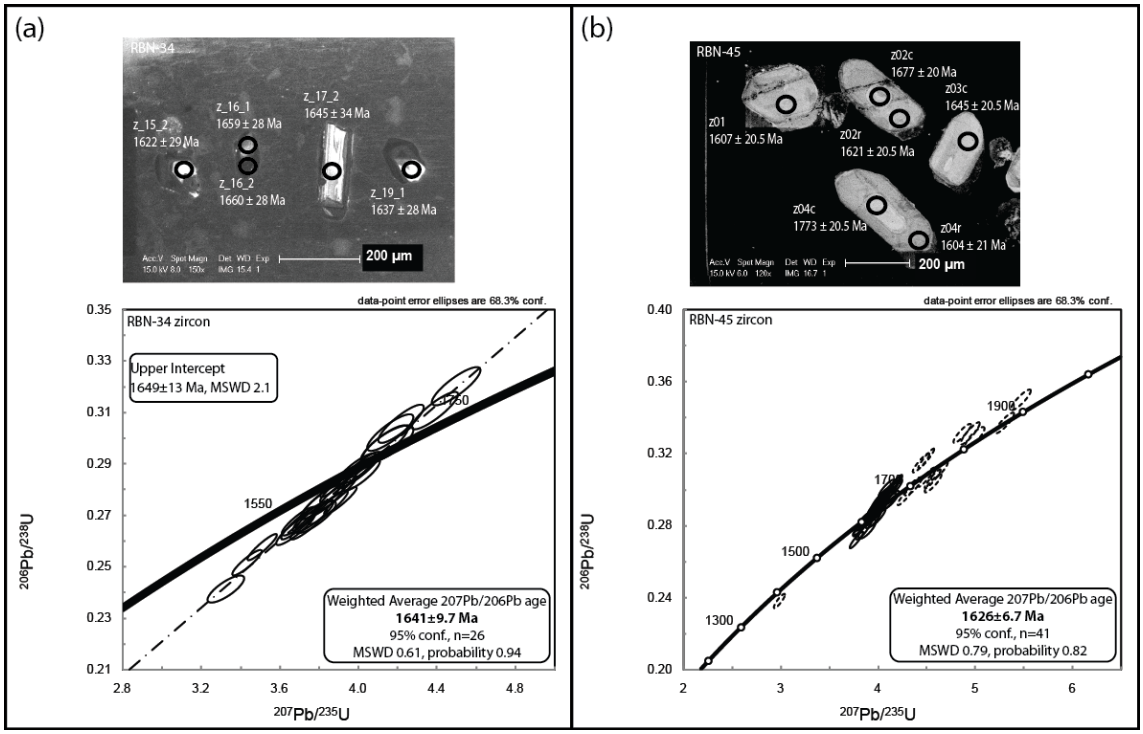

Figure 6- Concordia plots and representative CL images showing the results of U-Pb zircon geochronology for samples analysed in this study. All the analyses were conducted on grain mounts of zircons separated from crushed rock, using a 30 µm beam width as shown on the CL images with a black circle. (a) RBN-34: one distinct age group present with a weighted average 207Pb/206Pb age of 1641 ± 10 Ma (n=26). Grains are subhedral in shape and show concentric oscillatory zoning. (b) RBN-45: one distinct age population present with a weighted average 207Pb/206Pb age of 1626 ± 7 Ma (n=41). A number of spots from inherited grains were not included in the weighted average. One outlier was present with an age of 1446 Ma. Large euhedral grains (~300 µm) show minor oscillatory zoning, with the younger ages found on rims or more rounded grains.

Sample RBN-45

Sixty analyses were obtained from 38 individual weakly oscillatory-zoned zircon grains (Figure 6b). Of these, six analyses were rejected due to high ^{204}Pb causing concordancy

outside the set ±10% range. The analyses were plotted on a U-Pb concordia plot (Figure 6b), and the $^{207}Pb/^{206}Pb$ weighted average age was calculated to be 1627 ± 7 Ma (*n*=41, MSWD=0.79). Fifteen analyses were discounted from the population, with fourteen classed as inherited zircon (ages ranging ca. 1715-1870 Ma) and one outlier with an age of 1447 ± 23 Ma.

Pressure-Temperature conditions

A pressure-temperature pseudosection was calculated for the metapelitic sample RBN-11. The peak mineral assemblage observed within this migmatitic sample is garnet, sillimanite, biotite, quartz, plagioclase, K-feldspar and the presence of abundant migmatitic segregations suggests melt was present. Due to the absence of reaction microstructures, a retrograde path could not be established. The peak metamorphic conditions for this sample are constrained to the large biotite, garnet, sillimanite, K-feldspar, plagioclase, ilmanite, liquid and quartz field (Figure 7). This field occurs over the temperature and pressure range of 780-920°C and 5-10 kbars (Figure 7). This thermobarometric modelling is preliminary and aimed at providing a generalised picture of the thermobarometric regime. Detailed thermobarometric modelling is beyond the scope of the present work.

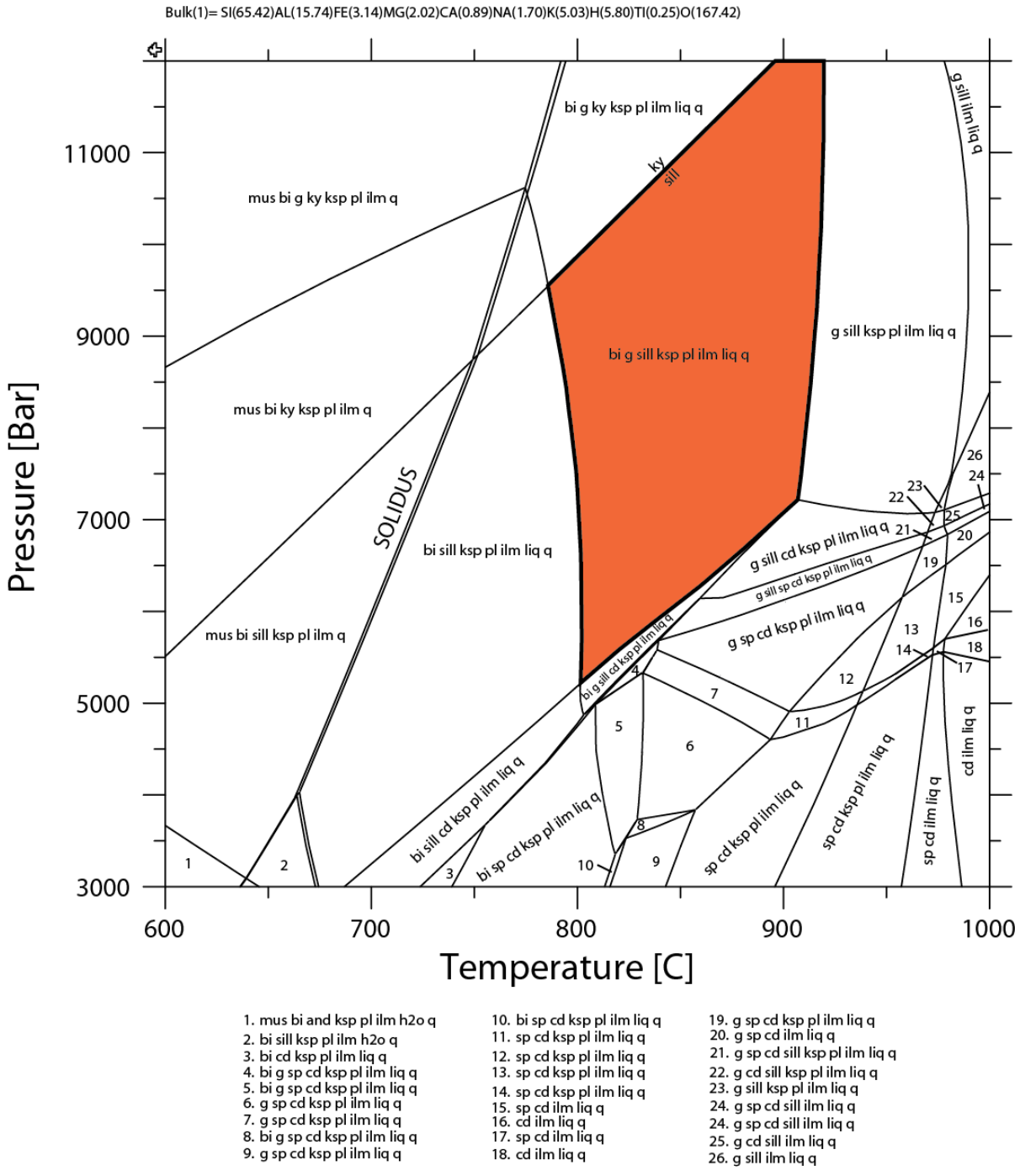

1. mus bi and ksp pl ilm h2o q
2. bi sill ksp pl ilm h2o q
3. bi cd ksp pl ilm liq q
4. bi g sp cd ksp pl ilm liq q
5. bi g sp cd ksp pl ilm liq q
6. g sp cd ksp pl ilm liq q
7. g sp cd ksp pl ilm liq q
8. bi g sp cd ksp pl ilm liq q
9. g sp cd ksp pl ilm liq q
10. bi sp cd ksp pl ilm liq q
11. sp cd ksp pl ilm liq q
12. sp cd ksp pl ilm liq q
13. sp cd ksp pl ilm liq q
14. sp cd ksp pl ilm liq q
15. sp cd ilm liq q
16. cd ilm liq q
17. sp cd ilm liq q
18. cd ilm liq q
19. g sp cd ksp pl ilm liq q
20. g sp cd ilm liq q
21. g sp cd sill ksp pl ilm liq q
22. g cd sill ksp pl ilm liq q
23. g sill ksp pl ilm liq q
24. g sp cd sill ilm liq q
24. g sp cd sill ilm liq q
25. g cd sill ilm liq q
26. g sill ilm liq q

Figure 7- Calculated *P-T* pseudosection for metapelitic sample RBN-11, from the northern area of the EW trending belt. The bulk composition is shown above the *P-T* section. The filled in field represents the peak temperature assemblage.

Mineral Chemistry

RBN-12

X-ray elemental maps of two garnet grains show no zoning of Fe, Mn or Mg (Figure 8). In the mapped area of the sample there is abundant biotite, plagioclase, sillimanite and quartz surrounding the central garnet grain. The apparent variation in Fe and Mg across the grains is caused by an error in sample mounting. Some local zoning to higher Ca content in the margins of garnet appears to occur primarily in proximity to plagioclase (white in the Ca map, Figure 8). However, Ca zoning does not always occur in garnet where garnet is in direct contact with plagioclase.

RBN-28

X-ray elemental maps of two garnet grains show zoning of all four elements Ca, Fe, Mg and Mn (Figure 9). In the mapped area of the sample there is abundant biotite, quartz, sillimanite and apatite surrounding the central garnet grain. Zoning in Ca is minor, with only slight local enrichment at the rim. In map RBN-28(2) (Figure, 9) there is minor local Fe enrichment in the rims of garnet. Mg zoning is obvious, with the garnet having lower Mg rims. Some of the Mg zoning post-dates fractures in garnet (see map RBN-28(2), Figure 9). Elevated Mn concentrations mimic zones of lower Mg.

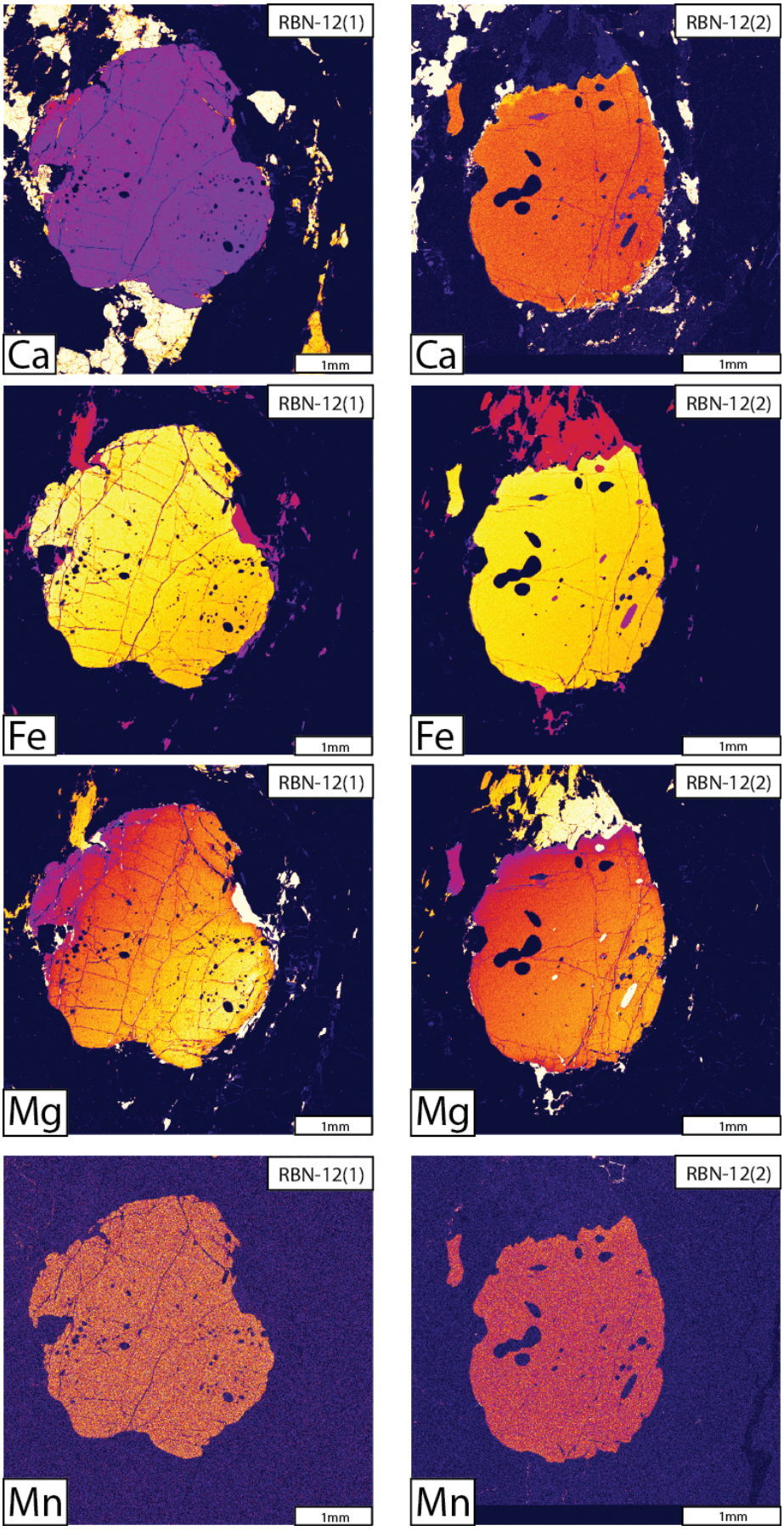

Figure 8- Microprobe-derived X-ray element maps for Ca, Fe, Mg and Mn for two garnet grains from sample RBN-12. White/yellow mineral in Ca maps is plagioclase. White/yellow mineral in Mg maps is biotite. Ca is the only element to show variation within garnet (Fe and Mg vary across grain due to sloping of the analytical surface).

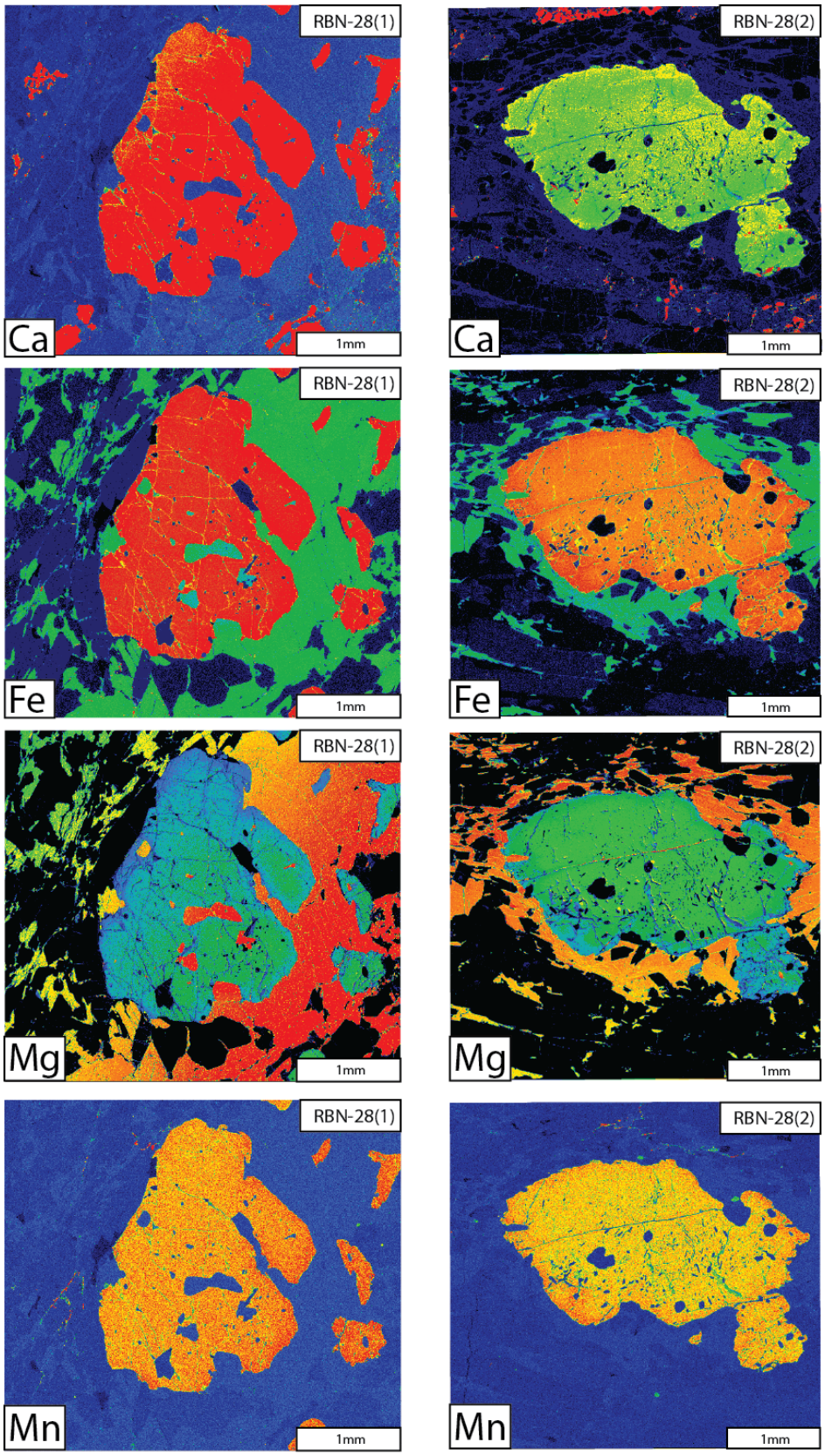

Figure 9- Microprobe-derived X-ray element maps for Ca, Fe, Mg and Mn for two garnet grains from sample RBN-28. These show zoning caused by the differences in the chemical concentration of the element analysed. Differences in colour within garnet reflect differences in concentration with warmer (redder) colours indicating higher concentration and cooler (purpler) colours indicating lower concentration. Small red mineral in Ca map for 28(2) is apatite; green mineral in Fe maps is biotite; blue mineral in Fe maps is sillimanite. Variation from green (left) to red (right) in biotite in 28(1) is due to sloping analytical surface.

DISCUSSION

The over-arching goal of this study is to define the age of fabric elements in a poorly outcropping but large (approximately 1120 km^2) EW-trending 'straight belt' that is clearly visible on aeromagnetic maps, occurring immediately north of the Redbank Deformed Zone and along strike from the mega-boudins of the Mt Chapple-Hay massifs. In trying to constrain the age of fabrics within this EW-trending belt, it is crucial to combine field outcrop data with U-Pb monazite and zircon geochronology.

U-Pb geochronology data

Table 3- Summary of U-Pb monazite and zircon geochronology results from all samples analysed in this study, listed in order of increasing age. The ages quoted are weighted average $^{207}Pb/^{206}Pb$ ages.

	Rock/sample type	**Monazite U-Pb age**	**Zircon U-Pb age**
RBN-46	Garnet-biotite pegmatite	1545 ± 7 Ma	
RBN-45	Garnet-bearing pegmatite	1573 ± 9 Ma	
RBN-12	Garnet-sillimanite metapelitic gneiss	1593 ± 20 Ma	
RBN-34	Granitic gneiss		1641 ± 10 Ma
RBN-45	Garnet-bearing pegmatite		1627 ± 7 Ma
RBN-28	Garnet-sillimanite metapelitic gneiss	1741 ± 7 Ma	
RBN-11	Garnet-sillimanite metapelitic gneiss	1743 ± 11 Ma	
RBN-47	Garnet-bearing leucosome	1744 ± 9 Ma	
RBN-26	Garnet-biotite granitic gneiss	1745 ± 6 Ma	
RBN-12	Garnet-sillimanite metapelitic gneiss	1750 ± 6 Ma	
RBN-31	Garnet-biotite psammitic gneiss	1750 ± 8 Ma	
RBN-45	Garnet-bearing pegmatite	1754 ± 10 Ma	

On the basis of all samples analysed for monazite U-Pb age data there are clearly two age clusters (Table 3). The older population ranges between 1750 and 1740 Ma and the younger ages range between ca. 1593 and 1544 Ma. Samples RBN-11, RBN-26, RBN-28, RBN-31 and RBN-47 all show a population in the range of 1750-1740 Ma, while RBN-46 shows a population between 1593 and 1544 Ma. Samples RBN-12 and RBN-45 record both populations. In contrast, zircon U-Pb age data (from two samples) is

distinct from the monazite geochronology. Zircon U-Pb ages define a grouping at ca. 1625 to 1640 Ma and thus do not overlap with monazite U-Pb ages.

The 1750−1740 Ma timeline recorded by monazite in this study is similar in age to the Inkamulla Event (Scrimgeour 2003, Betts & Giles 2006). The Inkamulla Event is poorly constrained and has thus far only been recognised as producing granitic and mafic magmatism in the Harts and Strangways Ranges in the southeastern Arunta Complex (Mortimer *et al.* 1987, Maidment *et al.* 2005). However, the prevalence of 1755−1740 Ma U-Pb monazite ages in gneissic metasediments and leucosomes in this study probably indicates that granulite grade metamorphism involving partial melting and regional-scale pervasive deformation occurred in the study area at the time of the Inkamulla event. Therefore this study is the first to document metamorphism and deformation during the Inkamulla Event time period.

Zircons analysed from a foliated granitic gneiss (RBN-34) located in the NE of the study area gave a weighted average age of 1641 ± 10 Ma, which is interpreted as the magmatic age. This sample appears to record relatively low strain, with large phenocrysts of K-feldspar only weakly aligned within a weak to moderately defined fabric. Moreover, the outcrop for this sample is located just north of the main EW-trending ‘straight belt’ (Figures 10 and 11) Because the interpreted magmatic age is younger than the Inkamulla-aged deformation within the “straight” belt to the south, the ENE trending deformational fabric in sample RBN-34 must be 1640 Ma or younger. This sample did not contain monazite or metamorphic rims on zircon, so it was not possible to conclusively date the age of the fabric within this sample.

Sample RBN-45 is a garnet-bearing pegmatite located in the northern part of the EW-trending ‘straight belt’ and is concordant with the gneissic fabric of the host rock.

The sample is located within several metres of metapelitic sample RBN-12 and planar pegmatite sample RBN-46. RBN-45 contains two monazite age populations, 1754 ± 10 and 1572 ± 9 Ma, and also a zircon age population of 1627 ± 7 Ma. This sample also contains older inherited zircon ages (n = 13) that are represented as cores in some of the zircons grains analysed. The unusual geochronological results from this sample, i.e. no overlap in monazite and zircon ages, may hold the key to understanding the age of the outcrop- and larger-scale fabric of the northern margin of the EW-trending straight belt. It is possible that the ca. 1754 Ma monazite grains were inherited from the host metasedimentary gneisses and due to their large size (50−300 μm; Figure 5b) and/or the possible saturation of REE's (and other monazite-forming components) in the pegmatitic melt (Kelsey *et al.* 2008). Neither recrystallisation nor substantial monazite dissolution occurred at ca. 1627 Ma, which corresponded to the timing of pegmatite crystallisation. This interpretation would imply that the pegmatite then underwent later deformation and metamorphism resulting in the recrystallisation of monazite around 1572 Ma. The lack of detectable (metamorphic) rim overgrowths on the zircon grains in this sample suggests there was no additional zircon growth after ca. 1627 Ma, which is not unexpected since there is no evidence that the pegmatite underwent renewed melting. Monazite ages of ca. 1572 Ma appear to involve either the growth of entirely new grains (50-200μm) and/or complete resetting of the older ca. 1754 Ma grains, as the younger ca. 1572 Ma monazite ages are not found as rims on ca. 1754 Ma monazite grains. The younger monazite population appears to be present in smaller, more rounded monazite grains, as opposed to the larger older grains.

A planar pegmatite (RBN-46) with a deformational fabric parallel to the gneissic foliation in the host gneiss (RBN-12) is oriented at a high angle to the gneissic layering

and has a monazite U-Pb age of 1544 ± 7 Ma. The fabric in the pegmatite is stronger at its diffuse margins, most likely reflecting intrusion late in a deforming system. The monazite age of ca. 1545 Ma inferred to date the pegmatite intrusion demonstrates that the rock system remained at elevated temperatures for a much longer period than is typically inferred for the Chewings Orogeny (Myers *et al.* 1996, Williams *et al.* 1996, Hand & Buick 2001, Rubatto *et al.* 2001, Betts & Giles 2006). However the age of ~1545 Ma overlaps with the timing of late monazite growth and partial melt crystallisation associated with the later stages of the Chewings Orogeny in the Reynolds Range (Morrissey pers. comm. 2012, Howlett 2012).

This is supported by the compositional maps for garnet in RBN-12 that show no zoning, suggesting any zoning that may have been present was annihilated by diffusional processes operating over a suitably lengthy time period.

Two distinct monazite age populations occur in two of the analysed samples, RBN-12 and RBN-45. The retention of radiogenic Pb monazite has been argued to be a function of grain size, cooling rate and other influences such as fluids and recrystallisation (Parrish 1990, Montel *et al.* 2000, Kelsey *et al.* 2003, Cherniak *et al.* 2004). However, if monazite grains are sufficiently large (approximately >50−100 μm) U-Pb growth ages can be preserved despite being subjected to temperatures in excess of 750−800 °C during later metamorphic events (Rubatto *et al.* 2001, Cherniak *et al.* 2004). This is especially the case if the subsequent events did not experience melting or fluid events. The grain size of monazite in samples RBN-12 and RBN-45 are 100−400 μm and 50−300 μm respectively. RBN-12 contains monazite grains with detectable zoning with BSE imaging, and the rims of monazite grains preserve a younger age. Younger ages are preserved in smaller monazite grains in sample RBN-45. Thus, grain size can be

argued to be a plausible explanation for the preservation of two monazite populations in a single sample.

Age of the outcrop- and larger-scale fabrics in study area

The spatial distribution of samples and their geochronological data is shown in Figures 10 and 11, and provides a foundation for attempting to constrain the age of the outcrop- and larger-scale fabrics in the study area. The most striking observation in Figure 10 is that samples preserving ages between ca. 1545–1595 Ma are restricted to the north of the EW 'straight belt', whereas the older ca. 1740–1755 Ma ages occur in the central and northern part of the EW 'straight belt'. A linear structure with a low TMI signal can be seen to truncate the northern margin of the EW-straight belt. This structure may well correspond to a Chewings Orogeny-aged (ca. 1545-1590 Ma) shear zone. The interpretation that the fabric is Chewings-aged is consistent with the interpretations that can be made from the geochronologically complex sample RBN-45. The overall interpretation of the age data from RBN-45 is that the outcrop-scale fabric is probably ca. 1570 Ma, reworking an older ca. 1750 Ma or composite 1750/1630 Ma fabric.

Samples from the central portion of the EW-straight belt only contain the ca. 1740–1755 Ma monazite ages, probably indicating the age of the regional and pervasive fabric of the EW-trending 'straight belt' is this age, corresponding to the Inkamulla Event timeline. This is the first documentation of regional deformation in the Arunta Complex with ages corresponding to the Inkamulla Event.

Table 4- Aileron Province Tectonic events

	Study	Sample Number	Type of Geochronology	Rock Type	Age
A	This study	RBN-46	Monazite	Pegmatite	1545±7 Ma
B	This study	RBN-45	Monazite Zircon Monazite	Pegmatite	1573±9 Ma 1627±7 Ma 1754±10 Ma
C	This study	RBN-12	Monazite	Adla Granulite	1593±20 Ma 1750±8 Ma
D	This study	RBN-11	Monazite	Adla Granulite	1743±11 Ma
E	This study	RBN-47	Monazite	Leucosome	1744±9 Ma
F	This study	RBN-28	Monazite	Adla Granulite	1741±7 Ma
G	This study	RBN-26	Monazite	Adla Granulite	1745±6 Ma
H	This study	RBN-31	Monazite	Adla Granulite	1750±8 Ma
I	This study	RBN-34	Zircon	Unnamed granite	1641±10 Ma
J	Smit (2012) (Unpublished data)	NAC-2011-016 NAC-2011-019 NAC-2011-033	Zircon	Maddens Yard Metamorphics (gneiss) Glen Helen Metamorphics (orthogneiss) Madderns Yard Metamorphics (microgranite)	1752±11 Ma 1640±6 Ma 1627±26 Ma
K	Anderson (2012) Preliminary results (unpublished data)	Hay_11_05a Hay_11_09a Hay_11_12	Monazite	Mt Hay Granulite	1750-1740 Ma 1600-1590 Ma 1790-1780 Ma 1750-1700 Ma 1600-1550 Ma
L	Wong (2011)	HAM2011-08	Zircon	Migmatitic Orthogneiss	1627±7 Ma
M	Fields (2012)	RBN-20 RBN-57 RBN-61 AS2012-1 AS2012-2	Zircon Zircon Zircon Monazite Zircon Zircon	Porphryoclastic granite Granitic gneiss Migmatitic Orthogneiss Granitic Gneiss Migmatitic orthgneiss	1626±7 Ma 1747±6 Ma 1739±9 Ma 1625±7 Ma 1633±9 Ma 1628±8 Ma

Rare open, upright folding observed in the central portion of the EW ‘straight belt’ could reflect the impact of the Chewings Orogeny, though there is no geochronology to support this. If the folding is later than the ca. 1740–1755 Ma tectonism, then the fabric in the straight belt is instead most probably a composite Inkamulla-Chewings fabric. One possible explanation for the strong striped pattern on the TMI image could be due to the folding of metasedimentary beds of differing magnetic susceptibilities. The northern outcrops preserve (rare) S-C fabrics with south-down kinematics, along a steeply plunging lineation. In its current (steep) orientation the kinematics indicate

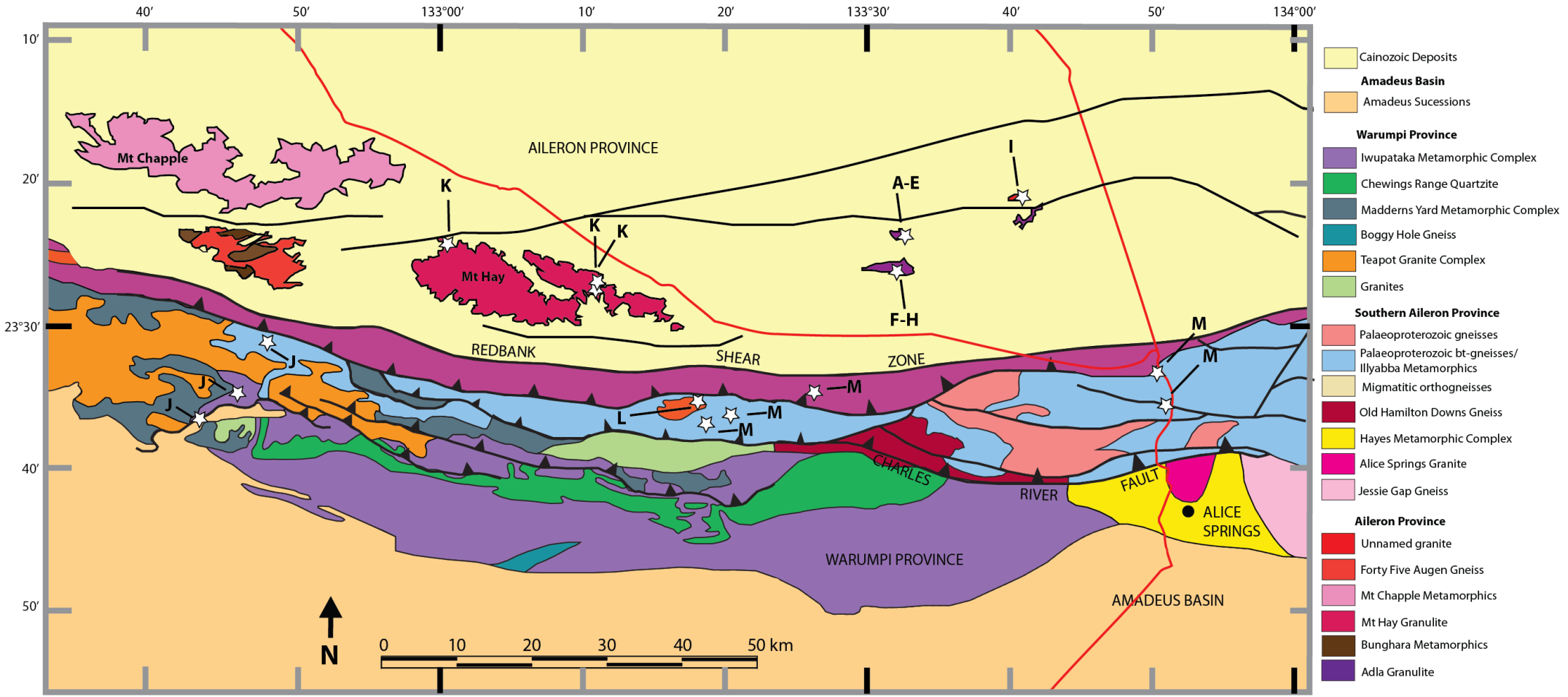

Figure 10- A simple geological map showing the Warumpi Province in relation to the southern Aileron Province outcrops (Mt Hay, Mt Chapple and Redbank Hill). White stars correspond to geochronological sample locations of this study and corresponding studies, with the letters indicating the corresponding sample from Table 4.

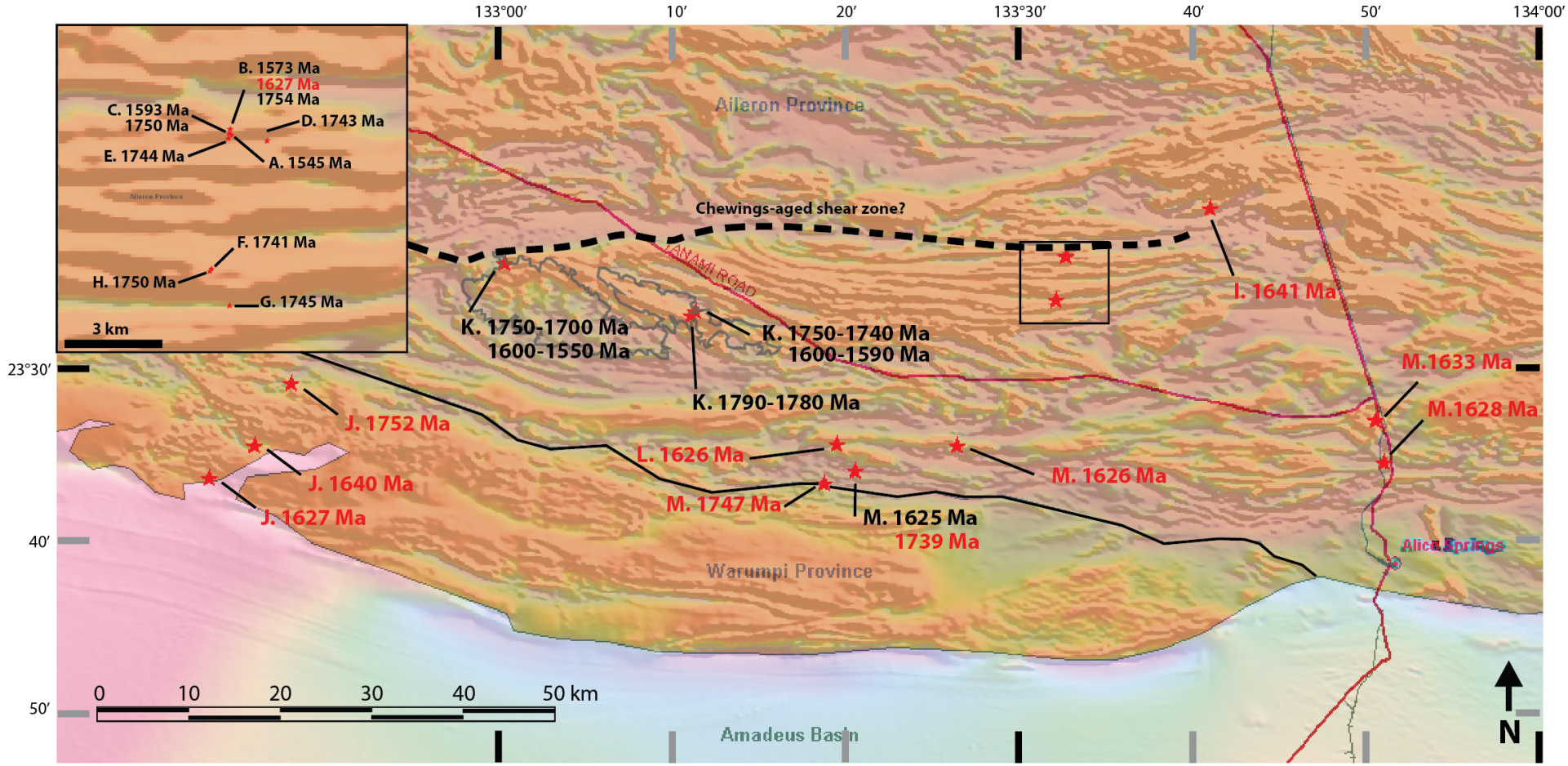

Figure 11- TMI aeromagnetic map of the southern Arunta Complex. The spatial distributions of geochronological results from this study are shown, as well as existing geochronology from the Hay-Chapple-Redbank Hill regions (Table 4). The red ages correspond to magmatic ages, while the black ages are metamorphic ages. (Anderson, pers. comm. 2012., Smit pers. comm. 2012., Fields, 2012).

an extensional zone, but given the steepness of the fabric it is difficult to definitively assign an extensional or contractional character to the fabric.

In an attempt to determine whether the Chewings- and Inkamulla-aged fabric domains have different petrological characteristics, thin sections of metapelitic gneisses RBN-12 (north) and RBN-28 (south) were assessed for mineralogy and microstructure, and in addition, x-ray element maps were collected for two garnet grains from each sample. The petrology of the samples show no obvious mineralogical differences between the samples (aside from the larger amount of biotite in sample RBN-28). The S-C fabrics in sample RBN-28 could not be seen at the scale of the thin section. Maps of garnet grains in sample RBN-12 indicate flat compositional profiles, suggesting that the thermal history was of long enough duration to annihilate any zoning that may have been present in garnet. There is also no indication of resorption of garnet since there is no evidence of elevated Mn at the margin of the garnet grains, which is a typical consequence of garnet resorption. In contrast, garnet grains in RBN-28 are zoned in all elements. Zoning to lower Mg and higher Mn at the rims/margins of the garnet grains is usually interpreted to reflect Fe-Mg compositional resetting with cooling (Fitzsimons & Harley 1994, Pattison & Begin 1994, Pattison & Bégin 2007) as well as resorption of garnet (presumably by biotite in this case) to explain the elevated Mn at the margins of garnet. This zoning was probably imprinted in the garnet grains during the ca. 1740–1755 Ma period since RBN-28 sample preserves only one monazite age population. It is curious that RBN-28 and not RBN-12 preserves zoning in garnet, since RBN-12 is interpreted to occur within a Chewings-aged reworking zone (reworking ca. 1740–1755 Ma fabrics). However a number of studies have shown that diffusion within minerals can be influenced by deformation (Worley *et al.* 1997, Van Orman *et al.* 2003), and

therefore it is possible that the Chewings deformation assisted in compositional modification of garnet.

Melting occurred at ca. 1625–1640 Ma, manifested as magmatism in the NE of the study area (sample RBN-34) and pegmatites in the northern part of the EW 'straight belt' (sample RBN-45). However, fabric development and the structural/tectonic significance of this timeline in the study area remains unclear.

Regional Implications

Existing geochronological data from the Mt Hay–Mt Chapple massifs encompasses timelines and events that do not correspond to the Inkamulla Event documented in this study. Magmatism in the Mt Chapple and Mt Hay regions occurred at ca. 1803 Ma (Stafford Event) and ca. 1774–1771 Ma (Yambah Event) (Claoue-Long & Hoatson, 2005), therefore predating the magmatism and deformation in this study. Tectonism (deformation, metamorphism) in the Chapple-Hay regions has been documented at ca. 1725, ca. 1700 (both Strangways Event) and ca. 1590 Ma (Claoué-Long & Hoatson 2005, Claoué-Long *et al.* 2008b) using U-Pb zircon geochronology, of which only the ca. 1590 Chewings Orogeny age corroborates with this study. No evidence of the Stafford or Yambah Events has been found in this study, with only a few LA–ICP–MS analyses showing ca. 1700 Ma (Strangways) ages. The proposed depositional age of the Adla Granulite metasediments (ca. 1820–1790 Ma; Black & Shaw 1992) does not assist in explaining the discrepancy in age 'matching'. Due to minimal zircon geochronology it is difficult to constrain a depositional age, or the effects of Yambah aged deformation/magmatism in this area, as it was not preserved in the monazite data.

The finding of Inkamulla-aged deformation and metamorphism in the EW 'straight belt' along strike of Mt Hay and Redbank Hill raises the possibility that Mt

Hay and Redbank Hill are mega-boudins wrapped by younger fabric with an Inkamulla Event age. If this interpretation is correct, the regional imprint/footprint of the Inkamulla Event is significantly increased. The Inkamulla Event timeline has only been defined by Scrimgeour (2003), based on the earlier work of Mortimer *et al.* (1987) and referenced in later works (Betts & Giles 2006, Betts *et al.* 2008).

Constraints on the thermal structure of the crust during the Inkamulla Event are provided by the *P–T* pseudosection for sample RBN-11 (Figure 7). The peak mineral assemblage containing garnet, sillimanite and biotite does not place tight constraints on the *P–T* conditions of metamorphism. However, using the location of the upper-left hand and lower right-hand boundaries of the peak assemblage field (Figure 7), conservative estimates on the apparent thermal gradient at the time of metamorphism are estimated to range between 32 and 55 °C km^{-1}. These values for the apparent thermal gradient are elevated (higher than normal) and therefore, simplistically, are suggestive of high heat flow (Hyndman *et al.* 2005, Brown 2007).

The regional footprint of Inkamulla-aged activity continues to be expanded by the finding of Inkamulla-aged magmatism in the vicinity of the Charles River Thrust and Redbank Shear Zone (Fields, 2012). Some of the Inkamulla-aged magmatism from Fields (2012) occurs south of the proposed boundary between the Aileron and Warumpi Province, which indicates that the Warumpi Province contains 'Aileron-type' magmatic rocks. The ca. 1635–1645 Ma timeline corresponding to the Liebig Orogeny has been documented in this study only in the form of magmatism and pegmatitic melting. The Liebig Orogeny is proposed as recording the subduction driven accretion of the exotic Warumpi Province with the southern margin of the Aileron Province within the NAC (Scrimgeour et al. 2005). One of the premises of this interpretation is that magmatic

rocks in the Warumpi and Aileron Province do not have common ages. Magmatism at ca. 1640 Ma is proposed by Close *et al.* (2003) and Scrimgeour *et al.* (2005b) to be restricted to the Warumpi Province. However, this study has demonstrated that ca. 1640 Ma magmatism occurs well within the Aileron Province (Table 4, Figure 10). In addition, ca. 1640 Ma magmatism has been documented from other locations in the Aileron Province (Claoué-Long & Hoatson 2005, Wong 2011, Fields 2012). Thus, it has been clearly demonstrated that Liebig-aged magmatism is not unique to the Warumpi Province. The presence of ca. 1640 Ma magmatism in the Aileron Province provides evidence to weaken the argument put forward by Scrimgeour et al. (2005) that the Warumpi Province is exotic to the Aileron Province. Additionally metasediments in the Warumpi Province contain detrital zircon populations that are similar to those in the Aileron Province. Wong (2011) suggested that the Warumpi Province may have been depositionally connected to the Aileron Province. Furthermore Thomas (2012) has shown that Warumpi aged granites in the Casey Inlier in the NE Amadeus basin have a similar crustal evolution to rocks belonging to the NAC. These lines of evidence point to the Warumpi Province as being lithospherically part of the Aileron Province.

The timeline of the Chewings Orogeny, ca. 1590–1570 Ma, has been documented throughout Proterozoic Australia (Neumann & Fraser 2007), where it is recognised as a compressional, possibly intracontinental event characterised by high geothermal gradient metamorphism (Betts & Giles 2006, Hand *et al.* 2007). In terms of the Arunta Complex, the Chewings Orogeny has long been thought to be a pervasive event causing extensive reworking without significant associated magmatism (Collins *et al.* 1995). However, whereas the Chewings Orogeny is well documented from the Reynolds Range in the central Arunta Complex (Hand & Buick 2001, Rubatto *et al.*

2001, Howlett 2012, Reid 2012), the Chewings Orogeny has been demonstrated to have had little effect in the southern Arunta Complex (Morrissey *et al.* 2011, Wong 2011). The absence of distinct Chewings-aged metamorphism in the central region of the EW-trending straight belt of this study tends to reinforce the findings of Morrissey *et al* (2011) and Wong (2011) that the Chewings Orogeny is not as pervasive in the southern Arunta Complex as has been previously believed. On the basis of the spatial distribution of Chewings-aged geochronology from this study, it appears that the impact of the Chewings Orogeny was variable and restricted to discrete (narrow) zones of reworking throughout the southern Arunta Complex (see Figure 11). This may account for the localised Chewings aged monazites found by Wong (2011) in granulites from the southernmost Aileron Province in the Colyer Creek region.

Grenvillian-aged tectonism has not been detected in the study area. Recent work by Morrissey *et al.* (2011), Wong (2011) and Fields (2012) has demonstrated that major EW-trending shear zones and large-scale isoclinal folds that control the outcrop pattern of the Warumpi Province are Grenvillian-aged, not Chewings-aged as had previously been assumed (Teyssier *et al.* 1988, Collins & Shaw 1995). Due to a lack of continuous outcrop in this study area, the relationship between the 1750-1580 Ma domain and the Redbank Shear Zone is obscure. However it appears that the Redbank Shear Zone represents the 'Grenville front'; the termination of Grenvillian-aged tectonism in the southern Arunta Complex. There is a consensus view that the Redbank Shear Zone represents a major crustal-scale feature, possibly even a suture (Scrimgeour *et al.* 2005b, Selway *et al.* 2009), given that it is known to have been reactivated during the Devonian-Carboniferous Alice Springs Orogeny, causing the Moho to be exhumed by

approximately 20 km (Teyssier 1985, Goleby *et al.* 1989, Korsch *et al.* 1998, Sandiford & Hand 1998).

The shared magmatic timelines of ca. 1640 Ma and ca. 1740-1755 Ma between the Warumpi and Aileron Province probably indicates that the Redbank Shear Zone does not represent a suture during these time periods. Whether or not the Redbank Shear Zone represents a younger, perhaps Grenvillian-aged suture, remains an open question. For this to be the case, extensional breakup of the southern NAC, and later reattachment during Grenvillian accretion (1200-1100 Ma) would be required. However, the Grenvillian reworking does appear to be characterised by high thermal gradient metamorphism (Morrissey *et al.* 2011), rather than by high-*P* metamorphism as might be expected for subduction-related tectonism.

There remains a number of unanswered questions about the tectonic setting and geodynamic significance of the southern margin of the Aileron Province, as well as the Warumpi Province, throughout the Paleo- and Meso-Proterozoic. The main reason for this continuing ambiguity is the fundamental issue of paucity of data from the southern Arunta Complex, despite the vast and often exceptional outcrop exposure. This project has set out to address this fundamental issue by collecting geochronological data that has been integrated with field structural observations, geophysical imagery, *P-T* data, mineral compositional data, published data and new data from concurrently running projects to shed more—and new—light on the tectonics of a part of the North Australian Craton that is held to be crucial to understanding the growth and assembly of the Australian continent during the Proterozoic.

CONCLUSIONS

1) Monazite U-Pb geochronology from metapelitic samples indicate a ca. 1740–1755 Ma aged fabric in a major regional EW-striking ‘straight belt’. This is the first documentation of Inkamulla-aged metamorphism in the Arunta Complex.

2) Monazite U-Pb geochronology indicates Chewings-aged reworking truncates the northern margin of the ‘straight belt’. The absence of Chewings-aged monazites in some samples indicates Chewings-aged deformation is not as pervasive as has been previously perceived.

3) Monazite U-Pb geochronology from a late pegmatite indicates the duration of Chewings-aged tectonism (and heat source) is significantly long-lived, on the order of ~60 Myr. This is much longer than has been documented for the Chewings Orogeny in other places such as the Reynolds Range.

4) Zircon U-Pb geochronology indicates the presence of ca. 1640 Ma magmatism in the Aileron Province, and ca. 1740-1750 Ma magmatism in the Warumpi Province. This weakens the argument that the Warumpi Province is exotic to the Aileron Province.

5) The finding of Inkamulla-aged tectonism in the southern Aileron Province begs the question of how regionally extensive is this deformation and metamorphism?

ACKNOWLEDGMENTS

I would like to thank my supervisors, David Kelsey, Martin Hand and Justin Payne for all their help, support and guidance this year. This project could not have been as successful without their unfaltering dedication. I would also like to thank the following PhD students; Jade Anderson, Alec Walsh, Kathleen Lane, Bonnie Henderson, Russell Smits and Laura Morrissey. Their help this year has been wonderful, especially their knowledge on all things theriac and isoplot. Many thanks to Katie Howard, who took the time to teach me how to use all the lab equipment I have needed this year. A very big thank-you to Ben Wade, Angus Netting and the staff at Adelaide Microscopy. Their technical support, guidance and patience has truly been invaluable. A big thanks to Brodie McBain and Claire Flint for their ongoing support and last minute proof-reading. Lastly I would like to thank the Centrals Group, Claire Thomas, Courtney Fields,

Mathew Reid and Daniel Howlett for their support and collaboration on our various projects, this year would not have been the same without them. This project was funded by ARC discovery project DP1095456 and ARC linkage project LP100200127.

REFERENCES

BALLÈVRE M., MÖLLER A. & HENSEN B. 2000. Exhumation of the lower crust during crustal shortening: an Alice Springs (380 Ma) age for a prograde amphibolite facies shear zone in the Strangways Metamorphic Complex (central Australia). *Journal of Metamorphic Geology* **18**, 737-747.

BETTS P., GILES D. & SCHAEFER B. F. 2008. Comparing 1800–1600Ma accretionary and basin processes in Australia and Laurentia: Possible geographic connections in Columbia. *Precambrian Research* **166**, 81-92.

BETTS P. G. & GILES D. 2006. The 1800–1100Ma tectonic evolution of Australia. *Precambrian Research* **144**, 92-125.

BLACK L. P. & SHAW R. D. 1995. An assessment, based on U□ Pb zircon data, of Rb□ Sr dating in the Arunta Inlier, central Australia. *Precambrian Research* **71**, 3-15.

BONAMICI C. E., TIKOFF B. & GOODWIN L. B. 2011. Anatomy of a 10 km scale sheath fold, Mount Hay ridge, Arunta Region, central Australia: The structural record of deep crustal flow. *Tectonics* **30**, TC6015.

BROWN M. 2007. Metamorphic conditions in orogenic belts: a record of secular change. *International Geology Review* **49**, 193-234.

BUICK I. S., HAND M., WILLIAMS I. S., MAWBY J., MILLER J. A. & NICOLL R. S. 2005. Detrital zircon provenance constraints on the evolution of the Harts Range Metamorphic Complex (central Australia): links to the Centralian Superbasin. *Journal of the Geological Society* **162**, 777-787.

CHERNIAK D., WATSON E. B., GROVE M. & HARRISON T. M. 2004. Pb diffusion in monazite: a combined RBS/SIMS study. *Geochimica et Cosmochimica Acta* **68**, 829-840.

CLAOUÉ-LONG J., EDGOOSE C. & WORDEN K. 2008a. A correlation of Aileron Province stratigraphy in central Australia. *Precambrian Research* **166**, 230-245.

CLAOUÉ-LONG J., MAIDMENT D., HUSSEY K. & HUSTON D. 2008b. The duration of the Strangways Event in central Australia: Evidence for prolonged deep crust processes. *Precambrian Research* **166**, 246-262.

CLAOUÉ-LONG J. C. & HOATSON D. M. 2005. Proterozoic mafic–ultramafic intrusions in the Arunta Region, central Australia: Part 2: Event chronology and regional correlations. *Precambrian Research* **142**, 134-158.

CLOSE D., SCRIMGEOUR I., EDGOOSE C., CROSS A., CLAOUÉ-LONG J., KINNY P. & MEIXNER T. 2003. Redefining the Warumpi Province. *Northern Territory Geological Survey Record* **1**, 1-3.

COGGAN R. & HOLLAND T. 2002. Mixing properties of phengitic micas and revised garnet–phengite thermometers. *J. Metamorph. Geol* **20**, 683-696.

COLLINS W., WILLIAMS I., SHAW S. & MCLAUGHLIN N. 1995. The age of the Ormiston Pound Granite: implications for Mesoproterozoic evolution of the Arunta Inlier, central Australia. *Precambrian Research* **71**, 91-105.

COLLINS W. J. & SHAW R. D. 1995. Geochronological constraints on orogenic events in the Arunta Inlier: a review. *Precambrian Research* **71**, 315-346.

COOPER J., MORTIMER G. & JAMES P. 1988. Rate of Arunta Inlier evolution at the eastern margin of the Entia Dome, central Australia. *Precambrian Research* **40**, 217-231.

CORFU F., HANCHAR J. M., HOSKIN P. W. O. & KINNY P. 2003. Atlas of zircon textures. *Reviews in Mineralogy and Geochemistry* **53**, 469-500.

DE CAPITANI C. & PETRAKAKIS K. 2010. The computation of equilibrium assemblage diagrams with Theriak/Domino software. *American Mineralogist* **95**, 1006-1016.

FIELDS C. E. 2012. Liebig-aged (ca. 1640 Ma) magmatism and metamorphism in ca. 1760 Ma crust in the Warumpi and Southern Aileron Province, Central Australia: A case for revising the tectonic framework of Proterozoic Australia. B.Sc (Honours) thesis, Geology and Geophysics, The University of Adelaide, Adelaide (unpubl.).

FITZSIMONS I. & HARLEY S. 1994. The influence of retrograde cation exchange on granulite PT estimates and a convergence technique for the recovery of peak metamorphic conditions. *Journal of Petrology* **35**, 543-576.

FODEN J., BUICK I. & MORTIMER G. 1988. The petrology and geochemistry of granitic gneisses from the East Arunta Inlier, central Australia: implications for Proterozoic crustal development. *Precambrian Research* **40**, 233-259.

GAGE J., GOODWIN L. & TIKOFF B. 2011. Metamorphism and deformation on western Mt Chapple, Arunta Region, central Australia: A record of multiple high-grade tectonic events. *Australian Journal of Earth Sciences* **58**, 273-284.

GLIKSON A. 1984. Granulite-gneiss terranes of the southwestern Arunta Block, central Australia: Glen Helen. *Narwietooma, and Anburla* **1**, 1984-1922.

GOLEBY B. R., SHAW R. D., WRIGHT C., KENNETT B. L. N. & LAMBECK K. 1989. Geophysical evidence for'thick-skinned' crustal deformation in central Australia. *Nature* **337**, 325-330.

HAINES P. W., HAND M. & SANDIFORD M. 2001. Palaeozoic synorogenic sedimentation in central and northern Australia: a review of distribution and timing with implications for the evolution of intracontinental orogens. *Australian Journal of Earth Sciences* **48**, 911-928.

HAND M. & BUICK I. 2001. Tectonic evolution of the Reynolds-Anmatjira Ranges: a case study in terrain reworking from the Arunta Inlier, central Australia. *Geological Society, London, Special Publications* **184**, 237-260.

HAND M., REID A. & JAGODZINSKI L. 2007. Tectonic framework and evolution of the Gawler craton, southern Australia. *Economic Geology* **102**, 1377-1395.

HARLEY S. L., FITZSIMONS I. C. W. & BUICK I. S. 1994. Reactions and textures in wollastonite-scapolite granulites and their significance for pressure-temperature-fluid histories of high-grade terranes. *Precambrian Research* **66**, 309-323.

HOATSON D., CLAOUÉ-LONG J. & SUN S. 2002. Event chronology and prospectivity of the mafic magmatic systems in the Arunta Province. *Northern Territory Geological Survey, Record* **3**.

HOLLAND T. & POWELL R. 1998. An internally consistent thermodynamic data set for phases of petrological interest. *Journal of Metamorphic Geology* **16**, 309-343.

HOLLAND T. & POWELL R. 2003. Activity–composition relations for phases in petrological calculations: an asymmetric multicomponent formulation. *Contributions to Mineralogy and Petrology* **145**, 492-501.

HOWLETT D. P. 2012. Geochronological constraints on Yambah and Chewings aged deformation at Mt Boothby in the south eastern Reynolds Range, central Australia. B. Sc (Honours) thesis, Geology and Geophysics, The University of Adelaide, Adelaide (unpubl.).

HYNDMAN R. D., CURRIE C. A. & MAZZOTTI S. P. 2005. Subduction zone backarcs, mobile belts, and orogenic heat. *GSA Today* **15**, 4-10.

KELSEY D. E., CLARK C. & HAND M. 2008. Thermobarometric modelling of zircon and monazite growth in melt-bearing systems: examples using model metapelitic and metapsammitic granulites. *Journal of Metamorphic Geology* **26**, 199-212.

KELSEY D. E., POWELL R., WILSON C. J. L. & STEELE D. 2003. (Th+ U)-Pb monazite ages from Al-Mg-rich metapelites, Rauer Group, east Antarctica. *Contributions to Mineralogy and Petrology* **146**, 326-340.

KORSCH R., GOLEBY B., LEVEN J. & DRUMMOND B. 1998. Crustal architecture of central Australia based on deep seismic reflection profiling. *Tectonophysics* **288**, 57-69.

LUDWIG K. R. 2012. *User's Manual for Isoplot 3.75* (Vol. Special Publication 5). Berkeley Geochronological Centre.

MAIDMENT D., HAND M. & WILLIAMS I. S. 2005. Tectonic cycles in the Strangways Metamorphic Complex, Arunta Inlier, central Australia: geochronological evidence for exhumation and basin formation between two high-grade metamorphic events*. *Australian Journal of Earth Sciences* **52**, 205-215.

MAWBY J., HAND M. & FODEN J. 1999. Sm-Nd evidence for high-grade Ordovician metamorphism in the Arunta Block, central Australia. *Journal of Metamorphic Geology* **17**, 653-668.

MONTEL J. M., KORNPROBST J. & VIELZEUF D. 2000. Preservation of old U-Th-Pb ages in shielded monazite: example from the Beni Bousera Hercynian kinzigites (Morocco). *Journal of Metamorphic Geology* **18**, 335-342.

MORRISSEY L., PAYNE J. L., KELSEY D. E. & HAND M. 2011. Grenvillian-aged reworking in the North Australian Craton, central Australia: Constraints from geochronology and modelled phase equilibria. *Precambrian Research*.

MORTIMER G., COOPER J. & JAMES P. 1987. U□ Pb and Rb□ Sr geochronology and geological evolution of the Harts Range ruby mine area of the Arunta Inlier, central Australia. *Lithos* **20**, 445-467.

MYERS J. S., SHAW R. D. & TYLER I. M. 1996. Tectonic evolution of Proterozoic Australia. *Tectonics* **15**, 1431-1446.

NEUMANN N. L. & FRASER G. L. 2007. *Geochronological synthesis and time-space plots for Proterozoic Australia*. Geoscience Australia.

PARRISH R. R. 1990. U-Pb dating of monazite and its application to geological problems. *Canadian Journal of Earth Sciences* **27**, 1431-1450.

PATTISON D. & BEGIN N. 1994. Hierarchy of closure temperatures in granulites and the importance of an intergranular exchange medium (melt?) in controlling maximum Fe-Mg exchange temperatures. *Mineralogical Magazine A* **58**, 694-695.

PATTISON D. & BÉGIN N. 2007. Zoning patterns in orthopyroxene and garnet in granulites: implications for geothermometry. *Journal of Metamorphic Geology* **12**, 387-410.

PAYNE J. L., BAROVICH K. M. & HAND M. 2006. Provenance of metasedimentary rocks in the northern Gawler Craton, Australia: Implications for Palaeoproterozoic reconstructions. *Precambrian Research* **148**, 275-291.

PAYNE J. L., FERRIS G., BAROVICH K. M. & HAND M. 2010. Pitfalls of classifying ancient magmatic suites with tectonic discrimination diagrams: An example from the Paleoproterozoic Tunkillia Suite, southern Australia. *Precambrian Research* **177**, 227-240.

PAYNE J. L., HAND M., BAROVICH K. M. & WADE B. P. 2008. Temporal constraints on the timing of high-grade metamorphism in the northern Gawler Craton: implications for assembly of the Australian Proterozoic. *Australian Journal of Earth Sciences* **55**, 623-640.

REID M. D. 2012. New constraints on Chewings-aged deformation and metamorphism of ca.≥ 1750 Ma crust in the Reynolds Range,central Australia. B.Sc (Honours) thesis, Geology and Geophysics, The University of Adelaide, Adelaide (unpubl.).

RUBATTO D., WILLIAMS I. S. & BUICK I. S. 2001. Zircon and monazite response to prograde metamorphism in the Reynolds Range, central Australia. *Contributions to Mineralogy and Petrology* **140**, 458-468.

SANDIFORD M. & HAND M. 1998. Controls on the locus of intraplate deformation in central Australia. *Earth and Planetary Science Letters* **162**, 97-110.

SCRIMGEOUR I., CLOSE D. & EDGOOSE C. 2005a. *Explanatory Notes, 1: 250 000 Geological Map Series, Mount Liebig SF52-16*. Northern Territory Geological Survey, Darwin.

SCRIMGEOUR I. R. 2003. Developing a revised framework for the Arunta Region. *Northern Territory Geological Survey Annual Geoscience Exploration Seminar (AGES) 2003 Record of Abstracts*.

SCRIMGEOUR I. R., KINNY P. D., CLOSE D. F. & EDGOOSE C. J. 2005b. High-*T* granulites and polymetamorphism in the southern Arunta Region, central Australia: Evidence for a 1.64 Ga accretional event. *Precambrian Research* **142**, 1-27.

SELWAY K., HAND M., HEINSON G. S. & PAYNE J. L. 2009. Magnetotelluric constraints on subduction polarity: Reversing reconstruction models for Proterozoic Australia. *Geology* **37**, 799-802.

SHAW R., STEWART A. & BLACK L. 1984. The Arunta Inlier: a complex ensialic mobile belt in central Australia. Part 2: tectonic history. *Australian Journal of Earth Sciences* **31**, 457-484.

SMITHIES R., HOWARD H. M., EVINS P., KIRKLAND C., KELSEY D. E., HAND M., WINGATE M., COLLINS A. S. & BELOUSOVA E. 2011. High-temperature granite magmatism, crust–mantle interaction and the Mesoproterozoic intracontinental evolution of the Musgrave Province, Central Australia. *Journal of Petrology* **52**, 931-958.

SUN S., WARREN R. & SHAW R. 1995. Nd isotope study of granites from the Arunta Inlier, central Australia: constraints on geological models and limitation of the method. *Precambrian Research* **71**, 301-314.

TEYSSIER C. 1985. A crustal thrust system in an intracratonic tectonic environment. *Journal of Structural Geology* **7**, 689-700.

TEYSSIER C., AMRI C. & HOBBS B. E. 1988. South Arunta Block: the internal zones of a Proterozoic overthrust in central Australia. *Precambrian Research* **40**, 157-173.

THOMAS C. M. 2012. Zircon Lu-Hf constraints on recently proposed models for the tectonic assembly of Proterozoic central Australia. B.Sc (Honours) thesis, Geology and Geophysics, The University of Adelaide, Adelaide (unpubl.).

VAN ORMAN J. A., FEI Y., HAURI E. H. & WANG J. 2003. Diffusion in MgO at high pressures: Constraints on deformation mechanisms and chemical transport at the core-mantle boundary. *Geophysical research letters* **30**, 1056.

WARREN R. & SHAW R. 1995. Hermannsburg Northern Territory 1: 250 000 Geological Series, Explanatory Notes SF53-13. *Northern Territory Geological Survey, Darwin*.

WHITE R., POWELL R. & CLARKE G. 2002. The interpretation of reaction textures in Fe-rich metapelitic granulites of the Musgrave Block, central Australia: constraints from mineral equilibria calculations in the system K2O–FeO–MgO–Al2O3–SiO2–H2O–TiO2–Fe2O3. *Journal of Metamorphic Geology* **20**, 41-55.

WHITE R., POWELL R. & HOLLAND T. 2007. Progress relating to calculation of partial melting equilibria for metapelites. *Journal of Metamorphic Geology* **25**, 511-527.

WHITE R., POWELL R., HOLLAND T. & WORLEY B. 2000. The effect of TiO~ 2 and Fe~ 2O~ 3 on metapelitic assemblages at greenschist and amphibolite facies conditions: mineral equilibria calculations in the system K~ 2O-FeO-MgO-Al~ 2O~ 3-SiO~ 2-H~ 2O-TiO~ 2-Fe~ 2O~ 3. *Journal of Metamorphic Geology* **18**, 497-512.

WILLIAMS I., BUICK I. & CARTWRIGHT I. 1996. An extended episode of early Mesoproterozoic metamorphic fluid flow in the Reynolds Range, central Australia*. *Journal of Metamorphic Geology* **14**, 29-47.

WONG B. 2011. Grenvillian-aged reworking of late Paleoproterozoic crust in the southern Ailerion Province, central Australia: implications for the assembly of Mesoproterozoic Australia. . B.Sc (Honours) thesis, Geology and Geophysics, The University of Adelaide, Adelaide (unpubl.).

WORLEY B., POWELL R. & WILSON C. J. L. 1997. Crenulation cleavage formation: Evolving diffusion, deformation and equilibration mechanisms with increasing metamorphic grade. *Journal of Structural Geology* **19**, 1121-1135.

YOUNG D., EDGOOSE C., BLAKE D. & SHAW R. 1995. Mount Doreen, Northern Territory. 1: 250 000 geological map series and explanatory notes, SF52-12. *Northern Territory Geological Survey, Darwin and Australian Geological Survey Organisation, Canberra*.

ZHAO J. & BENNETT V. C. 1995. SHRIMP U Pb zircon geochronology of granites in the Arunta Inlier, central Australia: implications for Proterozoic crustal evolution. *Precambrian Research* **71**, 17-43.

ZHAO J. X. & COOPER J. A. 1992. The Atnarpa Igneous Complex, southeast Arunta Inlier, central Australia: implications for subduction at an Early-Mid Proterozoic continental margin. *Precambrian Research* **56**, 227-253.

APPENDIX A: U-PB MONAZITE GEOCHRONOLOGY

APPENDIX B: U-PB ZIRCON GEOCHRONOLOGY

APPENDIX C: WHOLE ROCK GEOCHEMISTRY

APPENDIX D: MONAZITE AND ZIRCON MORPHOLOGY

APPENDIX E: MINERAL CHEMISTRY

*All of the above appendices have been attached in a separate document

APPENDIX A: U-PB MONAZITE GEOCHRONOLOGY

Analysis no.	$^{207}Pb/^{206}Pb$	1σ	$^{206}Pb/^{238}U$	1σ	$^{207}Pb/^{235}U$	1σ	Conc.	$^{207}Pb/^{206}Pb$ age	1σ	$^{206}Pb/^{238}U$ age	1σ	$^{207}Pb/^{235}U$ age	1σ	204 counts
Sample RBN-11														
11A_M01	4.53073	0.08047	0.30445	0.0052	4.53073	0.08047	97	1765.5	22.41	1713.3	25.7	1736.6	14.77	0
11A_M01_2	4.2414	0.07547	0.2943	0.00503	4.2414	0.07547	97	1706.8	22.46	1663	25.06	1682.1	14.62	8
11A_M01_3	4.56925	0.08266	0.30269	0.00521	4.56925	0.08266	95	1791.5	23.09	1704.7	25.78	1743.7	15.07	3
11A_M02_1	4.31932	0.07728	0.29788	0.00511	4.31932	0.07728	98	1718	22.51	1680.8	25.38	1697.1	14.75	3
11A_M02_2	4.47336	0.07966	0.30412	0.00523	4.47336	0.07966	98	1744.3	21.95	1711.7	25.83	1726	14.78	0
11A_M02_3	4.45727	0.08073	0.30541	0.00527	4.45727	0.08073	99	1729.9	22.83	1718.1	26.04	1723.1	15.02	0
11A_M03_1	4.21869	0.07753	0.29638	0.00514	4.21869	0.07753	99	1683.9	23.64	1673.4	25.56	1677.7	15.09	1
11A_M03_2	4.51483	0.0844	0.30457	0.00531	4.51483	0.0844	97	1758.5	24.12	1713.9	26.24	1733.7	15.54	6
11A_M04_1	4.51096	0.08604	0.30641	0.00538	4.51096	0.08604	99	1745.9	25.19	1723	26.55	1733	15.85	11
11A_M04_2	4.33959	0.08222	0.29914	0.00525	4.33959	0.08222	98	1718.9	24.81	1687.1	26.04	1700.9	15.63	0
11A_M05_1	4.26897	0.07977	0.29245	0.00516	4.26897	0.07977	96	1730.3	23.96	1653.8	25.73	1687.4	15.37	5
11A_M05_2	4.50084	0.08368	0.30619	0.0054	4.50084	0.08368	99	1743.1	23.54	1721.9	26.63	1731.1	15.45	0
11A_M05_3	4.66241	0.08745	0.31491	0.00556	4.66241	0.08745	100	1756.2	24.04	1764.8	27.24	1760.5	15.68	0
11A_M06_1	4.29707	0.07873	0.30154	0.00529	4.29707	0.07873	101	1686.1	22.84	1698.9	26.19	1692.8	15.09	6
11A_M06_2	4.27088	0.08008	0.29944	0.00528	4.27088	0.08008	100	1687.7	24.08	1688.5	26.2	1687.8	15.43	3
11A_M06_3	4.28438	0.07987	0.30062	0.00529	4.28438	0.07987	100	1686.2	23.7	1694.4	26.22	1690.4	15.35	4
11A_M07_1	4.21283	0.08125	0.29525	0.00524	4.21283	0.08125	99	1688.5	25.55	1667.7	26.08	1676.5	15.83	0
11A_M07_2	4.42386	0.08748	0.30322	0.00541	4.42386	0.08748	99	1729.3	26.74	1707.3	26.76	1716.8	16.38	12
11A_M08_1	4.57792	0.08833	0.31158	0.00552	4.57792	0.08833	100	1742.3	25.23	1748.5	27.13	1745.3	16.08	4
11A_M08_2	4.61156	0.0888	0.31449	0.00557	4.61156	0.0888	101	1738.7	25.16	1762.8	27.3	1751.4	16.07	0
11A_M08_3	4.28004	0.07924	0.2953	0.00523	4.28004	0.07924	97	1717.3	22.94	1668	26.02	1689.5	15.24	6
11A_M08_4	4.51497	0.08276	0.30765	0.00544	4.51497	0.08276	99	1740.1	22.45	1729.2	26.81	1733.7	15.24	2
11A_M09_1	4.52797	0.08576	0.30993	0.00553	4.52797	0.08576	100	1731.9	24.28	1740.4	27.2	1736.1	15.75	3
11A_M09_2	4.43914	0.08392	0.30476	0.00543	4.43914	0.08392	99	1726.4	24.01	1714.9	26.84	1719.7	15.67	6
11A_M10_1	4.29928	0.08306	0.2992	0.00537	4.29928	0.08306	99	1701.4	25.24	1687.3	26.64	1693.2	15.91	9
11A_M10_2	4.55725	0.08895	0.31017	0.00558	4.55725	0.08895	100	1742.3	25.55	1741.5	27.46	1741.5	16.25	3
11A_M10_3	4.5595	0.08836	0.30891	0.00555	4.5595	0.08836	99	1750.7	25.1	1735.3	27.33	1741.9	16.14	5
11A_M11_1	3.82374	0.07715	0.27857	0.00505	3.82374	0.07715	98	1616.7	27.85	1584.1	25.47	1597.8	16.24	7
11A_M12_1	4.49369	0.08868	0.30381	0.00548	4.49369	0.08868	97	1754.5	26.05	1710.2	27.11	1729.8	16.39	0
11A_M12_2	4.39247	0.08665	0.30133	0.00543	4.39247	0.08665	98	1727.9	26.08	1697.9	26.9	1710.9	16.32	3
11A_M13_1	4.62812	0.08676	0.31355	0.00563	4.62812	0.08676	100	1750.9	23.47	1758.1	27.61	1754.4	15.65	5
11A_M13_2	4.58394	0.08782	0.31349	0.00565	4.58394	0.08782	101	1733.6	24.86	1757.9	27.72	1746.4	15.97	0
11A_M13_3	4.48063	0.08248	0.31118	0.00554	4.48063	0.08248	102	1705.4	22.7	1746.5	27.23	1727.4	15.28	3
11A_M14_1	4.47039	0.08495	0.30799	0.00552	4.47039	0.08495	101	1720.1	24.51	1730.8	27.19	1725.5	15.77	0
11A_M14_2	4.36752	0.08077	0.29913	0.00532	4.36752	0.08077	97	1730.9	23.04	1687	26.38	1706.2	15.28	2
11A_M15_1	4.43048	0.08577	0.30442	0.00547	4.43048	0.08577	99	1725	25.57	1713.2	27.05	1718.1	16.04	1

11A_M15_2	4.49611	0.08873	0.30563	0.0055	4.49611	0.08873	99	1744.7	26.51	1719.2	27.15	1730.3	16.39	0
11A_M15_3	4.44392	0.08668	0.30587	0.00549	4.44392	0.08668	100	1721.9	26.24	1720.4	27.09	1720.6	16.17	0
11A_M16_1	3.01035	0.05922	0.23797	0.00426	3.01035	0.05922	94	1463.2	27.51	1376.1	22.19	1410.2	14.99	0
11A_M16_2	3.43976	0.06744	0.25875	0.00463	3.43976	0.06744	95	1557	26.95	1483.4	23.69	1513.5	15.42	7
11A_M17_1	4.13602	0.07743	0.29435	0.00521	4.13602	0.07743	100	1660.2	24.26	1663.2	25.94	1661.4	15.31	0
11A_M17_2	4.14153	0.07741	0.29129	0.00517	4.14153	0.07741	98	1682.1	23.95	1648	25.8	1662.5	15.29	9
11A_M17_3	4.13872	0.07715	0.29159	0.00516	4.13872	0.07715	98	1678.9	23.93	1649.5	25.74	1662	15.24	1
11A_M18_1	4.35147	0.08131	0.30165	0.00532	4.35147	0.08131	99	1708.7	24.18	1699.5	26.37	1703.2	15.43	7
11A_M18_2	4.55226	0.08879	0.30903	0.00551	4.55226	0.08879	99	1747.1	26.14	1735.9	27.14	1740.6	16.24	8
11A_M19_1	4.43878	0.08663	0.30435	0.00543	4.43878	0.08663	99	1728.8	26.43	1712.9	26.83	1719.6	16.17	0
11A_M19_2	4.51077	0.08905	0.30901	0.00553	4.51077	0.08905	100	1730.5	26.8	1735.8	27.23	1733	16.41	0
11A_M19_3	4.47579	0.087	0.30402	0.00541	4.47579	0.087	98	1746	25.92	1711.2	26.72	1726.5	16.13	0
11A_M20_1	4.48717	0.08938	0.30217	0.00541	4.48717	0.08938	97	1761.8	27.28	1702	26.76	1728.6	16.54	6
11A_M20_2	4.28438	0.0864	0.29156	0.00519	4.28438	0.0864	95	1742.7	28.54	1649.3	25.91	1690.4	16.6	2
11A_M20_3	4.41994	0.0846	0.30062	0.00536	4.41994	0.0846	97	1743.6	25.11	1694.4	26.59	1716.1	15.85	13
11A_M21_1	4.09705	0.07474	0.28937	0.0051	4.09705	0.07474	98	1674.2	22.66	1638.4	25.5	1653.7	14.89	0
11A_M21_2	4.18912	0.07756	0.29274	0.00519	4.18912	0.07756	98	1693.8	23.22	1655.2	25.87	1671.9	15.18	14
11A_M21_3	4.04511	0.0759	0.28603	0.0051	4.04511	0.0759	97	1672.1	23.77	1621.7	25.54	1643.3	15.28	5
11A_M22_1	4.23616	0.08053	0.29623	0.0053	4.23616	0.08053	99	1692.7	24.29	1672.6	26.34	1681.1	15.62	2
11A_M23_1	4.20857	0.08098	0.29625	0.00532	4.20857	0.08098	100	1680.4	25	1672.7	26.44	1675.7	15.79	0
11A_M24_1	4.49239	0.08722	0.30587	0.0055	4.49239	0.08722	99	1741.6	25.28	1720.3	27.16	1729.6	16.13	0
11A_M24_2	4.53087	0.08955	0.3106	0.00562	4.53087	0.08955	101	1729.2	26.15	1743.6	27.63	1736.7	16.44	11
11A_M25_1	4.52727	0.09074	0.31161	0.00565	4.52727	0.09074	102	1721.7	27.12	1748.6	27.79	1736	16.67	7
11A_M25_2	4.58184	0.09365	0.31182	0.00569	4.58184	0.09365	100	1742.5	27.85	1749.6	27.97	1746	17.03	7
11A_M26_1	4.5309	0.08606	0.30878	0.00558	4.5309	0.08606	100	1739.9	24.02	1734.7	27.51	1736.7	15.8	17
11A_M27_1	4.5695	0.08764	0.31051	0.00563	4.5695	0.08764	100	1745.2	24.41	1743.2	27.68	1743.7	15.98	0
11A_M28_1	4.149	0.07777	0.29386	0.00529	4.149	0.07777	100	1669	23.38	1660.8	26.37	1664	15.34	0
11A_M29_1	4.42428	0.08229	0.30461	0.00547	4.42428	0.08229	100	1721.2	23.12	1714.1	27.05	1716.9	15.4	3
11A_M30_1	4.41139	0.08515	0.30673	0.00556	4.41139	0.08515	101	1703.1	25.4	1724.6	27.41	1714.5	15.98	0
11A_M31_1	4.4248	0.08618	0.30344	0.0055	4.4248	0.08618	99	1728.5	25.77	1708.4	27.21	1717	16.13	0
11A_M32_1	4.54276	0.08801	0.31292	0.00567	4.54276	0.08801	102	1720.3	25.42	1755.1	27.83	1738.8	16.12	1
11A_M33_1	4.19966	0.08071	0.29504	0.00533	4.19966	0.08071	99	1684	25.13	1666.7	26.51	1674	15.76	9
11A_M34_1	4.67773	0.09097	0.31741	0.00574	4.67773	0.09097	102	1747.9	25.16	1777.1	28.07	1763.3	16.27	2
11A_M35_1	4.09163	0.07998	0.29366	0.00532	4.09163	0.07998	101	1644.5	26.22	1659.8	26.49	1652.6	15.95	0
Sample RBN-12														
12_M02_1	4.45042	0.07336	0.30865	0.00503	4.45042	0.07336	102	1707.8	21.28	1734.1	24.78	1721.8	13.67	0
12_M04_1	4.58491	0.07611	0.3139	0.00513	4.58491	0.07611	102	1731.8	21.29	1759.9	25.18	1746.5	13.84	14
12_M05_1	4.45583	0.07373	0.30637	0.005	4.45583	0.07373	100	1723.8	20.95	1722.8	24.68	1722.8	13.72	15
12_M06_1	4.6042	0.07725	0.31021	0.00509	4.6042	0.07725	99	1761.1	21.33	1741.8	25.02	1750	14	0
12_M07_1	3.76887	0.06512	0.28219	0.00466	3.76887	0.06512	102	1565.6	23.45	1602.4	23.42	1586.1	13.86	15
12_M08_1	4.65444	0.07931	0.31396	0.00517	4.65444	0.07931	100	1759	21.9	1760.2	25.36	1759.1	14.24	3

12_M09_1	4.52761	0.07807	0.30912	0.00512	4.52761	0.07807	100	1737.2	22.33	1736.4	25.19	1736.1	14.34	10
12_M10_1	4.54195	0.07816	0.30842	0.0051	4.54195	0.07816	99	1746.9	22.29	1732.9	25.13	1738.7	14.32	0
12_M11_1	4.48523	0.07882	0.30721	0.00516	4.48523	0.07882	100	1730.6	23.24	1727	25.44	1728.2	14.59	7
12_M11_2R	3.78587	0.06357	0.28193	0.00468	3.78587	0.06357	102	1575.6	21.48	1601.1	23.53	1589.8	13.49	0
12_M12_1C	4.56748	0.07622	0.31145	0.00516	4.56748	0.07622	101	1738.9	20.83	1747.8	25.38	1743.4	13.9	16
12_M12_2R	4.52244	0.08031	0.30966	0.00522	4.52244	0.08031	100	1731.2	23.57	1739.1	25.68	1735.1	14.77	0
12_M13_1	4.67441	0.07955	0.31601	0.00527	4.67441	0.07955	101	1754.7	21.35	1770.2	25.82	1762.7	14.24	0
12_M14_1C	4.54995	0.07929	0.30768	0.00515	4.54995	0.07929	99	1754.2	22.71	1729.3	25.4	1740.2	14.51	0
12_M14_2R	4.81921	0.08319	0.31248	0.00521	4.81921	0.08319	96	1830.8	22.1	1752.9	25.6	1788.3	14.51	33
12_M15_1C	4.43816	0.07759	0.30397	0.0051	4.43816	0.07759	99	1730.7	22.65	1711	25.19	1719.5	14.49	16
12_M16_1C	4.59083	0.08485	0.31238	0.00532	4.59083	0.08485	101	1742.7	25.39	1752.4	26.12	1747.6	15.41	0
12_M17_1C	4.61727	0.08223	0.31126	0.00523	4.61727	0.08223	99	1759.9	23.36	1746.9	25.69	1752.4	14.86	0
12_M18_1	4.517	0.07641	0.30504	0.00511	4.517	0.07641	98	1756.6	20.25	1716.2	25.24	1734.1	14.06	6
12_M19_1	4.51064	0.07771	0.30666	0.00516	4.51064	0.07771	99	1744.3	21.14	1724.2	25.47	1732.9	14.32	0
12_M20_1	4.68981	0.08001	0.31234	0.00524	4.68981	0.08001	98	1781.9	20.57	1752.2	25.75	1765.4	14.28	0
12_M21_1	4.54792	0.07841	0.30897	0.00521	4.54792	0.07841	99	1745.6	21.26	1735.6	25.64	1739.8	14.35	25
12_M22_1	4.63279	0.07995	0.30819	0.0052	4.63279	0.07995	97	1784	21.19	1731.8	25.6	1755.2	14.41	0
12_M23_1	4.56635	0.08156	0.30908	0.00525	4.56635	0.08156	99	1752.3	23.22	1736.2	25.86	1743.1	14.88	10
12_M24_1	4.55408	0.07896	0.30842	0.00521	4.55408	0.07896	99	1751.3	21.44	1732.9	25.65	1740.9	14.44	10
12_M25_1	4.59443	0.08353	0.31201	0.00534	4.59443	0.08353	100	1746.3	24.01	1750.6	26.25	1748.3	15.16	11
12_M26_1R	4.12217	0.0727	0.29482	0.00501	4.12217	0.0727	101	1650.8	22.69	1665.6	24.92	1658.7	14.41	9
12_M26_2C	4.59086	0.0823	0.3094	0.00526	4.59086	0.0823	99	1760.2	23.07	1737.7	25.91	1747.6	14.95	0
12_M27_1	4.53352	0.07852	0.30987	0.00525	4.53352	0.07852	100	1734.5	21.58	1740.1	25.83	1737.1	14.41	4
12_M28_1	4.6327	0.07889	0.31115	0.00525	4.6327	0.07889	99	1766.5	20.76	1746.3	25.83	1755.2	14.22	16
12_M29_1	4.48116	0.07851	0.30979	0.00526	4.48116	0.07851	102	1713.6	22.44	1739.7	25.89	1727.5	14.54	16
12_M30_1	4.50332	0.07722	0.30438	0.00514	4.50332	0.07722	98	1754.9	20.8	1713	25.4	1731.6	14.25	13
12_M31_1	4.70221	0.0833	0.31542	0.00537	4.70221	0.0833	100	1768.8	22.74	1767.3	26.3	1767.6	14.83	1
12_M32_1	4.5275	0.07964	0.30834	0.00524	4.5275	0.07964	100	1741.1	22.27	1732.5	25.83	1736	14.63	1
12_M33_1	4.57449	0.08243	0.30944	0.00528	4.57449	0.08243	99	1753.6	23.53	1737.9	26.01	1744.6	15.02	15
12_M34_1	4.53111	0.08284	0.30969	0.00531	4.53111	0.08284	100	1734.6	24.49	1739.2	26.13	1736.7	15.21	1
12_M35_1	4.52862	0.07974	0.30707	0.00521	4.52862	0.07974	99	1749.1	22.45	1726.3	25.67	1736.2	14.65	4
12_M36_1	4.65018	0.08314	0.31263	0.00532	4.65018	0.08314	99	1764.8	23.2	1753.7	26.11	1758.3	14.94	11
12_M37_1	4.44676	0.07706	0.30002	0.00508	4.44676	0.07706	96	1758.3	21.7	1691.4	25.18	1721.1	14.36	0
12_M38_1	4.5421	0.07784	0.3091	0.00523	4.5421	0.07784	100	1742.5	20.97	1736.3	25.76	1738.7	14.26	2
12_M39_1	4.46866	0.07817	0.30417	0.00517	4.46866	0.07817	98	1742.1	22.08	1712	25.57	1725.2	14.51	5
12_M40_1	4.55024	0.08278	0.30456	0.00524	4.55024	0.08278	97	1772.9	23.94	1713.9	25.88	1740.2	15.14	6
12_M41_1	4.46371	0.07811	0.30566	0.00519	4.46371	0.07811	99	1731.2	21.88	1719.3	25.64	1724.3	14.52	11
12_M42_1	4.45763	0.07937	0.30796	0.00525	4.45763	0.07937	101	1714.9	22.94	1730.7	25.86	1723.1	14.77	4
12_M43_1	4.59529	0.08356	0.30956	0.0053	4.59529	0.08356	99	1761.1	23.73	1738.6	26.11	1748.4	15.16	13
12_M44_1	4.59393	0.08149	0.3095	0.00525	4.59393	0.08149	99	1761	22.59	1738.2	25.86	1748.2	14.79	1
12_M45_1	4.5201	0.08082	0.30472	0.00518	4.5201	0.08082	97	1759.8	23.16	1714.7	25.59	1734.7	14.87	12

12_M46_1	4.36078	0.07883	0.29562	0.00503	4.36078	0.07883	95	1749.6	23.74	1669.6	25.02	1704.9	14.93	24
12_M47_1	4.28795	0.07282	0.2962	0.00501	4.28795	0.07282	98	1715.1	20.43	1672.4	24.94	1691	13.98	20
12_M48_1	4.55963	0.07825	0.30799	0.00522	4.55963	0.07825	99	1756.2	20.79	1730.8	25.72	1741.9	14.29	0
12_M49_1	4.54447	0.07769	0.30764	0.0052	4.54447	0.07769	99	1752.2	20.75	1729.1	25.63	1739.1	14.23	7
12_M50_1	4.45493	0.07838	0.30103	0.00512	4.45493	0.07838	97	1755.6	22.35	1696.4	25.36	1722.6	14.59	4
12_M51_1	4.17401	0.07298	0.29467	0.00501	4.17401	0.07298	99	1675.1	21.69	1664.8	24.96	1668.9	14.32	0
12_M52_1	4.60779	0.08188	0.30882	0.00527	4.60779	0.08188	98	1770.5	22.31	1734.9	25.98	1750.7	14.82	9
12_M53_1	3.81804	0.06862	0.27633	0.00472	3.81804	0.06862	97	1628.9	23.55	1572.9	23.84	1596.6	14.46	3
12_M53_2R	4.27665	0.07502	0.29538	0.00502	4.27665	0.07502	97	1715.4	21.62	1668.4	25	1688.9	14.44	0
12_M54_1	4.5167	0.0799	0.30435	0.00518	4.5167	0.0799	97	1760.8	21.92	1712.8	25.62	1734.1	14.71	1
12_M55_1	4.66818	0.08393	0.31289	0.00533	4.66818	0.08393	99	1770.4	23.12	1754.9	26.17	1761.6	15.04	0
12_M56_1	4.58732	0.08101	0.30964	0.00531	4.58732	0.08101	99	1757.6	21.71	1738.9	26.15	1747	14.72	0
12_M57_1	3.83371	0.06769	0.2817	0.00483	3.83371	0.06769	100	1600.8	22.13	1599.9	24.29	1599.9	14.22	0
12_M58_1	4.53485	0.08012	0.30511	0.00524	4.53485	0.08012	97	1763.5	21.61	1716.6	25.87	1737.4	14.7	25
12_M59_1	4.51206	0.08261	0.30568	0.00529	4.51206	0.08261	98	1750.8	23.66	1719.4	26.14	1733.2	15.22	5
12_M60_1	3.75075	0.06744	0.27609	0.00476	3.75075	0.06744	98	1597.4	22.96	1571.7	24.05	1582.3	14.41	5
12_M61_1	4.56349	0.08159	0.30981	0.00534	4.56349	0.08159	100	1747	22.22	1739.8	26.28	1742.6	14.89	0
12_M62_1	4.47618	0.08054	0.30678	0.00529	4.47618	0.08054	100	1729.6	22.5	1724.9	26.11	1726.6	14.93	1
12_M63_1	4.52684	0.08228	0.30484	0.00527	4.52684	0.08228	97	1761.9	23.06	1715.2	26.06	1735.9	15.12	12
12_M64_1	4.57566	0.08429	0.30797	0.00535	4.57566	0.08429	98	1762.7	23.6	1730.7	26.37	1744.8	15.35	8
12_M64_2R	4.54894	0.08471	0.31069	0.00542	4.54894	0.08471	100	1735.9	24.47	1744.1	26.64	1740	15.5	2
Sample RBN-26														
26_M01_1	4.40845	0.07021	0.29965	0.0047	4.40845	0.07021	97	1743.8	19.8	1689.6	23.31	1713.9	13.18	1
26_M012_1	4.5207	0.07194	0.3048	0.00479	4.5207	0.07194	98	1758.7	19.39	1715.1	23.67	1734.8	13.23	3
26_M03_1	4.51845	0.07279	0.30565	0.00483	4.51845	0.07279	98	1752.7	19.86	1719.2	23.85	1734.4	13.39	1
26_M04_1	4.45908	0.07126	0.30314	0.00479	4.45908	0.07126	98	1743.5	19.53	1706.8	23.67	1723.4	13.25	14
26_M05_1	4.47317	0.07294	0.30274	0.00482	4.47317	0.07294	97	1751.8	20.2	1704.9	23.83	1726	13.53	0
26_M06_1	4.51181	0.07326	0.30266	0.00481	4.51181	0.07326	96	1767.9	19.94	1704.5	23.82	1733.1	13.5	7
26_M07_1	4.50482	0.07435	0.30413	0.00486	4.50482	0.07435	97	1756.3	20.85	1711.8	24.01	1731.9	13.71	0
26_M08_1	4.47734	0.07374	0.30256	0.00484	4.47734	0.07374	97	1754.6	20.51	1704	23.97	1726.8	13.67	1
26_M09_1	4.44586	0.07366	0.30265	0.00483	4.44586	0.07366	98	1741.1	21.09	1704.4	23.91	1720.9	13.73	6
26_M10_1	4.49682	0.07439	0.30391	0.00488	4.49682	0.07439	98	1754.4	20.52	1710.7	24.14	1730.4	13.74	5
26_M11_1	4.51115	0.07363	0.30532	0.00495	4.51115	0.07363	98	1751.7	19.57	1717.6	24.42	1733	13.57	14
26_M12_1	4.4893	0.07374	0.30583	0.00496	4.4893	0.07374	99	1739.7	20	1720.1	24.5	1729	13.64	14
26_M13_1	4.47563	0.07387	0.30422	0.00494	4.47563	0.07387	98	1743.8	20.23	1712.2	24.44	1726.5	13.7	1
26_M14_1	4.51644	0.07434	0.3067	0.00498	4.51644	0.07434	99	1745.6	20	1724.4	24.58	1734	13.68	1
26_M15_1	4.47932	0.07377	0.30807	0.00501	4.47932	0.07377	101	1722.2	20.16	1731.2	24.67	1727.1	13.67	8
26_M16_1	4.52248	0.07442	0.31107	0.00505	4.52248	0.07442	101	1722.1	20.12	1746	24.85	1735.1	13.68	6
26_M17_1	3.97932	0.06601	0.2858	0.00465	3.97932	0.06601	99	1642.2	20.74	1620.5	23.33	1630	13.46	0
26_M18_1	4.39723	0.07306	0.29913	0.00487	4.39723	0.07306	97	1742.3	20.55	1687	24.18	1711.8	13.74	20
26_M19_1	4.40355	0.07325	0.30154	0.00491	4.40355	0.07325	98	1730.3	20.63	1698.9	24.34	1713	13.76	0

26_M20_1	4.4696	0.07462	0.30581	0.00499	4.4696	0.07462	99	1731.8	20.81	1720.1	24.63	1725.3	13.85	0
26_M21_1	4.2334	0.06983	0.29267	0.00475	4.2334	0.06983	97	1712.7	20.23	1654.9	23.67	1680.5	13.55	0
26_M22_1	4.47624	0.07396	0.30346	0.00493	4.47624	0.07396	98	1748.7	20.06	1708.4	24.4	1726.6	13.71	8
26_M23_1	4.60367	0.0764	0.30963	0.00504	4.60367	0.0764	99	1763.2	20.07	1738.9	24.8	1749.9	13.84	23
26_M24_1	4.49261	0.0757	0.30529	0.00498	4.49261	0.0757	98	1744.3	20.98	1717.5	24.58	1729.6	13.99	6
26_M25_1	4.45691	0.07414	0.30381	0.00494	4.45691	0.07414	98	1738.6	20.45	1710.2	24.41	1723	13.79	0
26_M26_1	4.57097	0.07658	0.30728	0.00501	4.57097	0.07658	98	1764.1	20.46	1727.3	24.69	1744	13.96	0
26_M27_1	4.52703	0.07633	0.30766	0.00501	4.52703	0.07633	99	1744.2	21.03	1729.2	24.7	1736	14.02	15
26_M28_1	4.55201	0.07679	0.31026	0.00505	4.55201	0.07679	100	1738.8	21.04	1742	24.82	1740.5	14.04	0
26_M29_1	4.44053	0.0758	0.3049	0.00498	4.44053	0.0758	99	1725.3	21.52	1715.6	24.62	1719.9	14.15	0
26_M30_1	4.5597	0.0782	0.30537	0.005	4.5597	0.0782	97	1770.9	21.6	1717.9	24.67	1741.9	14.28	3
26_M31_1	4.45007	0.07388	0.30225	0.00493	4.45007	0.07388	98	1745.2	20.15	1702.5	24.42	1721.7	13.76	2
26_M32_1	4.46334	0.07376	0.3049	0.00497	4.46334	0.07376	99	1734.7	19.92	1715.5	24.55	1724.2	13.71	15
26_M33_1	4.50416	0.0742	0.30599	0.00498	4.50416	0.0742	99	1744.8	19.73	1720.9	24.6	1731.7	13.69	14
26_M34_1	4.36992	0.07252	0.29723	0.00485	4.36992	0.07252	96	1742.6	20.12	1677.6	24.1	1706.7	13.71	2
26_M35_1	4.48522	0.07475	0.30481	0.00498	4.48522	0.07475	98	1744.1	20.33	1715.1	24.59	1728.2	13.84	13
26_M36_1	4.37864	0.07337	0.29981	0.0049	4.37864	0.07337	98	1730.4	20.64	1690.3	24.31	1708.3	13.85	6
26_M37_1	4.60548	0.07696	0.30972	0.00506	4.60548	0.07696	99	1763.4	20.36	1739.3	24.91	1750.3	13.94	0
26_M38_1	4.56361	0.07678	0.30707	0.00503	4.56361	0.07678	98	1762.4	20.7	1726.3	24.78	1742.6	14.01	6
26_M39_1	4.42287	0.07455	0.30195	0.00494	4.42287	0.07455	98	1735.8	20.91	1701	24.47	1716.6	13.96	0
26_M40_1	4.48486	0.07525	0.30228	0.00494	4.48486	0.07525	97	1759.3	20.54	1702.6	24.46	1728.2	13.93	0
Sample RBN-28														
28_M01_1	4.40143	0.0698	0.29835	0.00471	4.40143	0.0698	96	1748.8	18.99	1683.1	23.4	1712.6	13.12	3
28_M02_1	4.40308	0.07083	0.30036	0.00477	4.40308	0.07083	97	1737.2	19.67	1693.1	23.65	1712.9	13.31	0
28_M03_1	4.40497	0.0707	0.3016	0.0048	4.40497	0.0707	98	1730.4	19.43	1699.2	23.76	1713.3	13.28	0
28_M05_1	4.433	0.07186	0.30029	0.00481	4.433	0.07186	97	1750.1	19.47	1692.7	23.85	1718.5	13.43	0
28_M06_1	4.51492	0.07421	0.30819	0.00496	4.51492	0.07421	100	1736	20.15	1731.8	24.46	1733.7	13.66	7
28_M07_1	4.46128	0.07344	0.30534	0.00493	4.46128	0.07344	99	1731.1	20.06	1717.8	24.36	1723.8	13.65	0
28_M08_1	4.53964	0.07503	0.30602	0.00496	4.53964	0.07503	98	1758.9	19.96	1721.1	24.47	1738.3	13.75	0
28_M09_1	4.25418	0.07066	0.29399	0.00478	4.25418	0.07066	97	1713.4	20.19	1661.4	23.82	1684.5	13.66	0
28_M10_1	4.45621	0.07499	0.3067	0.00501	4.45621	0.07499	100	1720.8	20.75	1724.5	24.74	1722.9	13.96	8
28_M11_1	4.11174	0.06814	0.2912	0.00475	4.11174	0.06814	99	1668.3	20.3	1647.5	23.72	1656.6	13.53	5
28_M12_1	4.49929	0.07499	0.30427	0.00498	4.49929	0.07499	98	1753.2	20.02	1712.4	24.62	1730.8	13.85	0
28_M13_1	4.47275	0.07444	0.30429	0.00497	4.47275	0.07444	98	1742.2	20.21	1712.5	24.58	1725.9	13.81	18
28_M14_1	4.43629	0.07372	0.30182	0.00493	4.43629	0.07372	98	1742.2	20	1700.3	24.42	1719.1	13.77	26
28_M15_1	4.48835	0.07407	0.30599	0.00497	4.48835	0.07407	99	1738.4	20.1	1720.9	24.55	1728.8	13.7	3
28_M16_1	4.40073	0.07282	0.30047	0.00489	4.40073	0.07282	98	1735.5	20.34	1693.7	24.22	1712.5	13.69	19
28_M17_1	4.46691	0.07451	0.3042	0.00496	4.46691	0.07451	98	1740.2	20.77	1712.1	24.49	1724.8	13.84	0
28_M18_1	4.41582	0.07318	0.3025	0.0049	4.41582	0.07318	99	1729.4	20.74	1703.7	24.24	1715.3	13.72	6
28_M20_1	4.37751	0.07361	0.29955	0.00488	4.37751	0.07361	98	1731.3	21.19	1689.1	24.22	1708.1	13.9	12
28_M21_1	4.4562	0.07322	0.30118	0.0049	4.4562	0.07322	97	1754.3	19.57	1697.2	24.3	1722.9	13.63	0

28_M22_1	4.45204	0.07377	0.30232	0.00493	4.45204	0.07377	98	1745.7	20.02	1702.8	24.38	1722.1	13.74	1
28_M24_1	4.27228	0.07091	0.29292	0.00478	4.27228	0.07091	96	1727.9	20.06	1656.1	23.83	1688	13.66	0
28_M25_1	4.46422	0.07401	0.30241	0.00493	4.46422	0.07401	97	1750.1	19.96	1703.2	24.4	1724.3	13.75	2
28_M26_1	4.00196	0.06676	0.28285	0.00461	4.00196	0.06676	96	1671.9	20.51	1605.7	23.17	1634.6	13.55	6
28_M27_1	4.5128	0.07561	0.30581	0.00498	4.5128	0.07561	98	1749.4	20.63	1720	24.59	1733.3	13.93	0
28_M28_1	4.38943	0.07333	0.29589	0.00482	4.38943	0.07333	95	1759	20.23	1670.9	23.98	1710.4	13.81	13
28_M29_1	4.53349	0.07668	0.30639	0.005	4.53349	0.07668	98	1754.2	20.96	1722.9	24.67	1737.1	14.07	8
28_M30_1	4.52699	0.07716	0.30491	0.00499	4.52699	0.07716	97	1760.5	21.09	1715.6	24.66	1735.9	14.17	2
28_M32_1	4.50157	0.07219	0.30652	0.0049	4.50157	0.07219	99	1740.6	19.18	1723.6	24.2	1731.3	13.32	0
28_M33_1	4.23937	0.06874	0.29384	0.00473	4.23937	0.06874	97	1708	19.65	1660.7	23.55	1681.7	13.32	10
28_M34_1	4.42712	0.07244	0.30139	0.00487	4.42712	0.07244	98	1741	19.76	1698.2	24.12	1717.4	13.55	0
28_M35_1	4.48854	0.07342	0.30476	0.00494	4.48854	0.07342	98	1745.9	19.57	1714.9	24.38	1728.9	13.58	1
28_M36_1	4.46265	0.0734	0.30423	0.00494	4.46265	0.0734	98	1738.4	19.82	1712.3	24.4	1724.1	13.64	14
28_M37_1	4.4889	0.07511	0.3021	0.00494	4.4889	0.07511	97	1762.1	20.3	1701.7	24.45	1728.9	13.89	3
28_M38_1	4.25455	0.07086	0.29406	0.00481	4.25455	0.07086	97	1713.2	20.28	1661.8	23.95	1684.6	13.69	12
28_M39_1	4.51181	0.07544	0.30233	0.00496	4.51181	0.07544	96	1769.9	20.1	1702.9	24.57	1733.2	13.9	0
28_M40_1	4.4771	0.07498	0.30778	0.00506	4.4771	0.07498	100	1723.1	20.15	1729.8	24.96	1726.7	13.9	8
Sample RBN-31														
31_M01_1	4.47751	0.07137	0.30616	0.00482	4.47751	0.07137	99	1732.9	19.8	1721.8	23.78	1726.8	13.23	3
31_M02_1	5.61459	0.08984	0.3463	0.00547	5.61459	0.08984	100	1919.9	19.43	1916.9	26.21	1918.3	13.79	4
31_M03_1	4.52272	0.07209	0.30802	0.00487	4.52272	0.07209	99	1740.1	19.68	1730.9	23.98	1735.2	13.25	27
31_M04_1	4.59537	0.07303	0.31134	0.00494	4.59537	0.07303	100	1749.7	19.18	1747.3	24.27	1748.4	13.25	9
31_M051	4.5044	0.07211	0.30384	0.00484	4.5044	0.07211	97	1757.7	19.34	1710.3	23.92	1731.8	13.3	7
31_M06_1	4.54434	0.07316	0.30792	0.00492	4.54434	0.07316	99	1749.6	19.44	1730.5	24.27	1739.1	13.4	7
31_M07_1	4.03046	0.06555	0.28245	0.00455	4.03046	0.06555	95	1687.7	19.82	1603.7	22.85	1640.4	13.23	6
31_M08_1C	4.20535	0.06798	0.29013	0.00465	4.20535	0.06798	96	1716.4	19.92	1642.2	23.23	1675.1	13.26	0
31_M08_2R	3.62841	0.05929	0.27055	0.00437	3.62841	0.05929	98	1572.4	20.34	1543.6	22.15	1555.8	13.01	11
31_M09_1	4.47307	0.07506	0.30641	0.00501	4.47307	0.07506	100	1729.6	20.72	1723	24.72	1726	13.92	18
31_M13_1	4.48604	0.07467	0.30419	0.00503	4.48604	0.07467	98	1748.3	19.66	1712.1	24.86	1728.4	13.82	0
31_M14_1	4.41928	0.07345	0.3009	0.00497	4.41928	0.07345	97	1740.7	19.65	1695.8	24.65	1716	13.76	4
31_M15_1	4.49445	0.07488	0.30504	0.00505	4.49445	0.07488	98	1746.6	19.62	1716.3	24.93	1729.9	13.84	0
31_M16_1	4.35301	0.07261	0.29803	0.00493	4.35301	0.07261	97	1730.6	19.75	1681.5	24.5	1703.5	13.77	5
31_M17_1	3.99681	0.06716	0.28624	0.00475	3.99681	0.06716	98	1647.6	20.28	1622.7	23.8	1633.5	13.65	5
31_M18_1C	4.49748	0.07641	0.30651	0.00509	4.49748	0.07641	99	1739	20.74	1723.5	25.12	1730.5	14.11	0
31_M18_2R	3.32039	0.05652	0.25681	0.00428	3.32039	0.05652	98	1503.6	21.16	1473.5	21.93	1485.9	13.28	6
31_M19_1D	4.64411	0.07808	0.30913	0.00516	4.64411	0.07808	97	1782.1	19.34	1736.4	25.43	1757.2	14.05	0
31_M20_1D	4.23406	0.07145	0.29249	0.00489	4.23406	0.07145	96	1714.3	19.71	1653.9	24.39	1680.6	13.86	0
31_M22_1D	4.47825	0.0769	0.30437	0.00512	4.47825	0.0769	98	1744	20.28	1713	25.33	1726.9	14.25	6
31_M234_1C	4.74277	0.08149	0.31572	0.00531	4.74277	0.08149	99	1781.9	20.23	1768.8	26.01	1774.8	14.41	5
31_M234_2C	4.93082	0.0851	0.32632	0.0055	4.93082	0.0851	102	1792.6	20.26	1820.5	26.74	1807.5	14.57	0
31_M234_3C	4.77533	0.0829	0.31937	0.00539	4.77533	0.0829	101	1773.4	20.61	1786.6	26.35	1780.6	14.57	0

31_M234_4R	4.36933	0.07567	0.30629	0.00517	4.36933	0.07567	102	1687.2	20.64	1722.4	25.51	1706.6	14.31	1
31_M25_1C	4.44362	0.07597	0.30398	0.00515	4.44362	0.07597	99	1732	19.49	1711	25.47	1720.5	14.17	0
31_M25_2R	3.79326	0.06483	0.28174	0.00478	3.79326	0.06483	101	1579.6	19.88	1600.1	24.02	1591.3	13.73	12
31_M26_1	4.77217	0.08182	0.32057	0.00544	4.77217	0.08182	102	1765.3	19.55	1792.5	26.56	1780	14.39	0
31_M27_1	4.13382	0.0714	0.2931	0.00499	4.13382	0.0714	99	1666	20.21	1657	24.85	1661	14.12	0
31_M28_1	4.54973	0.0794	0.30462	0.0052	4.54973	0.0794	97	1771.3	20.52	1714.2	25.7	1740.1	14.53	0
31_M29_1	4.72207	0.08362	0.31426	0.0054	4.72207	0.08362	99	1782.4	21.18	1761.6	26.47	1771.2	14.84	12
31_M30_1	4.65112	0.08115	0.31363	0.00536	4.65112	0.08115	100	1758.4	20.36	1758.6	26.3	1758.5	14.58	0
31_M31_1	4.59905	0.08044	0.31379	0.00536	4.59905	0.08044	101	1736.8	20.65	1759.4	26.32	1749.1	14.59	0
31_M32_1	4.55717	0.08033	0.30829	0.00528	4.55717	0.08033	99	1752.5	20.97	1732.3	26.03	1741.5	14.68	0
31_M33_1	4.5054	0.07847	0.30594	0.00523	4.5054	0.07847	99	1745.6	20.34	1720.7	25.81	1732	14.47	16
Sample RBN-45														
45_M01	3.68525	0.0527	0.27379	0.00382	3.68525	0.0527	99	1579.1	20.07	1560	19.32	1568.2	11.42	7
45_M01A	3.74347	0.05437	0.27705	0.00388	3.74347	0.05437	99	1586.3	20.69	1576.5	19.57	1580.7	11.64	1
45_M02	3.84086	0.056	0.28229	0.00395	3.84086	0.056	100	1599.3	20.83	1602.9	19.86	1601.4	11.75	4
45_M03	4.54216	0.06401	0.30867	0.00427	4.54216	0.06401	99	1744.2	19.23	1734.2	21.02	1738.7	11.73	4
45_M04	3.80882	0.05496	0.28172	0.00392	3.80882	0.05496	101	1587.5	20.48	1600	19.73	1594.6	11.6	0
45_M04A	3.5661	0.053	0.26908	0.00366	3.5661	0.053	99	1550	22.8	1536.1	18.6	1542	11.79	0
45_M05	3.8134	0.0552	0.28362	0.00393	3.8134	0.0552	102	1577.2	20.89	1609.6	19.74	1595.6	11.64	10
45_M06	3.85797	0.05536	0.28684	0.00398	3.85797	0.05536	103	1577.8	20.34	1625.7	19.94	1604.9	11.57	6
45_M06A	4.13783	0.06023	0.29545	0.00412	4.13783	0.06023	101	1653.1	20.64	1668.7	20.49	1661.8	11.9	0
45_M07	3.62068	0.05193	0.26961	0.00373	3.62068	0.05193	98	1574.9	20.45	1538.8	18.95	1554.1	11.41	0
45_M08	3.58309	0.04949	0.26852	0.00365	3.58309	0.04949	98	1562.6	19.48	1533.3	18.57	1545.8	10.96	0
45_M08A	3.89625	0.05523	0.29038	0.00396	3.89625	0.05523	104	1572.9	20.72	1643.4	19.78	1612.9	11.45	0
45_M09	4.82633	0.06617	0.3232	0.00438	4.82633	0.06617	102	1770.8	18.91	1805.3	21.36	1789.5	11.53	7
45_M09A	4.8687	0.06675	0.32238	0.00437	4.8687	0.06675	101	1791.4	18.84	1801.3	21.32	1796.9	11.55	0
45_M10	4.5987	0.06399	0.31228	0.00425	4.5987	0.06399	100	1745.3	19.53	1751.9	20.85	1749	11.6	0
45_M10A	4.52249	0.06264	0.30915	0.0042	4.52249	0.06264	100	1733.2	19.36	1736.5	20.69	1735.1	11.52	0
45_M11	4.33265	0.06021	0.30328	0.00412	4.33265	0.06021	101	1689.6	19.63	1707.5	20.37	1699.6	11.46	3
45_M11A	4.36314	0.06067	0.30741	0.00419	4.36314	0.06067	103	1677.6	19.57	1727.9	20.64	1705.4	11.49	2
45_M12	4.58584	0.06301	0.31073	0.00421	4.58584	0.06301	100	1749.4	18.93	1744.3	20.72	1746.7	11.45	14
45_M12A	4.57531	0.06359	0.30732	0.00418	4.57531	0.06359	98	1765.4	19.23	1727.5	20.6	1744.8	11.58	0
45_M12B	4.8238	0.06715	0.3223	0.00438	4.8238	0.06715	101	1775.1	19.32	1801	21.37	1789.1	11.71	10
45_M13	3.85064	0.05454	0.28506	0.00389	3.85064	0.05454	102	1585.8	20.42	1616.8	19.53	1603.4	11.42	0
45_M13A	3.79307	0.05369	0.2829	0.00386	3.79307	0.05369	102	1571.8	20.49	1606	19.39	1591.3	11.37	9
45_M13B	3.78816	0.05361	0.28374	0.00387	3.78816	0.05361	103	1563.9	20.44	1610.2	19.44	1590.2	11.37	0
45_M14	3.79202	0.05427	0.28236	0.00387	3.79202	0.05427	102	1574.9	20.74	1603.2	19.46	1591.1	11.5	10
45_M14A	3.58013	0.05156	0.27306	0.00375	3.58013	0.05156	102	1529.8	21.11	1556.3	18.97	1545.1	11.43	0
45_M15	3.89427	0.05548	0.29052	0.00398	3.89427	0.05548	105	1571.4	20.6	1644.1	19.86	1612.5	11.51	0
45_M16	4.76631	0.06684	0.32113	0.00438	4.76631	0.06684	102	1760	19.41	1795.3	21.37	1779	11.77	4
45_M16A	4.53308	0.06332	0.30755	0.00418	4.53308	0.06332	99	1747.3	19.4	1728.6	20.61	1737.1	11.62	0

45_M16B	4.59801	0.06545	0.31874	0.00436	4.59801	0.06545	104	1707.8	20.04	1783.6	21.32	1748.9	11.87	2
45_M17	4.89468	0.06994	0.32989	0.00451	4.89468	0.06994	104	1759.4	20.04	1837.9	21.88	1801.3	12.05	0
45_M17A	4.81742	0.06929	0.32524	0.00447	4.81742	0.06929	103	1756.4	20.19	1815.3	21.73	1787.9	12.09	4
45_M18	3.75888	0.05573	0.27981	0.00386	3.75888	0.05573	101	1575.6	22.02	1590.4	19.44	1584	11.89	0
45_M18A	3.83548	0.05696	0.28608	0.00396	3.83548	0.05696	103	1571.9	21.91	1621.9	19.87	1600.2	11.96	3
45_M19	3.80631	0.055	0.2826	0.00387	3.80631	0.055	102	1580.5	21.02	1604.5	19.45	1594.1	11.62	0
45_M20	4.63835	0.06818	0.315	0.00435	4.63835	0.06818	101	1745.6	20.99	1765.3	21.32	1756.2	12.28	6
45_M21	3.76083	0.05513	0.28282	0.00388	3.76083	0.05513	103	1556.5	21.6	1605.6	19.52	1584.4	11.76	0
45_M22	3.50097	0.05069	0.26495	0.00363	3.50097	0.05069	98	1544.7	21.05	1515.1	18.52	1527.4	11.43	0
45_M23	3.90431	0.05738	0.28608	0.00394	3.90431	0.05738	101	1605.2	21.44	1621.9	19.76	1614.6	11.88	8
Sample RBN-46														
46_M01	3.55613	0.04624	0.26659	0.00333	3.55613	0.04624	98	1562.3	20.01	1523.5	16.94	1539.8	10.31	7
46_M02	3.51652	0.04582	0.26508	0.00331	3.51652	0.04582	98	1551.9	20.07	1515.8	16.88	1530.9	10.3	7
46_M03	3.5639	0.04649	0.26365	0.0033	3.5639	0.04649	95	1587.1	20	1508.5	16.81	1541.5	10.34	89
46_M04	3.5097	0.04596	0.26579	0.00333	3.5097	0.04596	98	1543.2	20.22	1519.4	16.94	1529.4	10.35	0
46_M05	3.40428	0.0448	0.25755	0.00323	3.40428	0.0448	96	1545	20.36	1477.3	16.54	1505.4	10.33	46
46_M06	3.44499	0.04553	0.26042	0.00327	3.44499	0.04553	96	1546.4	20.45	1492	16.71	1514.7	10.4	0
46_M07	3.47016	0.04599	0.26416	0.00332	3.47016	0.04599	99	1533.3	20.56	1511.1	16.91	1520.5	10.45	7
46_M08	3.44459	0.04599	0.25911	0.00326	3.44459	0.04599	95	1555.6	20.7	1485.3	16.69	1514.6	10.51	0
46_M09	3.34662	0.04487	0.25439	0.0032	3.34662	0.04487	95	1536	20.87	1461.1	16.47	1492	10.48	0
46_M10	3.46785	0.04665	0.26145	0.0033	3.46785	0.04665	97	1551.3	20.91	1497.3	16.84	1519.9	10.6	36
46_M11	3.56634	0.04673	0.27053	0.00341	3.56634	0.04673	100	1539.8	20.17	1543.5	17.31	1542.1	10.39	0
46_M12	3.51739	0.04617	0.26933	0.0034	3.51739	0.04617	101	1522.2	20.27	1537.4	17.26	1531.1	10.38	11
46_M13	3.58726	0.04726	0.26732	0.00338	3.58726	0.04726	97	1573.2	20.25	1527.2	17.17	1546.7	10.46	51
46_M14	3.46057	0.04576	0.26357	0.00333	3.46057	0.04576	98	1532.3	20.46	1508.1	17.01	1518.3	10.42	1
46_M15	3.49238	0.04642	0.26196	0.00331	3.49238	0.04642	96	1560.9	20.6	1499.9	16.93	1525.5	10.49	18
46_M16	3.45328	0.04599	0.25975	0.00329	3.45328	0.04599	96	1555.7	20.64	1488.6	16.83	1516.6	10.49	8
46_M16A	3.47232	0.04645	0.26511	0.00336	3.47232	0.04645	99	1527.8	20.83	1515.9	17.13	1521	10.54	15
46_M17	3.47342	0.04669	0.26152	0.00332	3.47342	0.04669	96	1554	20.92	1497.6	16.97	1521.2	10.6	5
46_M18	3.42957	0.04636	0.2619	0.00333	3.42957	0.04636	98	1527.4	21.18	1499.5	17.01	1511.2	10.63	0
46_M20	3.42588	0.04535	0.26187	0.00334	3.42588	0.04535	98	1526.6	20.14	1499.4	17.04	1510.4	10.4	64
46_M21	3.52855	0.04669	0.26402	0.00336	3.52855	0.04669	96	1566.7	20	1510.4	17.15	1533.6	10.47	15
46_M22	2.60652	0.03522	0.22099	0.00283	2.60652	0.03522	97	1328.8	21.36	1287.1	14.95	1302.5	9.92	4
46_M23	3.57705	0.04803	0.27331	0.0035	3.57705	0.04803	102	1527.5	20.49	1557.6	17.71	1544.5	10.65	3
46_M24	3.46871	0.04673	0.2644	0.00339	3.46871	0.04673	99	1532	20.55	1512.3	17.28	1520.1	10.62	9
46_M24A	3.48072	0.04717	0.2668	0.00342	3.48072	0.04717	100	1521.5	20.76	1524.5	17.43	1522.9	10.69	0
46_M25	3.49167	0.04747	0.264	0.00339	3.49167	0.04747	98	1547.2	20.76	1510.3	17.3	1525.3	10.73	2
46_M26	3.4775	0.04753	0.26476	0.00341	3.4775	0.04753	99	1534.1	20.95	1514.2	17.37	1522.1	10.78	14
46_M27	3.64639	0.05026	0.2722	0.00351	3.64639	0.05026	99	1571.1	21.12	1552	17.79	1559.7	10.98	58
46_M27	3.56623	0.04815	0.27186	0.00351	3.56623	0.04815	101	1531.8	20.39	1550.3	17.79	1542.1	10.71	0
46_M29	3.31914	0.04476	0.25456	0.00328	3.31914	0.04476	96	1520.4	20.39	1462	16.87	1485.6	10.52	12

46_M30	3.51651	0.04806	0.26669	0.00345	3.51651	0.04806	99	1541.5	20.74	1524	17.56	1530.9	10.81	14
46_M31	3.42553	0.04711	0.26242	0.0034	3.42553	0.04711	99	1522.5	20.94	1502.2	17.37	1510.3	10.81	12
46_M32	3.45236	0.04757	0.26155	0.00339	3.45236	0.04757	97	1543.5	20.96	1497.8	17.32	1516.4	10.85	9
46_M33	3.57655	0.04953	0.26881	0.00349	3.57655	0.04953	98	1558.4	21.08	1534.7	17.71	1544.3	10.99	8
46_M34	3.55916	0.04953	0.26716	0.00347	3.55916	0.04953	98	1560.8	21.21	1526.4	17.64	1540.5	11.03	4
Sample RBN-47														
47_M02	4.62337	0.06386	0.3148	0.00424	4.62337	0.06386	101	1740.3	19.78	1764.3	20.81	1753.5	11.53	0
47_M03	4.64676	0.06437	0.31272	0.00422	4.64676	0.06437	100	1761.7	19.73	1754.1	20.72	1757.7	11.57	1
47_M04	4.25239	0.05784	0.29726	0.00399	4.25239	0.05784	99	1691.9	19.27	1677.7	19.83	1684.2	11.18	0
47_M05	4.37702	0.05997	0.30106	0.00405	4.37702	0.05997	99	1721.7	19.51	1696.6	20.07	1708	11.33	12
47_M06	4.25723	0.05897	0.29466	0.00398	4.25723	0.05897	97	1710.2	19.89	1664.8	19.79	1685.1	11.39	11
47_M07	4.49225	0.06224	0.30379	0.0041	4.49225	0.06224	98	1752.9	19.72	1710.1	20.27	1729.5	11.51	0
47_M08	4.50773	0.06337	0.30479	0.00413	4.50773	0.06337	98	1753.1	20.25	1715	20.4	1732.4	11.68	0
47_M09	4.61711	0.06382	0.31109	0.0042	4.61711	0.06382	99	1759.6	19.61	1746	20.63	1752.4	11.54	2
47_M10	4.65163	0.06499	0.31438	0.00425	4.65163	0.06499	100	1753.9	20	1762.2	20.85	1758.6	11.68	6
47_M11	4.69011	0.06539	0.31807	0.0043	4.69011	0.06539	102	1747.7	19.89	1780.3	21.02	1765.5	11.67	0
47_M12	4.71758	0.06469	0.31868	0.00429	4.71758	0.06469	102	1754.9	19.27	1783.3	20.96	1770.4	11.49	0
47_M13	4.59853	0.06465	0.31558	0.00427	4.59853	0.06465	102	1726	20.32	1768.1	20.94	1749	11.72	0
47_M13A	4.67788	0.06566	0.31842	0.00431	4.67788	0.06566	102	1740.9	20.2	1782	21.08	1763.3	11.74	9
47_M13B	4.58112	0.06438	0.31131	0.00422	4.58112	0.06438	100	1744	20.25	1747.1	20.72	1745.8	11.71	11
47_M14	4.74816	0.0659	0.32273	0.00436	4.74816	0.0659	103	1743.6	19.78	1803	21.23	1775.8	11.64	0
47_M15	4.52461	0.06305	0.31349	0.00423	4.52461	0.06305	103	1708.4	20.01	1757.8	20.78	1735.5	11.59	0
47_M16	4.58363	0.06426	0.30904	0.00418	4.58363	0.06426	99	1758.3	20.04	1736	20.59	1746.3	11.68	0
47_M18A	4.70085	0.06607	0.31971	0.00433	4.70085	0.06607	103	1742.5	20.18	1788.3	21.13	1767.4	11.77	2
47_M19	4.74912	0.06794	0.32257	0.00439	4.74912	0.06794	103	1744.9	20.74	1802.3	21.38	1776	12	2
47_M20	4.71145	0.06816	0.32328	0.00441	4.71145	0.06816	105	1726.3	21.28	1805.7	21.47	1769.3	12.12	1
47_M21	4.72648	0.06714	0.32215	0.00437	4.72648	0.06714	104	1738.5	20.56	1800.2	21.31	1771.9	11.9	5
47_M22	4.6948	0.06689	0.32256	0.00438	4.6948	0.06689	105	1723.8	20.7	1802.2	21.34	1766.3	11.93	0
47_M23	4.77791	0.06808	0.32546	0.00442	4.77791	0.06808	104	1739.6	20.66	1816.3	21.49	1781	11.96	3
47_M24	4.71375	0.06664	0.31715	0.0043	4.71375	0.06664	101	1762.2	20.25	1775.8	21.02	1769.7	11.84	4
47_M25	4.68485	0.06675	0.31505	0.00428	4.68485	0.06675	100	1763.1	20.53	1765.5	20.96	1764.5	11.92	23
47_M26	4.42451	0.06367	0.29881	0.00407	4.42451	0.06367	96	1755.4	20.91	1685.4	20.18	1716.9	11.92	7
47_M30	4.2395	0.06204	0.29715	0.00406	4.2395	0.06204	99	1687.1	21.71	1677.2	20.16	1681.7	12.02	5
47_M32	4.74347	0.0686	0.32479	0.00442	4.74347	0.0686	105	1730.1	21.13	1813.1	21.5	1775	12.13	0
47_M35	4.76473	0.0697	0.32082	0.00438	4.76473	0.0697	102	1760.9	21.4	1793.7	21.36	1778.7	12.28	0
47_M36	4.58106	0.06666	0.31579	0.0043	4.58106	0.06666	103	1717.7	21.36	1769.2	21.07	1745.8	12.13	18
47_M37	4.72843	0.06947	0.31778	0.00434	4.72843	0.06947	101	1764.3	21.55	1778.9	21.23	1772.3	12.31	2

APPENDIX B: U-PB ZIRCON GEOCHRONOLOGY

Analysis no.	$^{207}Pb/^{206}Pb$	1σ	$^{206}Pb/^{238}U$	1σ	$^{207}Pb/^{235}U$	1σ	Conc.	$^{207}Pb/^{206}Pb$ age	1σ	$^{206}Pb/^{238}U$ age	1σ	$^{207}Pb/^{235}U$ age	1σ	204 counts	208 counts
Sample- RBN-34															
34_Z03_2	3.7483	0.06257	0.26654	0.00407	3.7483	0.06257	92	1661.1	23.57	1523.2	20.71	1581.8	13.38	8	21249
34_Z13_1_	4.39076	0.07817	0.31068	0.00482	4.39076	0.07817	104	1671.2	26.54	1744	23.68	1710.6	14.72	12	24807
34_Z15_2_	4.16176	0.0771	0.30222	0.0047	4.16176	0.0771	105	1622.7	28.84	1702.3	23.25	1666.5	15.17	0	9362
34_Z16_1_	4.49643	0.08185	0.32011	0.00493	4.49643	0.08185	108	1659.5	28	1790.3	24.06	1730.3	15.12	0	10797
34_Z16_2_	3.78345	0.06893	0.26925	0.00413	3.78345	0.06893	93	1660.1	28.15	1537	20.98	1589.2	14.63	48	29137
34_Z17_2_	4.14906	0.08602	0.29752	0.00475	4.14906	0.08602	102	1645.8	34.44	1679	23.59	1664	16.96	0	7488
34_Z19_1	3.81976	0.07107	0.27516	0.00441	3.81976	0.07107	96	1636.9	28.11	1566.9	22.27	1596.9	14.97	70	11478
34_Z21_1	4.00962	0.07017	0.28775	0.00452	4.00962	0.07017	99	1643.9	25.11	1630.3	22.61	1636.1	14.22	69	25700
34_Z24_1	4.2173	0.07753	0.30553	0.00485	4.2173	0.07753	106	1626.3	27.43	1718.7	23.96	1677.4	15.09	66	16057
34_Z25_1	3.77165	0.06864	0.2696	0.00426	3.77165	0.06864	93	1651.2	26.83	1538.8	21.65	1586.7	14.61	78	44366
34_Z26_2	4.13239	0.07818	0.29757	0.00474	4.13239	0.07818	103	1637.5	28.63	1679.3	23.55	1660.7	15.47	75	11787
34_Z28_1	3.8918	0.06723	0.27848	0.0045	3.8918	0.06723	96	1649.3	23.21	1583.7	22.68	1612	13.95	0	8048
34_Z29_1	3.84616	0.06777	0.27314	0.00443	3.84616	0.06777	94	1663.2	24.17	1556.7	22.44	1602.5	14.2	5	19949
34_Z30_1	3.70405	0.06503	0.26691	0.00432	3.70405	0.06503	93	1636.3	24.08	1525.1	21.98	1572.2	14.04	8	15649
34_Z33_1	3.80533	0.06811	0.27503	0.00445	3.80533	0.06811	96	1630.8	25.07	1566.3	22.52	1593.9	14.39	11	8969
34_Z33_2	3.68019	0.06621	0.26466	0.00429	3.68019	0.06621	92	1640	25.3	1513.6	21.84	1567.1	14.36	20	9856
34_Z35R	3.89438	0.05855	0.28047	0.00381	3.89438	0.05855	97	1637.3	22.71	1593.7	19.19	1612.5	12.15	400	20026
34_Z37C	4.01464	0.06334	0.28547	0.00394	4.01464	0.06334	97	1661	24.37	1618.8	19.75	1637.2	12.82	19	134604
34_Z37R	3.88754	0.05501	0.28246	0.00369	3.88754	0.05501	99	1620.8	21.78	1603.7	18.54	1611.1	11.43	18	8422
34_Z40R	3.4324	0.04974	0.25138	0.00329	3.4324	0.04974	90	1606	22.87	1445.6	16.94	1511.8	11.39	22	21249
34_Z41R	3.90791	0.05427	0.27551	0.00358	3.90791	0.05427	94	1677.1	21.31	1568.7	18.1	1615.3	11.23	29	13487
34_Z42C	3.51038	0.04966	0.25749	0.00337	3.51038	0.04966	92	1603.6	22.05	1477	17.25	1529.6	11.18	18	30183
34_Z45C	3.99361	0.06616	0.28795	0.00406	3.99361	0.06616	100	1635.6	26.36	1631.3	20.33	1632.9	13.45	3	8859
34_Z46C	3.32638	0.06162	0.24118	0.00353	3.32638	0.06162	86	1625.6	30.5	1392.8	18.32	1487.3	14.46	18	15498
34_Z47C	3.69879	0.05732	0.26754	0.00363	3.69879	0.05732	94	1629.7	24.14	1528.3	18.48	1571.1	12.39	29	13333
34_Z48R	3.98092	0.0602	0.28631	0.00385	3.98092	0.0602	99	1640.2	23.37	1623.1	19.3	1630.3	12.27	0	7829
Sample RBN-45															
45_Z01C	3.9686	0.04819	0.29052	0.00329	3.9686	0.04819	102	1607.1	20.72	1644.1	16.43	1627.8	9.85	6	5092
45_Z02C	4.49923	0.05384	0.31709	0.00358	4.1518	0.05059	106	1677.5	20.1	1775.5	16.92	1664.6	9.97	0	3852
45_Z02R	4.1518	0.05059	0.30164	0.00342	4.49923	0.05384	105	1621.1	20.79	1699.4	17.52	1730.8	9.94	14	3543
45_Z03C	4.01078	0.04888	0.28753	0.00326	4.01078	0.04888	99	1645.9	20.72	1629.2	16.3	1636.4	9.9	0	3029
45_Z04C	4.9494	0.06654	0.3311	0.00401	3.84621	0.04743	104	1773.6	21.73	1843.7	16.08	1602.5	9.94	3	2944
45_Z04R	3.84621	0.04743	0.28192	0.0032	4.9494	0.06654	100	1604.7	21.18	1601	19.43	1810.7	11.36	0	1008
45_Z05C	4.56228	0.05501	0.30568	0.00345	4.56228	0.05501	97	1770.3	20.17	1719.4	17.02	1742.4	10.04	9	4864
45_Z06AC	4.07889	0.04953	0.2978	0.00336	4.03216	0.04915	104	1611.9	20.76	1680.4	16.54	1640.7	9.92	0	5663
45_Z06C	4.03216	0.04915	0.29387	0.00332	4.07889	0.04953	103	1615.2	20.85	1660.8	16.68	1650.1	9.9	0	6796

45_Z07C	4.50171	0.0546	0.30677	0.00349	4.50171	0.0546	99	1739.3	20.1	1724.8	17.24	1731.3	10.08	4	5976
45_Z08R	4.44521	0.05502	0.3148	0.00356	4.44521	0.05502	106	1668.5	21.17	1764.3	17.43	1720.8	10.26	0	2761
45_Z09C	5.47041	0.06818	0.34983	0.00386	5.47041	0.06818	104	1854.7	21.43	1933.8	18.46	1896	10.7	0	10602
45_Z10R	3.88313	0.04908	0.28312	0.00321	3.88313	0.04908	100	1614.4	21.92	1607.1	16.13	1610.2	10.21	0	2611
45_Z11AR	4.08319	0.05091	0.2974	0.00336	4.12759	0.05148	104	1616.3	21.51	1678.4	16.74	1659.8	10.19	0	5627
45_Z11R	4.12759	0.05148	0.29868	0.00337	4.08319	0.05091	103	1628.5	21.5	1684.8	16.68	1651	10.17	0	5305
45_Z12C	5.30511	0.06627	0.33682	0.00371	5.30511	0.06627	100	1867.8	21.47	1871.3	17.87	1869.7	10.67	15	9169
45_Z12R	3.8536	0.04902	0.27708	0.00314	3.8536	0.04902	96	1640.3	22.04	1576.6	15.85	1604	10.26	1	2743
45_Z13R	4.00372	0.05056	0.28443	0.00322	4.48639	0.05582	97	1662.6	21.77	1613.6	14.75	1728.5	10.33	147	17565
45_Z14C	3.89274	0.06118	0.27779	0.00351	3.89274	0.06118	96	1654.6	26.98	1580.2	17.69	1612.2	12.7	0	3328
45_Z15C	3.98139	0.0513	0.28822	0.00325	3.98139	0.0513	100	1627.7	22.5	1632.6	16.29	1630.4	10.46	10	4742
45_Z16C	4.08892	0.05272	0.30036	0.0034	4.08892	0.05272	106	1600.5	22.54	1693.1	16.84	1652.1	10.52	0	5021
45_Z17C	3.9536	0.05275	0.28318	0.00317	3.9536	0.05275	98	1647.3	23.86	1607.4	15.9	1624.7	10.81	5	3399
45_Z18C	3.85655	0.05062	0.28251	0.0032	3.85655	0.05062	100	1605.6	23.07	1604	16.1	1604.6	10.58	4	3063
45_Z19C	4.16719	0.05472	0.30085	0.00341	4.16719	0.05472	104	1632.8	23.04	1695.5	16.88	1667.6	10.75	0	2903
45_Z20R	4.36231	0.05717	0.30162	0.00341	4.36231	0.05717	99	1712.6	22.79	1699.3	16.87	1705.2	10.83	7	2303
45_Z21C	4.99851	0.06667	0.32914	0.0037	4.60851	0.06027	102	1802.1	23.27	1834.2	17.01	1750.8	10.91	20	2295
45_Z22C	4.01136	0.04703	0.28864	0.00316	4.01136	0.04703	100	1639.1	20.55	1634.8	15.81	1636.5	9.53	0	4703
45_Z22R	3.82295	0.04526	0.27876	0.00306	3.82295	0.04526	98	1614.4	20.84	1585.1	15.43	1597.6	9.53	3	5648
45_Z23C	3.87618	0.04627	0.28251	0.0031	3.87618	0.04627	99	1615.3	21.07	1604	15.59	1608.7	9.63	0	4001
45_Z24C	3.78088	0.04533	0.27199	0.00299	3.78088	0.04533	95	1639.6	21.07	1550.9	15.16	1588.7	9.63	4	6305
45_Z26C	3.88462	0.04777	0.28221	0.00312	3.88462	0.04777	99	1621.3	21.73	1602.5	15.7	1610.5	9.93	0	4782
45_Z26R	2.98743	0.03703	0.23812	0.00263	2.98743	0.03703	95	1446.7	22.47	1376.9	13.7	1404.4	9.43	0	4742
45_Z27R	4.03637	0.05093	0.29485	0.00328	4.03637	0.05093	103	1611	22.4	1665.7	16.32	1641.6	10.27	9	3829
45_Z28C	4.56597	0.05677	0.30353	0.00339	4.56597	0.05677	96	1784.6	21.35	1708.8	16.75	1743.1	10.36	0	3318
45_Z28R	4.03768	0.04863	0.29431	0.00325	4.03768	0.04863	103	1615	21.21	1663	16.17	1641.8	9.8	2	4211
45_Z29AR	3.99546	0.04807	0.29128	0.00318	4.28129	0.05097	102	1614.7	21.42	1647.9	16.19	1689.8	9.8	0	3367
45_Z29C	4.28129	0.05097	0.296	0.00325	4.17992	0.05037	98	1712.7	20.65	1671.5	16.39	1670.1	9.87	0	4895
45_Z29R	4.17992	0.05037	0.30292	0.00331	3.99546	0.04807	105	1625.8	21.38	1705.8	15.86	1633.3	9.77	0	8819
45_Z30C	3.92865	0.0478	0.28674	0.00314	3.92865	0.0478	101	1612.5	21.72	1625.2	15.71	1619.6	9.85	0	5300
45_Z31C	3.96078	0.04909	0.28786	0.00315	3.96078	0.04909	101	1620.4	22.28	1630.8	15.78	1626.2	10.05	6	3009
45_Z32C	4.86577	0.05914	0.33106	0.0036	4.86577	0.05914	106	1742.2	21.46	1843.5	17.43	1796.3	10.24	0	3468
45_Z32R	4.10795	0.05162	0.29306	0.00321	4.10795	0.05162	100	1654.9	22.63	1656.8	15.99	1655.9	10.26	0	2999
45_Z33AC	4.63726	0.05735	0.31058	0.00337	4.00503	0.05011	98	1770.9	21.97	1743.6	15.93	1635.2	10.16	0	4647
45_Z33C	4.00503	0.05011	0.29346	0.0032	4.63726	0.05735	103	1605.2	22.72	1658.8	16.59	1756	10.33	13	4300
45_Z34C	3.93437	0.04698	0.28719	0.00309	3.93437	0.04698	101	1612.5	21.57	1627.4	15.46	1620.8	9.67	0	3636
45_Z35AC	4.00577	0.04782	0.28889	0.00311	3.94438	0.04669	100	1635	21.41	1636	15.29	1622.8	9.59	0	7088
45_Z35C	3.94438	0.04669	0.28416	0.00305	4.00577	0.04782	98	1636.9	21.26	1612.3	15.55	1635.4	9.7	6	6839
45_Z36AR	4.0356	0.04896	0.29554	0.00319	3.91965	0.04709	104	1606.6	21.87	1669.1	15.38	1617.7	9.72	0	2366
45_Z36C	3.91965	0.04709	0.28365	0.00306	4.0356	0.04896	99	1628.7	21.54	1609.7	15.88	1641.4	9.87	0	5912
45_Z36R	3.91477	0.04839	0.28518	0.00309	3.91477	0.04839	100	1616.5	22.32	1617.4	15.52	1616.7	10	0	3738

45_Z37R	3.81899	0.04815	0.27839	0.00303	3.81899	0.04815	98	1615.3	22.81	1583.2	15.3	1596.8	10.14	0	3337
45_Z38C	4.14115	0.05205	0.29447	0.0032	4.14115	0.05205	100	1661.4	22.58	1663.8	15.95	1662.5	10.28	0	5286
45_Z38R	3.97928	0.05154	0.2891	0.00317	3.97928	0.05154	101	1621.6	23.47	1637	15.86	1630	10.51	7	3038

APPENDIX C: WHOLE ROCK GEOCHEMISTRY

	RBN-11	RBN-13	RBN-28	RBN-37
major elements (wt%)				
SiO_2	72.5	48.7	48.1	52.5
TiO_2	0.37	2.135	1.01	0.585
Al_2O_3	14.8	17.4	28	23
Cr (ppm)	160	220	215	185
Cr_2O_3	0.016	0.022	0.0215	0.0185
Fe_2O_3	4.21	14.6	12	12.2
MnO	0.05	0.16	0.1	0.11
MgO	1.5	5.67	4.28	3
Zn (ppm)	85	205	130	105
CaO	0.92	5.39	0.57	1.09
Na_2O	0.97	0.55	0.57	0.85
K_2O	4.37	4.21	5.35	5.11
P_2O_5	0.03	0.94	0.04	0.05
LOI	0.75	0.97	0.53	1.88
Trace and REE (ppm)				
Sc	5	30	25	5
V	60	385	185	130
Ba	925	490	875	1825
Be	5	3.5	5.5	16
Hf	7	4	3	6
Sn	<10	<10	<10	<10
Ta	<2	3	<2	<2
Zr	220	100	120	240
Cs	1.1	9.5	2.3	2.3
Ga	17	32	33.5	36
Mo	1.2	0.8	1.3	0.8
Nb	4	29.5	16	3.5
Rb	170	550	165	190
Sr	150	110	140	165
Th	16.5	2.7	24.5	65
U	1	1.8	2.6	1.2
Y	14.5	60	22	17
Zr	48	47.5	32	26.5
Ce	70	70	85	200
Dy	3.5	13	6	5.5
Er	1.5	5	3.4	1.85
Eu	1.65	1.7	1.45	2.7
Gd	4.7	14.5	7.5	12
Ho	0.58	2	1.1	0.78
La	37.5	29	39.5	100
Lu	1.5	0.56	0.44	0.22
Nd	28.5	39	40.5	90
Pr	7.5	8.5	10.5	24
Sm	4.9	11	8	14
Tb	0.66	2.2	1	1.35
Tm	0.15	0.45	0.35	0.15
Yb	2.1	3.2	2.3	0.95

APPENDIX D: MONAZITE AND ZIRCON MORPHOLOGY

Monazite

RBN-11
Grains ranged in size between 100-400 µm and exhibited no zoning under BSE. The grains appeared rounded with a few broken fragments included. Some grains appeared to show inclusions and also included fractures.
RBN-12
Grains ranged in size between 100-400 µm and exhibited some zoning under BSE. The majority of grains appeared to be whole grains with a round or slightly elongate shape. Some grains were anhedral and these appeared to be partial grains. Quite a few of the grains were fractured. The cores of the grains showed 1750 ages while the rims and broken segments appeared to show younger ages.
RBN-26
Grains ranged in size between 100-400 µm and exhibit no zoning. There is an even mix of partial grains and whole grains, with the whole grains showing sub-rounded or slightly elongate shape. Fracturing within the grains appears minimal with only a few grains showing internal fracturing. Only one spot showed an age younger than the 1750 population, and this was taken from the centre of a partial grain.
RBN-28
Grains ranged in size between 100-200 µm and exhibit no zoning. The majority of grains are whole grains with a few partial grains. The grains appear well rounded with no elongation, only a few showing internal fracturing. Two spots that show a younger age come from a couple of the smaller grains.
RBN-31
Minimal monazites located within the sample. Of those found grains ranged in size from 100-150 µm and exhibited some zoning. The whole grains appeared sub-rounded with a few of them being partial grains which showed angular edges. Internal fractures were found only a a couple of monazites. Younger ages in this sample appear to be located either within smaller whole grains or on the rims of larger grains.
RBN-45
Minimal monazites are located within this sample. The grains range in size from 50-300 µm and exhibit no zoning. The grains appear to be partial grains which are very angular in shape and show large amounts of internal fracturing. Multiple spots on the same grain show the same age. The grains which appear more rounded and less fractured give a younger age, while the more fractured and angular partial grains tend to give the older age.
RBN-46
Highly angular and fractured monazites are located in this sample. They range in size from 200-600 µm and show no zoning. Highly anhedral grains with no set shape. One younger age was recorded in this sample and it was a spot located on a anhedral grain.
RBN-47
Grains range in size between 200-400 µm and exhibit no zoning. Very well rounded monazite grains showing no elongation, with only a few partial grains present. One significantly younger age was located on the edge of a partial monazite grain. Grains showing ages around 1700 appear to be smaller grains or cracked grains.

Zircon

RBN-34
Grains generally appear either elongate or rounded with a euhedral to subhedral crystal shape. They range in size from 100-200 µm. Minimal fracturing was found within the grains. Under CL the grains appeared to have bright concentric oscillatory zoning within the cores, with the rims showing less oscillatory zoning and are darker in nature. The rims dated did not seem to give any concordant age data.
RBN-45
Grains are a mix of elongate or rounded, with euhedral crystal shape. They are generally 200-400 µm in length, with an aspect ratio of 1:3 for the elongate grains. The grains are quite fractured. The older ages can be found in the cores of the grains which appear to be weakly oscillatory zoned. The younger ages can be found on more rounded grains which show minimal zoning, or on the rims of older zircon cores which also show minimal zoning.

APPENDIX E: MINERAL CHEMISTRY

Label	1	Gt1a__3	Gt1a__4	Gt1a__5	Gt1a__6	Gt1a__8	Gt1a__10	Gt1a__11	Gt1a__12	Gt1a__13
No	1	4	5	6	7	9	11	12	13	14
X	16889	9584	9434	9284	9134	8835	8535	8386	8236	8086
Y	-34805	-14894	-14651	-14408	-14165	-13679	-13193	-12950	-12707	-12464
Z	-305	226	226	226	226	226	226	226	227	227
Mineral	Gt	Gt1a__3	Gt1a__4	Gt1a__5	Gt1a__6	Gt1a__8	Gt1a__10	Gt1a__11	Gt1a__12	Gt1a__13
Ox%(Si)	39.56	37.25	35.03	37.16	37.12	36.19	35.83	37.71	35.45	35.22
Ox%(Ti)	0.09	0.04	0.02	0.00	0.01	0.03	0.00	0.06	0.05	0.00
Ox%(Al)	21.83	21.63	22.52	21.50	21.60	21.31	20.90	22.72	20.94	20.62
Ox%(Cr)	0.02	0.00	0.02	0.00	0.00	0.03	0.00	0.03	0.01	0.00
Ox%(Fe)	23.42	31.67	30.78	31.70	30.69	30.47	30.19	31.08	30.62	30.26
Ox%(Mn)	0.55	0.43	0.49	0.35	0.37	0.49	0.49	0.40	0.48	0.49
Ox%(Mg)	10.66	7.52	8.23	7.59	7.63	7.44	7.59	7.77	7.39	7.52
Ox%(Zn)										
Ox%(Ca)	4.07	1.38	1.31	1.29	1.41	1.45	1.44	1.23	1.41	1.40
Ox%(Na)	0.01	0.04	0.04	0.04	0.00	0.01	0.01	0.04	0.02	0.00
Ox%(K)	0.01	0.00	0.01	0.00	0.00	0.00	0.00	0.05	0.00	0.00
total	100.21	99.97	98.45	99.66	98.83	97.42	96.45	101.09	96.38	95.52
No. Oxygens	12	12	12	12	12	12	12	12	12	12
Si	3.00	2.93	2.81	2.94	2.94	2.92	2.92	2.92	2.90	2.91
Ti	0.01	0.00	0.00	0.00	0.00	0.00	0.00	0.00	0.00	0.00
Al	1.95	2.01	2.13	2.00	2.02	2.03	2.01	2.07	2.02	2.01
Cr	0.00	0.00	0.00	0.00	0.00	0.00	0.00	0.00	0.00	0.00
Fe2+	1.49	2.09	2.06	2.09	2.04	2.06	2.06	2.01	2.10	2.09
Mn2+	0.04	0.03	0.03	0.02	0.03	0.03	0.03	0.03	0.03	0.03
Mg	1.21	0.88	0.98	0.89	0.90	0.89	0.92	0.90	0.90	0.93
Zn	0.00	0.00	0.00	0.00	0.00	0.00	0.00	0.00	0.00	0.00
Ca	0.33	0.12	0.11	0.11	0.12	0.13	0.13	0.10	0.12	0.12
Na	0.00	0.01	0.01	0.01	0.00	0.00	0.00	0.01	0.00	0.00
K	0.00	0.00	0.00	0.00	0.00	0.00	0.00	0.00	0.00	0.00
total	8.02	8.06	8.13	8.07	8.05	8.06	8.07	8.05	8.09	8.09
X(alm)	0.49	0.67	0.65	0.67	0.66	0.66	0.66	0.66	0.66	0.66
X(py)	0.39	0.28	0.31	0.29	0.29	0.29	0.29	0.30	0.29	0.29
X(grs)	0.11	0.04	0.04	0.03	0.04	0.04	0.04	0.03	0.04	0.04
X(spss)	0.01	0.01	0.01	0.01	0.01	0.01	0.01	0.01	0.01	0.01
z(g)	0.11	0.04	0.04	0.04	0.04	0.04	0.04	0.03	0.04	0.04
X(Fe)	0.55	0.70	0.68	0.70	0.69	0.70	0.69	0.69	0.70	0.69

Gt1a__14	Gt1b__1	Gt1b__2	Gt1b__3	Gt1b__4	Gt1b__5	Gt1b__7	Gt1b__8	Gt1b__9	Gt1b__14	Gt1b__15
15	69	70	71	72	73	75	76	77	82	83
7936	9883	9797	9711	9625	9539	9367	9281	9195	8766	8680
-12221	-14721	-14543	-14365	-14187	-14009	-13653	-13475	-13297	-12407	-12229
227	232	232	233	233	234	235	236	236	240	240
Gt1a__14	Gt1b__1	Gt1b__2	Gt1b__3	Gt1b__4	Gt1b__5	Gt1b__7	Gt1b__8	Gt1b__9	Gt1b__14	Gt1b__15
34.97	37.30	37.61	36.84	35.93	37.01	97.14	97.85	96.70	36.28	36.16
0.00	0.00	0.00	0.04	0.04	0.00	0.01	0.00	0.04	0.00	0.00
20.60	21.42	22.05	21.34	19.43	21.35	0.00	0.00	0.02	21.16	20.83
0.01	0.00	0.01	0.02	0.00	0.00	0.00	0.00	0.00	0.00	0.01
29.88	31.24	30.64	31.93	31.13	31.73	0.05	0.03	0.05	31.10	30.49
0.45	0.47	0.42	0.39	0.47	0.39	0.00	0.04	0.00	0.43	0.30
7.68	7.48	7.74	7.52	7.24	7.70	0.03	0.00	0.00	7.55	7.41
1.47	1.37	1.35	1.38	1.38	1.47	0.00	0.00	0.00	1.46	1.45
0.04	0.00	0.02	0.02	0.01	0.00	0.00	0.03	0.01	0.00	0.00
0.01	0.00	0.00	0.00	0.01	0.00	0.00	0.02	0.00	0.00	0.01
95.11	99.27	99.85	99.48	95.65	99.65	97.24	97.98	96.84	97.97	96.67
12	12	12	12	12	12	12	12	12	12	12
2.90	2.95	2.95	2.92	2.97	2.93	6.00	6.00	5.99	2.92	2.94
0.00	0.00	0.00	0.00	0.00	0.00	0.00	0.00	0.00	0.00	0.00
2.01	2.00	2.04	2.00	1.89	1.99	0.00	0.00	0.00	2.01	2.00
0.00	0.00	0.00	0.00	0.00	0.00	0.00	0.00	0.00	0.00	0.00
2.07	2.07	2.01	2.12	2.15	2.10	0.00	0.00	0.00	2.09	2.07
0.03	0.03	0.03	0.03	0.03	0.03	0.00	0.00	0.00	0.03	0.02
0.95	0.88	0.90	0.89	0.89	0.91	0.00	0.00	0.00	0.91	0.90
0.00	0.00	0.00	0.00	0.00	0.00	0.00	0.00	0.00	0.00	0.00
0.13	0.12	0.11	0.12	0.12	0.12	0.00	0.00	0.00	0.13	0.13
0.01	0.00	0.00	0.00	0.00	0.00	0.00	0.00	0.00	0.00	0.00
0.00	0.00	0.00	0.00	0.00	0.00	0.00	0.00	0.00	0.00	0.00
8.10	8.05	8.04	8.08	8.08	8.08	6.00	6.01	6.00	8.08	8.06
0.65	0.67	0.66	0.67	0.67	0.66	0.52	0.42	0.88	0.66	0.66
0.30	0.28	0.30	0.28	0.28	0.29	0.47	0.02	0.01	0.29	0.29
0.04	0.04	0.04	0.04	0.04	0.04	0.00	0.04	0.11	0.04	0.04
0.01	0.01	0.01	0.01	0.01	0.01	0.00	0.51	0.00	0.01	0.01
0.04	0.04	0.04	0.04	0.04	0.04	0.00	0.08	0.11	0.04	0.04
0.69	0.70	0.69	0.70	0.71	0.70	0.53	0.95	0.99	0.70	0.70

Gt1b__17	gt1c start test	Gt1a_repeat__2	Gt1a_repeat__5	Gt1a_repeat__6	Gt1a_repeat__7	Gt1a_repeat__11
85	139	141	144	145	146	150
8508	-68	9704	9254	9104	8955	8355
-11873	879	-15204	-14476	-14233	-13990	-13019
241	267	226	228	228	229	231
Gt1b__17	gt1c start test	Gt1a_repeat__2	Gt1a_repeat__5	Gt1a_repeat__6	Gt1a_repeat__7	Gt1a_repeat__11
35.71	37.73	37.38	36.50	37.37	37.71	37.13
0.03	0.03	0.03	0.00	0.02	0.00	0.05
21.22	21.95	21.41	20.64	21.61	21.68	21.68
0.00	0.00	0.00	0.02	0.00	0.00	0.00
31.84	30.79	32.04	32.08	31.48	31.46	31.24
0.49	0.39	0.49	0.43	0.33	0.42	0.40
6.91	7.80	7.12	7.10	7.60	7.66	7.91
1.55	1.48	1.53	1.40	1.37	1.50	1.52
0.05	0.06	0.06	0.01	0.00	0.03	0.00
0.02	0.00	0.00	0.01	0.00	0.00	0.00
97.82	100.24	100.06	98.19	99.79	100.46	99.94
12	12	12	12	12	12	12
2.89	2.95	2.95	2.94	2.94	2.95	2.92
0.00	0.00	0.00	0.00	0.00	0.00	0.00
2.03	2.02	1.99	1.96	2.01	2.00	2.01
0.00	0.00	0.00	0.00	0.00	0.00	0.00
2.16	2.01	2.11	2.16	2.07	2.06	2.06
0.03	0.03	0.03	0.03	0.02	0.03	0.03
0.84	0.91	0.84	0.85	0.89	0.89	0.93
0.00	0.00	0.00	0.00	0.00	0.00	0.00
0.13	0.12	0.13	0.12	0.12	0.13	0.13
0.01	0.01	0.01	0.00	0.00	0.00	0.00
0.00	0.00	0.00	0.00	0.00	0.00	0.00
8.09	8.05	8.06	8.08	8.05	8.05	8.07
0.68	0.66	0.68	0.68	0.67	0.66	0.66
0.26	0.30	0.27	0.27	0.29	0.29	0.30
0.04	0.04	0.04	0.04	0.04	0.04	0.04
0.01	0.01	0.01	0.01	0.01	0.01	0.01
0.04	0.04	0.04	0.04	0.04	0.04	0.04
0.72	0.69	0.72	0.72	0.70	0.70	0.69

Gt1a_repeat__12	Gt1a_repeat__13	Gt1a_repeat__14	Gt1a_repeat__16	Gt1a_repeat__62	Gt1a_repeat__63
151	152	153	155	201	202
8205	8055	7905	7605	710	560
-12777	-12534	-12291	-11805	-638	-395
232	233	233	234	262	262
Gt1a_repeat__12	Gt1a_repeat__13	Gt1a_repeat__14	Gt1a_repeat__16	Gt1a_repeat__62	Gt1a_repeat__63
37.13	38.40	37.11	37.61	37.20	37.67
0.05	0.07	0.02	0.06	0.06	0.04
21.58	21.95	21.57	21.40	21.87	21.44
0.01	0.01	0.00	0.00	0.03	0.00
30.86	32.21	30.83	31.83	31.00	31.54
0.37	0.52	0.43	0.50	0.52	0.37
7.73	7.29	7.80	7.68	7.71	7.95
1.49	1.47	1.47	1.50	1.45	1.47
0.03	0.02	0.00	0.00	0.03	0.02
0.00	0.03	0.00	0.02	0.01	0.01
99.26	101.97	99.23	100.60	99.88	100.50
12	12	12	12	12	12
2.94	2.96	2.94	2.95	2.92	2.95
0.00	0.00	0.00	0.00	0.00	0.00
2.01	2.00	2.01	1.97	2.03	1.98
0.00	0.00	0.00	0.00	0.00	0.00
2.04	2.08	2.04	2.08	2.04	2.06
0.02	0.03	0.03	0.03	0.03	0.02
0.91	0.84	0.92	0.90	0.90	0.93
0.00	0.00	0.00	0.00	0.00	0.00
0.13	0.12	0.12	0.13	0.12	0.12
0.00	0.00	0.00	0.00	0.00	0.00
0.00	0.00	0.00	0.00	0.00	0.00
8.06	8.04	8.06	8.07	8.06	8.07
0.66	0.68	0.66	0.66	0.66	0.66
0.29	0.27	0.30	0.29	0.29	0.30
0.04	0.04	0.04	0.04	0.04	0.04
0.01	0.01	0.01	0.01	0.01	0.01
0.04	0.04	0.04	0.04	0.04	0.04
0.69	0.71	0.69	0.70	0.69	0.69

Gt1a_repeat__64	Gt1a_repeat__65	Gt1a_repeat__66	Gt1a_repeat__67	Gt1b__1	Gt1b__2	Gt1b__3	Gt1b__5
203	204	205	206	207	208	209	211
410	260	110	-40	9883	9797	9711	9539
-152	90	333	576	-14721	-14543	-14365	-14009
263	263	264	265	237	237	238	239
Gt1a_repeat__64	Gt1a_repeat__65	Gt1a_repeat__66	Gt1a_repeat__67	Gt1b__1	Gt1b__2	Gt1b__3	Gt1b__5
37.22	37.11	38.33	37.98	38.14	37.77	37.56	37.30
0.02	0.07	0.01	0.03	0.00	0.02	0.03	0.02
21.64	21.58	22.21	21.75	21.63	21.56	21.65	21.53
0.00	0.02	0.00	0.00	0.00	0.00	0.00	0.02
30.87	31.20	30.98	30.91	31.96	31.36	31.75	30.96
0.42	0.36	0.46	0.42	0.39	0.40	0.29	0.50
7.75	7.85	8.07	7.71	7.51	7.81	7.34	7.40
1.50	1.46	1.41	1.50	1.45	1.37	1.31	1.31
0.04	0.00	0.03	0.00	0.00	0.02	0.03	0.03
0.00	0.00	0.02	0.01	0.00	0.00	0.02	0.00
99.45	99.65	101.53	100.30	101.09	100.32	99.99	99.07
12	12	12	12	12	12	12	12
2.94	2.93	2.95	2.96	2.97	2.96	2.95	2.95
0.00	0.00	0.00	0.00	0.00	0.00	0.00	0.00
2.01	2.01	2.02	2.00	1.98	1.99	2.01	2.01
0.00	0.00	0.00	0.00	0.00	0.00	0.00	0.00
2.04	2.06	1.99	2.02	2.08	2.05	2.09	2.05
0.03	0.02	0.03	0.03	0.03	0.03	0.02	0.03
0.91	0.92	0.93	0.90	0.87	0.91	0.86	0.87
0.00	0.00	0.00	0.00	0.00	0.00	0.00	0.00
0.13	0.12	0.12	0.13	0.12	0.11	0.11	0.11
0.01	0.00	0.00	0.00	0.00	0.00	0.00	0.00
0.00	0.00	0.00	0.00	0.00	0.00	0.00	0.00
8.06	8.07	8.04	8.03	8.04	8.05	8.05	8.04
0.66	0.66	0.65	0.66	0.67	0.66	0.68	0.67
0.29	0.30	0.30	0.29	0.28	0.29	0.28	0.28
0.04	0.04	0.04	0.04	0.04	0.04	0.04	0.04
0.01	0.01	0.01	0.01	0.01	0.01	0.01	0.01
0.04	0.04	0.04	0.04	0.04	0.04	0.04	0.04
0.69	0.69	0.68	0.69	0.70	0.69	0.71	0.70

Gt1b__14	Gt1b__15	Gt1b__17	Gt1b__50	Gt1b__52	Gt1b__53	Gt1b__54	Gt1b__55	Gt1b__56	Gt1b__57
220	221	223	256	258	259	260	261	262	263
8766	8680	8508	5672	5500	5414	5328	5242	5156	5070
-12407	-12229	-11873	-5999	-5643	-5465	-5287	-5109	-4931	-4753
246	247	248	272	274	274	275	276	277	277
Gt1b__14	Gt1b__15	Gt1b__17	Gt1b__50	Gt1b__52	Gt1b__53	Gt1b__54	Gt1b__55	Gt1b__56	Gt1b__57
36.58	39.59	36.67	36.35	35.97	35.47	35.70	36.10	36.50	35.57
0.00	0.04	0.00	0.02	0.00	0.00	0.00	0.00	0.02	0.04
21.65	20.10	21.47	21.03	21.37	20.96	20.99	21.30	21.53	21.05
0.02	0.00	0.00	0.00	0.02	0.00	0.01	0.00	0.00	0.00
31.24	29.20	31.84	32.35	31.95	32.17	33.12	31.85	32.03	31.37
0.41	0.45	0.40	0.47	0.38	0.56	0.42	0.54	0.45	0.44
7.39	6.95	7.02	6.41	6.74	6.82	6.29	7.08	7.30	7.36
1.57	1.46	1.51	1.45	1.37	1.41	1.43	1.42	1.43	1.35
0.00	0.03	0.02	0.05	0.00	0.04	0.04	0.01	0.03	0.05
0.00	0.04	0.01	0.00	0.00	0.00	0.00	0.00	0.00	0.03
98.86	97.85	98.93	98.13	97.80	97.43	98.01	98.30	99.28	97.27
12	12	12	12	12	12	12	12	12	12
2.91	3.13	2.93	2.94	2.91	2.89	2.90	2.91	2.91	2.89
0.00	0.00	0.00	0.00	0.00	0.00	0.00	0.00	0.00	0.00
2.03	1.88	2.02	2.00	2.04	2.02	2.01	2.02	2.02	2.02
0.00	0.00	0.00	0.00	0.00	0.00	0.00	0.00	0.00	0.00
2.08	1.93	2.12	2.19	2.16	2.19	2.25	2.14	2.13	2.13
0.03	0.03	0.03	0.03	0.03	0.04	0.03	0.04	0.03	0.03
0.88	0.82	0.83	0.77	0.81	0.83	0.76	0.85	0.87	0.89
0.00	0.00	0.00	0.00	0.00	0.00	0.00	0.00	0.00	0.00
0.13	0.12	0.13	0.13	0.12	0.12	0.12	0.12	0.12	0.12
0.00	0.00	0.00	0.01	0.00	0.01	0.01	0.00	0.00	0.01
0.00	0.00	0.00	0.00	0.00	0.00	0.00	0.00	0.00	0.00
8.07	7.93	8.07	8.06	8.07	8.10	8.09	8.08	8.08	8.10
0.67	0.67	0.68	0.70	0.69	0.69	0.71	0.68	0.68	0.67
0.28	0.28	0.27	0.25	0.26	0.26	0.24	0.27	0.27	0.28
0.04	0.04	0.04	0.04	0.04	0.04	0.04	0.04	0.04	0.04
0.01	0.01	0.01	0.01	0.01	0.01	0.01	0.01	0.01	0.01
0.04	0.04	0.04	0.04	0.04	0.04	0.04	0.04	0.04	0.04
0.70	0.70	0.72	0.74	0.73	0.73	0.75	0.72	0.71	0.70

Gt1b__59	Gt1b__61	Gt1b__62	Gt1b__63	Gt1b__64	Gt1c__1	Gt1c__2	Gt1c__3	Gt1c__4	Gt1c__29	Gt1c__34
265	267	268	269	270	323	324	325	326	351	356
4899	4727	4641	4555	4469	9883	9758	9633	9508	6380	5755
-4396	-4040	-3862	-3684	-3506	-8954	-8831	-8707	-8584	-5500	-4884
279	280	281	282	283	303	303	303	302	291	288
Gt1b__59	Gt1b__61	Gt1b__62	Gt1b__63	Gt1b__64	Gt1c__1	Gt1c__2	Gt1c__3	Gt1c__4	Gt1c__29	Gt1c__34
35.80	38.57	35.68	35.94	38.99	36.81	36.23	37.14	38.76	35.09	35.46
0.00	0.07	0.00	0.00	0.00	0.02	0.01	0.02	0.00	0.01	0.00
21.24	22.76	21.02	21.25	21.70	21.58	21.12	21.60	22.68	20.50	20.98
0.01	0.02	0.00	0.01	0.02	0.00	0.02	0.01	0.02	0.00	0.00
31.25	30.36	31.20	32.34	32.86	31.57	31.30	31.94	32.09	33.46	32.45
0.40	0.37	0.54	0.44	0.46	0.45	0.47	0.50	0.48	0.43	0.57
7.23	8.02	7.00	6.89	6.29	7.51	7.10	7.22	7.08	4.55	6.17
1.50	1.40	1.48	1.38	1.35	1.45	1.45	1.43	1.32	1.60	1.40
0.00	0.03	0.00	0.00	0.04	0.01	0.05	0.03	0.02	0.00	0.03
0.01	0.02	0.00	0.00	0.02	0.03	0.02	0.02	0.03	0.02	0.00
97.44	101.62	96.91	98.27	101.73	99.45	97.75	99.90	102.48	95.66	97.06
12	12	12	12	12	12	12	12	12	12	12
2.90	2.95	2.91	2.90	3.02	2.92	2.93	2.93	2.96	2.94	2.91
0.00	0.00	0.00	0.00	0.00	0.00	0.00	0.00	0.00	0.00	0.00
2.03	2.05	2.02	2.02	1.98	2.02	2.01	2.01	2.04	2.02	2.03
0.00	0.00	0.00	0.00	0.00	0.00	0.00	0.00	0.00	0.00	0.00
2.12	1.94	2.13	2.18	2.13	2.09	2.11	2.11	2.05	2.34	2.22
0.03	0.02	0.04	0.03	0.03	0.03	0.03	0.03	0.03	0.03	0.04
0.87	0.92	0.85	0.83	0.73	0.89	0.85	0.85	0.81	0.57	0.75
0.00	0.00	0.00	0.00	0.00	0.00	0.00	0.00	0.00	0.00	0.00
0.13	0.12	0.13	0.12	0.11	0.12	0.13	0.12	0.11	0.14	0.12
0.00	0.00	0.00	0.00	0.01	0.00	0.01	0.00	0.00	0.00	0.00
0.00	0.00	0.00	0.00	0.00	0.00	0.00	0.00	0.00	0.00	0.00
8.08	8.02	8.08	8.09	8.00	8.07	8.07	8.06	8.02	8.05	8.08
0.67	0.65	0.68	0.69	0.71	0.67	0.68	0.68	0.68	0.76	0.71
0.28	0.31	0.27	0.26	0.24	0.28	0.27	0.27	0.27	0.18	0.24
0.04	0.04	0.04	0.04	0.04	0.04	0.04	0.04	0.04	0.05	0.04
0.01	0.01	0.01	0.01	0.01	0.01	0.01	0.01	0.01	0.01	0.01
0.04	0.04	0.04	0.04	0.04	0.04	0.04	0.04	0.04	0.05	0.04
0.71	0.68	0.71	0.72	0.75	0.70	0.71	0.71	0.72	0.80	0.75

Gt1c__36	Gt1c__37	Gt1c__43	Gt1c__44	Gt1c__45	Gt1c__47	Gt1c__49	Gt1c__79	Gt1c__80	Gt2a__1	Gt2a__8
358	359	365	366	367	369	371	401	402	403	410
5504	5379	4629	4504	4379	4128	3878	125	0	-4669	-4200
-4637	-4514	-3774	-3650	-3527	-3280	-3034	667	790	-1696	-1454
288	287	284	284	283	283	282	268	267	169	178
Gt1c__36	Gt1c__37	Gt1c__43	Gt1c__44	Gt1c__45	Gt1c__47	Gt1c__49	Gt1c__79	Gt1c__80	Gt2a__1	Gt2a__8
35.70	37.29	36.53	36.48	35.92	36.13	36.00	37.19	37.70	36.24	36.79
0.02	0.00	0.03	0.02	0.04	0.00	0.00	0.01	0.03	0.04	0.00
21.11	22.11	21.05	21.27	21.26	21.29	20.95	21.57	21.79	61.52	21.25
0.02	0.01	0.00	0.01	0.01	0.01	0.02	0.00	0.00	0.02	0.01
32.93	32.65	31.39	32.62	32.53	32.22	33.33	30.39	30.87	0.62	34.04
0.47	0.52	0.59	0.56	0.45	0.53	0.50	0.47	0.54	0.00	0.49
6.12	6.74	6.96	6.25	6.57	6.81	5.37	7.82	7.89	0.00	5.48
1.41	1.42	1.47	1.50	1.40	1.40	1.47	1.54	1.54	0.01	1.47
0.04	0.02	0.02	0.01	0.03	0.02	0.00	0.06	0.02	0.00	0.02
0.02	0.00	0.02	0.00	0.04	0.00	0.00	0.01	0.00	0.01	0.03
97.85	100.77	98.07	98.71	98.26	98.41	97.64	99.07	100.39	98.46	99.57
12	12	12	12	12	12	12	12	12	12	12
2.91	2.92	2.94	2.93	2.90	2.91	2.94	2.94	2.94	2.39	2.95
0.00	0.00	0.00	0.00	0.00	0.00	0.00	0.00	0.00	0.00	0.00
2.03	2.04	2.00	2.01	2.03	2.02	2.02	2.01	2.01	4.78	2.01
0.00	0.00	0.00	0.00	0.00	0.00	0.00	0.00	0.00	0.00	0.00
2.24	2.14	2.11	2.19	2.20	2.17	2.28	2.01	2.02	0.03	2.28
0.03	0.03	0.04	0.04	0.03	0.04	0.03	0.03	0.04	0.00	0.03
0.74	0.79	0.84	0.75	0.79	0.82	0.65	0.92	0.92	0.00	0.65
0.00	0.00	0.00	0.00	0.00	0.00	0.00	0.00	0.00	0.00	0.00
0.12	0.12	0.13	0.13	0.12	0.12	0.13	0.13	0.13	0.00	0.13
0.01	0.00	0.00	0.00	0.00	0.00	0.00	0.01	0.00	0.00	0.00
0.00	0.00	0.00	0.00	0.00	0.00	0.00	0.00	0.00	0.00	0.00
8.08	8.06	8.06	8.06	8.08	8.08	8.05	8.06	8.05	7.21	8.05
0.71	0.69	0.68	0.71	0.70	0.69	0.74	0.65	0.65	0.99	0.74
0.24	0.26	0.27	0.24	0.25	0.26	0.21	0.30	0.30	0.00	0.21
0.04	0.04	0.04	0.04	0.04	0.04	0.04	0.04	0.04	0.01	0.04
0.01	0.01	0.01	0.01	0.01	0.01	0.01	0.01	0.01	0.00	0.01
0.04	0.04	0.04	0.04	0.04	0.04	0.04	0.04	0.04	0.01	0.04
0.75	0.73	0.72	0.75	0.74	0.73	0.78	0.69	0.69	1.00	0.78

Gt2a__9	Gt2a__14	Gt2a__15	Gt2a__16	Gt2a__17	Gt2a__18	Gt2a__51	Gt2a__52	Gt2a__53	Gt2a__56	Gt2a__57
411	416	417	418	419	420	453	454	455	458	459
-4133	-3798	-3731	-3664	-3597	-3530	-1318	-1251	-1184	-982	-915
-1420	-1247	-1212	-1178	-1143	-1109	31	66	100	204	238
180	187	188	190	191	192	239	240	241	246	247
Gt2a__9	Gt2a__14	Gt2a__15	Gt2a__16	Gt2a__17	Gt2a__18	Gt2a__51	Gt2a__52	Gt2a__53	Gt2a__56	Gt2a__57
37.10	36.86	37.02	37.14	37.36	36.81	37.38	37.19	36.72	37.18	36.93
0.03	0.00	0.02	0.00	0.03	0.05	0.00	0.02	0.01	0.04	0.01
21.07	21.33	21.87	21.36	21.48	21.29	21.72	21.12	21.54	21.67	21.54
0.01	0.02	0.00	0.00	0.03	0.01	0.00	0.00	0.01	0.01	0.00
33.58	34.20	32.71	33.37	33.37	33.39	30.91	30.64	30.81	31.11	30.84
0.54	0.60	0.50	0.52	0.56	0.46	0.41	0.34	0.51	0.44	0.44
5.66	5.57	6.30	6.32	5.91	5.34	7.63	7.43	7.72	7.73	7.62
1.40	1.42	1.42	1.48	1.45	1.56	1.48	1.45	1.43	1.53	1.51
0.02	0.03	0.07	0.00	0.02	0.04	0.05	0.00	0.01	0.00	0.02
0.00	0.00	0.00	0.01	0.02	0.00	0.01	0.00	0.01	0.02	0.00
99.41	100.03	99.91	100.20	100.23	98.96	99.60	98.19	98.78	99.72	98.90
12	12	12	12	12	12	12	12	12	12	12
2.97	2.94	2.93	2.94	2.96	2.96	2.94	2.97	2.92	2.93	2.93
0.00	0.00	0.00	0.00	0.00	0.00	0.00	0.00	0.00	0.00	0.00
1.99	2.01	2.04	1.99	2.00	2.02	2.02	1.99	2.02	2.01	2.02
0.00	0.00	0.00	0.00	0.00	0.00	0.00	0.00	0.00	0.00	0.00
2.25	2.28	2.17	2.21	2.21	2.24	2.04	2.05	2.05	2.05	2.05
0.04	0.04	0.03	0.03	0.04	0.03	0.03	0.02	0.03	0.03	0.03
0.68	0.66	0.74	0.75	0.70	0.64	0.90	0.88	0.92	0.91	0.90
0.00	0.00	0.00	0.00	0.00	0.00	0.00	0.00	0.00	0.00	0.00
0.12	0.12	0.12	0.13	0.12	0.13	0.13	0.12	0.12	0.13	0.13
0.00	0.01	0.01	0.00	0.00	0.01	0.01	0.00	0.00	0.00	0.00
0.00	0.00	0.00	0.00	0.00	0.00	0.00	0.00	0.00	0.00	0.00
8.04	8.06	8.05	8.06	8.04	8.03	8.05	8.04	8.07	8.06	8.06
0.73	0.73	0.71	0.71	0.72	0.74	0.66	0.66	0.66	0.66	0.66
0.22	0.21	0.24	0.24	0.23	0.21	0.29	0.29	0.29	0.29	0.29
0.04	0.04	0.04	0.04	0.04	0.04	0.04	0.04	0.04	0.04	0.04
0.01	0.01	0.01	0.01	0.01	0.01	0.01	0.01	0.01	0.01	0.01
0.04	0.04	0.04	0.04	0.04	0.04	0.04	0.04	0.04	0.04	0.04
0.77	0.78	0.74	0.75	0.76	0.78	0.69	0.70	0.69	0.69	0.69

Gt2a__59	Gt2a__60	Gt2a__61	Gt2a__62	Gt2a__63	Gt2a__64	Gt2a__65	Gt2a__66	Gt2a__67	Gt2a__68
461	462	463	464	465	466	467	468	469	470
-781	-714	-647	-580	-513	-446	-379	-312	-245	-178
307	342	377	411	446	480	515	549	584	618
250	251	253	254	255	257	258	260	261	262
Gt2a__59	Gt2a__60	Gt2a__61	Gt2a__62	Gt2a__63	Gt2a__64	Gt2a__65	Gt2a__66	Gt2a__67	Gt2a__68
38.65	37.23	37.45	36.95	37.18	37.22	37.35	37.84	37.37	37.24
0.01	0.02	0.00	0.03	0.01	0.06	0.03	0.00	0.04	0.00
22.44	21.51	21.36	21.19	21.54	21.50	21.75	21.39	21.49	21.47
0.00	0.03	0.01	0.00	0.00	0.00	0.03	0.00	0.00	0.00
30.48	30.43	30.34	30.29	30.31	30.61	30.48	31.10	30.71	30.49
0.42	0.42	0.38	0.37	0.46	0.39	0.43	0.44	0.38	0.51
8.20	7.69	7.52	7.45	7.83	7.76	7.85	7.65	7.75	7.91
1.47	1.50	1.52	1.51	1.41	1.40	1.47	1.52	1.49	1.50
0.02	0.03	0.00	0.04	0.00	0.02	0.04	0.00	0.01	0.02
0.00	0.00	0.01	0.00	0.00	0.01	0.00	0.00	0.02	0.00
101.68	98.87	98.61	97.84	98.74	98.97	99.44	99.94	99.27	99.14
12	12	12	12	12	12	12	12	12	12
2.96	2.95	2.97	2.96	2.95	2.95	2.94	2.97	2.95	2.94
0.00	0.00	0.00	0.00	0.00	0.00	0.00	0.00	0.00	0.00
2.03	2.01	2.00	2.00	2.01	2.01	2.02	1.98	2.00	2.00
0.00	0.00	0.00	0.00	0.00	0.00	0.00	0.00	0.00	0.00
1.95	2.02	2.01	2.03	2.01	2.03	2.01	2.04	2.03	2.02
0.03	0.03	0.03	0.03	0.03	0.03	0.03	0.03	0.03	0.03
0.94	0.91	0.89	0.89	0.93	0.92	0.92	0.90	0.91	0.93
0.00	0.00	0.00	0.00	0.00	0.00	0.00	0.00	0.00	0.00
0.12	0.13	0.13	0.13	0.12	0.12	0.12	0.13	0.13	0.13
0.00	0.01	0.00	0.01	0.00	0.00	0.01	0.00	0.00	0.00
0.00	0.00	0.00	0.00	0.00	0.00	0.00	0.00	0.00	0.00
8.03	8.05	8.03	8.04	8.05	8.05	8.05	8.04	8.05	8.06
0.64	0.65	0.66	0.66	0.65	0.66	0.65	0.66	0.66	0.65
0.31	0.29	0.29	0.29	0.30	0.30	0.30	0.29	0.29	0.30
0.04	0.04	0.04	0.04	0.04	0.04	0.04	0.04	0.04	0.04
0.01	0.01	0.01	0.01	0.01	0.01	0.01	0.01	0.01	0.01
0.04	0.04	0.04	0.04	0.04	0.04	0.04	0.04	0.04	0.04
0.68	0.69	0.69	0.70	0.68	0.69	0.69	0.70	0.69	0.68

Gt2a__69	Gt2a__71	Gt2b__1	Gt2b__2	Gt2b__3	Gt2b__4	Gt2b__5	Gt2b__6	Gt2b__7	Gt2b__10	Gt2b__11
471	473	474	475	476	477	478	479	480	483	484
-111	23	-4656	-4553	-4449	-4346	-4242	-4139	-4035	-3725	-3621
653	722	-2395	-2292	-2189	-2085	-1982	-1879	-1776	-1466	-1363
264	267	157	159	162	165	168	171	173	182	185
Gt2a__69	Gt2a__71	Gt2b__1	Gt2b__2	Gt2b__3	Gt2b__4	Gt2b__5	Gt2b__6	Gt2b__7	Gt2b__10	Gt2b__11
37.14	37.63	36.24	37.05	35.98	36.52	36.27	36.02	36.39	36.08	36.33
0.00	0.01	0.05	0.07	0.05	0.01	0.04	0.04	0.00	0.00	0.00
21.47	21.58	21.40	22.09	21.33	21.05	20.99	21.23	21.28	21.10	21.07
0.00	0.00	0.00	0.00	0.00	0.00	0.00	0.00	0.00	0.00	0.01
30.93	30.60	32.32	31.25	31.68	31.24	31.43	31.68	32.09	33.18	31.97
0.34	0.43	0.48	0.48	0.48	0.41	0.59	0.48	0.42	0.52	0.38
7.64	7.72	6.96	7.17	6.64	6.87	6.66	6.45	6.45	5.65	6.47
1.51	1.49	1.46	1.32	1.32	1.39	1.47	1.43	1.48	1.40	1.55
0.01	0.01	0.04	0.02	0.00	0.02	0.03	0.02	0.05	0.02	0.03
0.00	0.00	0.00	0.00	0.01	0.02	0.00	0.01	0.01	0.00	0.02
99.06	99.46	98.95	99.43	97.48	97.54	97.48	97.37	98.17	97.96	97.82
12	12	12	12	12	12	12	12	12	12	12
2.94	2.96	2.90	2.93	2.92	2.95	2.94	2.93	2.93	2.93	2.94
0.00	0.00	0.00	0.00	0.00	0.00	0.00	0.00	0.00	0.00	0.00
2.01	2.00	2.02	2.06	2.04	2.00	2.01	2.03	2.02	2.02	2.01
0.00	0.00	0.00	0.00	0.00	0.00	0.00	0.00	0.00	0.00	0.00
2.05	2.01	2.16	2.06	2.15	2.11	2.13	2.15	2.16	2.26	2.16
0.02	0.03	0.03	0.03	0.03	0.03	0.04	0.03	0.03	0.04	0.03
0.90	0.91	0.83	0.84	0.80	0.83	0.80	0.78	0.77	0.69	0.78
0.00	0.00	0.00	0.00	0.00	0.00	0.00	0.00	0.00	0.00	0.00
0.13	0.13	0.13	0.11	0.11	0.12	0.13	0.12	0.13	0.12	0.13
0.00	0.00	0.01	0.00	0.00	0.00	0.01	0.00	0.01	0.00	0.00
0.00	0.00	0.00	0.00	0.00	0.00	0.00	0.00	0.00	0.00	0.00
8.06	8.04	8.09	8.04	8.06	8.05	8.06	8.06	8.06	8.06	8.06
0.66	0.66	0.69	0.68	0.69	0.68	0.69	0.70	0.70	0.73	0.70
0.29	0.29	0.26	0.28	0.26	0.27	0.26	0.25	0.25	0.22	0.25
0.04	0.04	0.04	0.04	0.04	0.04	0.04	0.04	0.04	0.04	0.04
0.01	0.01	0.01	0.01	0.01	0.01	0.01	0.01	0.01	0.01	0.01
0.04	0.04	0.04	0.04	0.04	0.04	0.04	0.04	0.04	0.04	0.04
0.69	0.69	0.72	0.71	0.73	0.72	0.73	0.73	0.74	0.77	0.73

Gt2b__12	Gt2b__13	Gt2c__1	Gt2c__2	Gt2c__4	Gt2c__5	Gt2c__6	Gt2c__7	Gt2c__8	Gt2c__9	Gt2c__11	Gt2c__12
485	486	520	521	523	524	525	526	527	528	530	531
-3518	-3414	-4656	-4573	-4407	-4323	-4240	-4157	-4074	-3991	-3825	-3741
-1260	-1156	-4669	-4576	-4389	-4295	-4202	-4109	-4015	-3922	-3735	-3642
187	190	133	135	140	142	144	147	149	151	156	158
Gt2b__12	Gt2b__13	Gt2c__1	Gt2c__2	Gt2c__4	Gt2c__5	Gt2c__6	Gt2c__7	Gt2c__8	Gt2c__9	Gt2c__11	Gt2c__12
36.52	38.48	36.21	36.04	36.98	38.99	35.84	36.49	36.34	36.06	36.58	36.52
0.03	0.00	0.00	0.01	0.01	0.00	0.01	0.09	0.03	0.07	0.02	0.00
21.29	22.46	21.31	21.21	21.15	23.17	20.95	21.04	21.23	21.19	21.20	21.15
0.00	0.02	0.03	0.01	0.00	0.00	0.01	0.01	0.00	0.00	0.00	0.02
32.35	31.13	31.32	31.80	31.88	31.55	31.30	31.87	31.98	32.01	32.01	31.98
0.43	0.51	0.49	0.41	0.49	0.38	0.40	0.45	0.44	0.51	0.44	0.41
6.47	6.37	6.82	6.95	6.84	7.78	6.79	6.75	6.97	7.05	6.77	6.79
1.48	1.89	1.45	1.41	1.44	1.45	1.37	1.45	1.36	1.49	1.43	1.34
0.07	0.05	0.01	0.03	0.05	0.01	0.00	0.00	0.01	0.04	0.02	0.04
0.01	0.01	0.00	0.01	0.00	0.03	0.03	0.01	0.00	0.01	0.00	0.00
98.65	100.92	97.64	97.88	98.85	103.36	96.69	98.16	98.35	98.42	98.50	98.24
12	12	12	12	12	12	12	12	12	12	12	12
2.93	2.98	2.93	2.91	2.95	2.95	2.93	2.94	2.92	2.90	2.94	2.94
0.00	0.00	0.00	0.00	0.00	0.00	0.00	0.01	0.00	0.00	0.00	0.00
2.01	2.05	2.03	2.02	1.99	2.06	2.02	2.00	2.01	2.01	2.01	2.01
0.00	0.00	0.00	0.00	0.00	0.00	0.00	0.00	0.00	0.00	0.00	0.00
2.17	2.02	2.12	2.15	2.13	1.99	2.14	2.15	2.15	2.15	2.15	2.15
0.03	0.03	0.03	0.03	0.03	0.02	0.03	0.03	0.03	0.03	0.03	0.03
0.77	0.74	0.82	0.84	0.81	0.88	0.83	0.81	0.84	0.85	0.81	0.81
0.00	0.00	0.00	0.00	0.00	0.00	0.00	0.00	0.00	0.00	0.00	0.00
0.13	0.16	0.13	0.12	0.12	0.12	0.12	0.13	0.12	0.13	0.12	0.12
0.01	0.01	0.00	0.01	0.01	0.00	0.00	0.00	0.00	0.01	0.00	0.01
0.00	0.00	0.00	0.00	0.00	0.00	0.00	0.00	0.00	0.00	0.00	0.00
8.06	7.99	8.06	8.08	8.05	8.02	8.06	8.06	8.07	8.09	8.06	8.06
0.70	0.69	0.68	0.69	0.69	0.66	0.69	0.69	0.69	0.68	0.69	0.69
0.25	0.25	0.27	0.27	0.26	0.29	0.27	0.26	0.27	0.27	0.26	0.26
0.04	0.05	0.04	0.04	0.04	0.04	0.04	0.04	0.04	0.04	0.04	0.04
0.01	0.01	0.01	0.01	0.01	0.01	0.01	0.01	0.01	0.01	0.01	0.01
0.04	0.05	0.04	0.04	0.04	0.04	0.04	0.04	0.04	0.04	0.04	0.04
0.74	0.73	0.72	0.72	0.72	0.69	0.72	0.73	0.72	0.72	0.73	0.73

Gt2c__13	Gt2c__14	Gt2c__15	Gt2c__16	Gt2c__17	Gt2c__18	Gt2c__19	Gt2c__20	Gt2c__21	Gt2c__22	Gt2c__45
532	533	534	535	536	537	538	539	540	541	564
-3658	-3575	-3492	-3409	-3326	-3243	-3159	-3076	-2993	-2910	-998
-3548	-3455	-3362	-3268	-3175	-3082	-2988	-2895	-2801	-2708	-560
161	163	166	168	170	173	175	177	180	182	236
Gt2c__13	Gt2c__14	Gt2c__15	Gt2c__16	Gt2c__17	Gt2c__18	Gt2c__19	Gt2c__20	Gt2c__21	Gt2c__22	Gt2c__45
36.37	36.84	37.53	36.78	36.30	36.67	36.30	36.53	36.24	35.12	37.80
0.05	0.07	0.02	0.00	0.02	0.00	0.03	0.02	0.02	0.03	0.00
21.18	21.05	21.65	21.15	21.09	21.30	21.08	21.14	21.34	20.54	21.71
0.00	0.00	0.03	0.00	0.00	0.00	0.00	0.00	0.04	0.00	0.01
31.88	31.96	29.90	32.61	31.83	32.09	31.66	32.04	32.03	32.71	30.68
0.50	0.55	0.48	0.45	0.53	0.48	0.48	0.46	0.52	0.51	0.40
6.74	6.76	6.45	7.01	7.06	6.98	6.97	6.92	6.70	5.97	7.26
1.52	1.48	1.43	1.43	1.51	1.47	1.39	1.50	1.54	1.44	1.62
0.01	0.03	0.01	0.03	0.02	0.03	0.00	0.03	0.05	0.03	0.01
0.00	0.00	0.04	0.01	0.00	0.00	0.00	0.00	0.00	0.00	0.00
98.25	98.73	97.55	99.47	98.34	99.04	97.91	98.64	98.50	96.35	99.49
12	12	12	12	12	12	12	12	12	12	12
2.93	2.95	3.00	2.93	2.92	2.93	2.93	2.93	2.91	2.91	2.97
0.00	0.00	0.00	0.00	0.00	0.00	0.00	0.00	0.00	0.00	0.00
2.01	1.99	2.04	1.99	2.00	2.00	2.01	2.00	2.02	2.01	2.01
0.00	0.00	0.00	0.00	0.00	0.00	0.00	0.00	0.00	0.00	0.00
2.15	2.14	2.00	2.17	2.14	2.14	2.14	2.15	2.15	2.27	2.02
0.03	0.04	0.03	0.03	0.04	0.03	0.03	0.03	0.04	0.04	0.03
0.81	0.81	0.77	0.83	0.85	0.83	0.84	0.83	0.80	0.74	0.85
0.00	0.00	0.00	0.00	0.00	0.00	0.00	0.00	0.00	0.00	0.00
0.13	0.13	0.12	0.12	0.13	0.13	0.12	0.13	0.13	0.13	0.14
0.00	0.00	0.00	0.00	0.00	0.01	0.00	0.00	0.01	0.00	0.00
0.00	0.00	0.00	0.00	0.00	0.00	0.00	0.00	0.00	0.00	0.00
8.06	8.06	7.98	8.08	8.08	8.07	8.07	8.07	8.07	8.09	8.02
0.69	0.69	0.68	0.69	0.68	0.68	0.68	0.69	0.69	0.72	0.67
0.26	0.26	0.26	0.26	0.27	0.27	0.27	0.26	0.26	0.23	0.28
0.04	0.04	0.04	0.04	0.04	0.04	0.04	0.04	0.04	0.04	0.05
0.01	0.01	0.01	0.01	0.01	0.01	0.01	0.01	0.01	0.01	0.01
0.04	0.04	0.04	0.04	0.04	0.04	0.04	0.04	0.04	0.04	0.05
0.73	0.73	0.72	0.72	0.72	0.72	0.72	0.72	0.73	0.75	0.70

Gt2c__47	Gt2c__48	Gt2c__49	Gt2c__50	Gt2c__51	Gt2c__52	Gt2c__53	Gt2c__54	Gt2c__55	Gt2c__57	Bt2__12
566	567	568	569	570	571	572	573	574	576	616
-831	-748	-665	-582	-499	-416	-333	-249	-166	0	-1110
-374	-280	-187	-94	0	93	187	280	373	560	-430
241	243	246	248	250	253	255	257	260	265	236
Gt2c__47	Gt2c__48	Gt2c__49	Gt2c__50	Gt2c__51	Gt2c__52	Gt2c__53	Gt2c__54	Gt2c__55	Gt2c__57	gt
37.17	36.76	37.44	37.02	36.69	36.92	36.59	36.45	37.57	37.21	36.96
0.01	0.02	0.04	0.00	0.02	0.02	0.01	0.00	0.00	0.00	0.00
21.45	21.31	21.46	22.90	21.28	21.38	21.37	21.19	21.89	21.52	21.16
0.02	0.00	0.00	0.01	0.00	0.01	0.01	0.00	0.01	0.00	0.02
30.47	30.01	30.56	28.99	30.56	30.29	30.48	30.40	30.21	30.89	30.69
0.41	0.49	0.47	0.41	0.40	0.48	0.36	0.37	0.47	0.42	0.45
7.72	7.68	7.96	8.05	7.72	7.82	7.81	7.54	7.89	7.91	7.60
1.46	1.39	1.44	1.30	1.51	1.46	1.43	1.45	1.42	1.50	1.47
0.03	0.00	0.00	0.03	0.02	0.01	0.01	0.02	0.00	0.05	0.02
0.00	0.01	0.00	0.03	0.00	0.01	0.00	0.01	0.00	0.04	0.00
98.75	97.66	99.37	98.73	98.19	98.38	98.06	97.43	99.46	99.53	98.38
12	12	12	12	12	12	12	12	12	12	12
2.95	2.95	2.95	2.91	2.93	2.94	2.93	2.94	2.95	2.94	2.95
0.00	0.00	0.00	0.00	0.00	0.00	0.00	0.00	0.00	0.00	0.00
2.01	2.01	1.99	2.12	2.01	2.01	2.02	2.01	2.03	2.00	1.99
0.00	0.00	0.00	0.00	0.00	0.00	0.00	0.00	0.00	0.00	0.00
2.02	2.01	2.01	1.91	2.04	2.02	2.04	2.05	1.98	2.04	2.05
0.03	0.03	0.03	0.03	0.03	0.03	0.02	0.03	0.03	0.03	0.03
0.91	0.92	0.94	0.94	0.92	0.93	0.93	0.91	0.92	0.93	0.90
0.00	0.00	0.00	0.00	0.00	0.00	0.00	0.00	0.00	0.00	0.00
0.12	0.12	0.12	0.11	0.13	0.12	0.12	0.12	0.12	0.13	0.13
0.00	0.00	0.00	0.01	0.00	0.00	0.00	0.00	0.00	0.01	0.00
0.00	0.00	0.00	0.00	0.00	0.00	0.00	0.00	0.00	0.00	0.00
8.05	8.04	8.05	8.03	8.06	8.06	8.06	8.06	8.04	8.07	8.06
0.65	0.65	0.65	0.64	0.65	0.65	0.65	0.66	0.65	0.65	0.66
0.30	0.30	0.30	0.32	0.30	0.30	0.30	0.29	0.30	0.30	0.29
0.04	0.04	0.04	0.04	0.04	0.04	0.04	0.04	0.04	0.04	0.04
0.01	0.01	0.01	0.01	0.01	0.01	0.01	0.01	0.01	0.01	0.01
0.04	0.04	0.04	0.04	0.04	0.04	0.04	0.04	0.04	0.04	0.04
0.69	0.69	0.68	0.67	0.69	0.68	0.69	0.69	0.68	0.69	0.69

-999	-888	-777	-666	-555	-444	-111	0	-254	-244	-234	-224
-366	-302	-238	-174	-110	-46	146	210	-7179	-7181	-7183	-7185
239	241	244	247	249	252	260	263	176	176	176	176
gt	gt	gt	gt	gt	gt	gt	gt	gt	gt	gt	gt
36.52	36.83	37.05	36.26	38.20	36.04	37.47	37.52	36.42	36.08	37.12	36.99
0.08	0.04	0.00	0.04	0.08	0.00	0.00	0.03	0.03	0.04	0.02	0.01
21.42	21.38	21.16	21.25	22.54	20.84	21.76	21.58	20.93	20.85	21.36	21.50
0.00	0.00	0.00	0.01	0.00	0.00	0.00	0.01	0.00	0.03	0.00	0.01
31.15	30.40	30.00	30.51	30.17	30.63	30.40	30.34	32.24	32.25	32.85	32.58
0.43	0.49	0.52	0.42	0.45	0.46	0.40	0.40	0.52	0.43	0.38	0.49
7.90	7.67	7.80	7.70	7.99	7.46	7.86	7.89	6.42	6.33	6.35	6.59
1.40	1.47	1.52	1.41	1.37	1.41	1.50	1.35	1.45	1.39	1.32	1.39
0.01	0.00	0.02	0.00	0.06	0.03	0.01	0.00	0.02	0.02	0.04	0.01
0.02	0.02	0.00	0.00	0.00	0.01	0.00	0.00	0.01	0.00	0.00	0.00
98.92	98.32	98.07	97.60	100.86	96.89	99.39	99.12	98.04	97.42	99.44	99.57
12	12	12	12	12	12	12	12	12	12	12	12
2.91	2.94	2.96	2.92	2.95	2.93	2.95	2.96	2.94	2.94	2.95	2.94
0.00	0.00	0.00	0.00	0.00	0.00	0.00	0.00	0.00	0.00	0.00	0.00
2.01	2.01	1.99	2.02	2.05	2.00	2.02	2.01	1.99	2.00	2.00	2.01
0.00	0.00	0.00	0.00	0.00	0.00	0.00	0.00	0.00	0.00	0.00	0.00
2.07	2.03	2.00	2.05	1.95	2.08	2.00	2.00	2.18	2.20	2.19	2.17
0.03	0.03	0.04	0.03	0.03	0.03	0.03	0.03	0.04	0.03	0.03	0.03
0.94	0.91	0.93	0.92	0.92	0.90	0.92	0.93	0.77	0.77	0.75	0.78
0.00	0.00	0.00	0.00	0.00	0.00	0.00	0.00	0.00	0.00	0.00	0.00
0.12	0.13	0.13	0.12	0.11	0.12	0.13	0.11	0.13	0.12	0.11	0.12
0.00	0.00	0.00	0.00	0.01	0.00	0.00	0.00	0.00	0.00	0.01	0.00
0.00	0.00	0.00	0.00	0.00	0.00	0.00	0.00	0.00	0.00	0.00	0.00
8.08	8.05	8.05	8.07	8.02	8.07	8.04	8.04	8.06	8.06	8.05	8.05
0.66	0.65	0.65	0.66	0.65	0.66	0.65	0.65	0.70	0.71	0.71	0.70
0.30	0.29	0.30	0.30	0.31	0.29	0.30	0.30	0.25	0.25	0.24	0.25
0.04	0.04	0.04	0.04	0.04	0.04	0.04	0.04	0.04	0.04	0.04	0.04
0.01	0.01	0.01	0.01	0.01	0.01	0.01	0.01	0.01	0.01	0.01	0.01
0.04	0.04	0.04	0.04	0.04	0.04	0.04	0.04	0.04	0.04	0.04	0.04
0.69	0.69	0.68	0.69	0.68	0.70	0.68	0.68	0.74	0.74	0.74	0.73

-214	-205	-195	-185	-175	-165	-156	-146	-136	-126	-116	-107
-7187	-7189	-7191	-7193	-7195	-7197	-7199	-7201	-7203	-7205	-7207	-7209
177	177	177	177	177	177	177	178	178	178	178	178
gt	gt	gt	gt	gt	gt	gt	gt	gt	gt	gt	gt
36.73	37.40	37.13	37.07	37.33	36.93	37.33	36.62	36.83	37.17	36.89	37.22
0.00	0.00	0.00	0.04	0.00	0.01	0.00	0.05	0.03	0.00	0.12	0.01
20.97	21.47	21.32	21.44	21.73	21.23	21.46	21.37	21.41	21.11	21.11	21.57
0.01	0.00	0.03	0.00	0.01	0.00	0.01	0.00	0.00	0.03	0.00	0.01
32.34	32.35	32.26	32.71	32.91	33.09	33.06	32.60	33.68	33.08	32.99	33.35
0.45	0.53	0.53	0.49	0.44	0.44	0.49	0.43	0.48	0.41	0.53	0.39
6.38	6.51	6.48	6.54	6.44	6.24	6.32	6.15	6.05	5.97	5.92	5.91
1.40	1.35	1.41	1.31	1.32	1.40	1.36	1.36	1.36	1.35	1.61	1.40
0.00	0.01	0.02	0.02	0.02	0.00	0.00	0.00	0.00	0.03	0.04	0.03
0.02	0.00	0.00	0.01	0.01	0.00	0.01	0.00	0.00	0.01	0.25	0.01
98.29	99.63	99.18	99.62	100.21	99.34	100.04	98.57	99.84	99.14	99.47	99.89
12	12	12	12	12	12	12	12	12	12	12	12
2.96	2.96	2.96	2.95	2.95	2.95	2.96	2.94	2.94	2.97	2.95	2.95
0.00	0.00	0.00	0.00	0.00	0.00	0.00	0.00	0.00	0.00	0.01	0.00
1.99	2.00	2.00	2.01	2.02	2.00	2.00	2.02	2.01	1.99	1.99	2.02
0.00	0.00	0.00	0.00	0.00	0.00	0.00	0.00	0.00	0.00	0.00	0.00
2.18	2.14	2.15	2.17	2.17	2.21	2.19	2.19	2.24	2.21	2.21	2.21
0.03	0.04	0.04	0.03	0.03	0.03	0.03	0.03	0.03	0.03	0.04	0.03
0.77	0.77	0.77	0.77	0.76	0.74	0.75	0.74	0.72	0.71	0.71	0.70
0.00	0.00	0.00	0.00	0.00	0.00	0.00	0.00	0.00	0.00	0.00	0.00
0.12	0.11	0.12	0.11	0.11	0.12	0.12	0.12	0.12	0.12	0.14	0.12
0.00	0.00	0.00	0.00	0.00	0.00	0.00	0.00	0.00	0.00	0.01	0.00
0.00	0.00	0.00	0.00	0.00	0.00	0.00	0.00	0.00	0.00	0.03	0.00
8.05	8.03	8.04	8.05	8.04	8.05	8.04	8.04	8.06	8.04	8.06	8.04
0.70	0.70	0.70	0.70	0.71	0.71	0.71	0.71	0.72	0.72	0.71	0.72
0.25	0.25	0.25	0.25	0.25	0.24	0.24	0.24	0.23	0.23	0.23	0.23
0.04	0.04	0.04	0.04	0.04	0.04	0.04	0.04	0.04	0.04	0.04	0.04
0.01	0.01	0.01	0.01	0.01	0.01	0.01	0.01	0.01	0.01	0.01	0.01
0.04	0.04	0.04	0.04	0.04	0.04	0.04	0.04	0.04	0.04	0.05	0.04
0.74	0.74	0.74	0.74	0.74	0.75	0.75	0.75	0.76	0.76	0.76	0.76

-97	-87
-7211	-7213
178	179
gt	gt
37.02	36.49
0.00	0.02
21.15	21.15
0.02	0.01
33.47	33.31
0.54	0.44
6.22	5.98
1.28	1.31
0.00	0.04
0.01	0.00
99.72	98.76
12	12
2.95	2.94
0.00	0.00
1.99	2.01
0.00	0.00
2.23	2.24
0.04	0.03
0.74	0.72
0.00	0.00
0.11	0.11
0.00	0.01
0.00	0.00
8.06	8.06
0.72	0.72
0.24	0.23
0.03	0.04
0.01	0.01
0.04	0.04
0.75	0.76